PhD degree in Molecular Medicine

SEMM – European School of Molecular Medicine

University of Milan, Faculty of Medicine, Bio/11

THE ROLE OF RNA AND DNA:RNA HYBRIDS AT DNA DOUBLE-STRAND BREAKS

Giuseppina D'Alessandro

IFOM, Milan

Supervisor	Dr. Fabrizio d'Adda di Fagagna IFOM, Milan
Internal co-supervisor	Dr. Vincenzo Costanzo IFOM, Milan
External co-supervisor	Dr. Jos Jonkers NKI, Amsterdam

2017-2018

Table of contents

Figures Index

Abstract

The stability of our genome is constantly challenged by several genotoxic threats. DNA double-strand breaks (DSBs) are the most dangerous DNA lesions that, if not repaired, can lead to cancer initiation and progression and/or ageing. These detrimental consequences can only be avoided if cells promptly recognize the lesions and signal their presence, thus promoting either efficient repair and transient cell cycle arrest or cell death and cellular senescence. This is the role of the DNA damage response (DDR) proteins and the newly identified damage-induced non coding RNAs. We recently discovered that RNA polymerase II is recruited to DSBs and synthetizes damage-induced non-coding RNAs (dilncRNAs). DROSHA- and DICER-mediated processing of dilncRNAs generates small RNA species, named DNA damage response RNA (DDRNAs) (Francia, 2012), that localize to DSBs via pairing with dilncRNAs and promote DDR signaling (Michelini et al., in press). Similar small non-coding RNA species discovered in plants are involved in DNA repair by homologous recombination (HR) (Wei, 2012, Gao, 2014, Wang, 2016). In line with these results, I report that transcriptional inhibition impairs recruitment of the HR proteins BRCA1, BRCA2, and RAD51 to DSBs, while partially promoting DNA end resection. Moreover, I show DNA:RNA hybrids accumulation at DSBs in mammalian cells by both DRIP analyses and imaging techniques. Damage-induced DNA:RNA hybrids form upon the hybridization of RNA species, likely dilncRNAs, to the resected DSBs DNA ends generated during the S/G2 cell cycle phase. I also report that purified recombinant BRCA1 binds DNA:RNA hybrids *in vitro*; moreover, DNA:RNA hybrids *in vivo* contribute to BRCA1 recruitment to DSBs. Consistent with the need to tightly regulate DNA:RNA hybrid levels, I demonstrate that RNase H2, the major RNase H activity in mammalian nuclei, is recruited to DSBs through direct interaction with RAD51. In summary, I report for the first time that DNA:RNA hybrids accumulate at DSBs in mammalian cells in a cell-cycle- and DNA end resection-depended way. At DSBs, BRCA1 directly recognizes DNA:RNA hybrids and likely controls their turn-over by mediating the recruitment of RNase H2 via RAD51.

1 Introduction

1.1 DNA damage: from signaling to repair

1.1.1 Types of DNA damage

It has been estimated that every day the stability of our genome is challenged by thousands of lesions (Lindahl and Barnes, 2000). In the majority of the cases, these lesions are efficiently repaired, while their inefficient repair has been associated to malignant transformation and cancer progression (Hanahan and Weinberg, 2011).

Genotoxic stimuli mainly target the nitrogen bases of the DNA, causing their loss or modification. However, they may also severely challenge the stability of our genome by breaking simultaneously the sugar-phosphate backbones of the two complementary DNA strands, generating a DNA double-strand break (DSB). A DSB is the most toxic DNA lesion since its inaccurate repair not only results in insertions or deletions, but can also cause gross genetic rearrangements, such as translocations, that are common in many cancers (Jackson and Bartek, 2009). This is the case, for example, for Burkitts Lymphoma, where a translocation event juxtaposes the strong immunoglobulin heavy chain promoter to the oncogene c-myc, causing aberrant expression of the oncogene, thus leading to cancer initiation and progression (Taub et al., 1982). In addition to cancer, DSBs have been linked to developmental, neurological, and immunological disorders (Jackson and Bartek, 2009).

DSBs may be generated upon exposure to several exogenous factors, including chemicals, or ionizing radiation (IR), for instance generated during radiotherapy and chemotherapy for medical treatments. Additionally, DSBs may be caused by endogenous free-radical oxygen species produced during cellular metabolism, or may arise during several other physiological processes, including DNA replication, transcription, or when these two processes collide (Aguilera and Gaillard, 2014). In addition to being a by-product of cellular processes, DSBs formation may be a key step of other specialized processes. Indeed, scheduled DSBs are generated during class switch and V(D)J recombination, two mechanisms required for the antibody repertoire diversification in the immune system (Soulas-Sprauel et al., 2007), and

meiotic recombination (Neale and Keeney, 2006).

1.1.2 The DNA damage response (DDR)

When our genome is damaged, the cell orchestrates a cellular response known as DNA damage response (DDR), that senses the damage, signals its presence, coordinates the repair, and finally leads to the activation of checkpoint responses that slow down or arrest cell-cycle progression, until the damage has been repaired (Ciccia and Elledge, 2010, d'Adda di Fagagna, 2008).

In order to activate DDR, the cell should be alerted of the presence of the DNA lesions. This is the job of the sensor proteins, Meiotic Recombination 11 (MRE11)/ Nijmegen breakage syndrome 1 (NBS1)/ RAD50 (MRN) and Replication Protein A (RPA), that recognize, respectively, exposed DNA ends or ssDNA stretches generated either upon DSBs end resection or replication stress (d'Adda di Fagagna, 2008).

MRN is a trimeric protein complex that associates with DNA through its globular "head", composed of MRE11 dimer and two RAD50 ATP-binding cassette (ABC) ATPase domains, and recruits ATM through the flexible adapter NBS1 (Williams et al., 2010). Once recruited to DSBs, ATM gets activated via a not yet fully defined mechanism that determines the transition from a multimeric inactive to a monomeric active form (Blackford and Jackson, 2017).

RPA is a heterotrimeric complex composed of the RPA70, RPA32 and RPA14 subunits, which binds to DNA through the oligonucleotide/oligosaccharide (OB) binding domains of the RPA70 and the RPA32 subunits (Zou and Elledge, 2003). RPA recruits the ATR kinase via the ATR interacting protein (ATRIP) and, through the RAD17/RCF complex, facilitates the loading of the RAD9–HUS1–RAD1 (9–1–1) clamp complex on ssDNA-dsDNA junctions. The 9-1-1 complex, in turn, recruits the topoisomerase II binding protein 1 (TopBP1) that binds the ATR-ATRIP complex and leads to ATR activation (Zou and

Elledge, 2003). Recently, a role for PRP19, an E3 ubiquitin ligase involved in pre-mRNA splicing, in ATR-ATRIP accumulation and signaling has been reported (Polo et al., 2012).

ATM and ATR are members of the phosphatidylinositol 3-kinase-like family of serine/threonine protein kinases (PIK kinases), which phosphorylate their substrates on a serine or threonine followed by glutamine, the S/TQ motif (Blackford and Jackson, 2017). The histone variant H2AX is one of the major targets of ATM and ATR, as well as of the PIK kinase DNA-PK. DNA damage induced phosphorylation of H2AX on serine 139 (named γH2AX) is recognized by DNA-damage checkpoint 1 (MDC1), which interacts with and mediates additional loading of the MRN complex. This, in turn, fuels ATM activation and H2AX phosphorylation, thus generating a positive feedback loop that strongly amplifies DDR signaling and results in the spreading of γH2AX for several kilobases around the DSB, generating a sort of "molecular velcro" for the retention of DDR proteins (Rogakou et al., 1999, d'Adda di Fagagna, 2008). This is a key point in DDR activation since the initial recruitment of DDR proteins through direct recognition of DNA ends (primary recruitment) is reinforced by a more complicated γH2AX dependent recruitment (secondary recruitment) (Celeste et al., 2003). Among the others, MDC1 mediates the recruitment of the E3 ubiquitin ligase RNF8 that, together with RNF168, mediates ubiquitylation of H2AX that is crucial for recruitment of mediator proteins, such as BRCA1 and 53BP1(Bekker-Jensen and Mailand, 2010). In addition to phosphorylation and ubiquitylation events, other reversible post-translational modifications like sumoylation and metylation are essential for DDR activation (Jackson and Durocher, 2013).

Additional major targets of ATM and ATR phosphorylation are the downstream protein kinases CHK2 and CHK1, respectively (Bekker-Jensen and Mailand, 2010). Activated CHK1 and CHK2 diffuse in the nucleoplasm, spreading the signal by phosphorylating their substrates throughout the nuclear space, and ultimately leading to the activation of p53 and the CDC25 phosphatases. At this point, DDR activation and cell cycle progression becomes strongly intertwined. On one hand, DNA damage dependent phosphorylation of the CDC25

phosphatases leads to inactivation of the CDK-Cyclin complexes that are responsible for the progression throughout the cell-cycle phases. On the other hand, cell-cycle arrest is obtained by p53-mediated transcription of the CDK1 inhibitor p21 (Branzei and Foiani, 2008). DNA damage-induced cell-cycle arrest is usually transient and cells restart proliferating normally once damage has been repaired. However, when the damage is not repaired cells may undergo apoptosis or enter a prolonged DDR-induced cell-cycle arrest known as cellular senescence (d'Adda di Fagagna, 2008).

1.1.2.1 The multiple roles of BRCA1 in the DDR

The breast and ovarian cancer type 1 susceptibility protein (BRCA1) is a protein with a key role in the maintenance of genome stability since it coordinates various aspects of the DNA damage response, from cell cycle activation to homologous recombination (HR)-mediated DSB repair (Huen et al., 2010). BRCA1 and breast and ovarian cancer type 2 susceptibility (BRCA2) genes are the most frequently mutated genes in breast and ovarian cancer (Venkitaraman, 2002) and recently-developed drugs exploit their key function in DNA repair to selectively target cancer cells (Polyak and Garber, 2011).

At the protein level, BRCA1 interacts with BARD1, through its N-terminal RING domain, forming a constitutive heterodimer with E3 ubiquitin ligase activity (Wu et al., 1996). Although the role of BRCA1-BARD1 mediated ubiquitylation in DDR is still poorly understood, it has been shown that BRCA1-mediated ubiquitylation of H2A at pericentromeric heterochromatin represses the expression of satellite DNA, thus promoting genome stability (Zhu et al., 2011).

The BRCT domain located at BRCA1 C-terminus, mediates the mutually exclusive interaction of the BRCA1-BARD1 heterodimer with phosphorylated ABRAXAS, BACH1, or CtIP, forming three different complexes, respectively known as BRCA1-A, BRCA1-B, and BRCA1-C (Huen et al., 2010). A fourth BRCA1 (BRCA1-D) complex is generated by interaction with BRCA2 and its associated partners PALB2 and RAD51 (Huen et al., 2010)

(figure 1). BRCA1-A complex is composed of RAP80, ABRAXAS, BRCC36, BRCC45 (also known as BRE), and mediator of RAP80 interactions and targeting subunit of 40 kDa (MERIT40). This complex mainly targets BRCA1 to DSBs through RAP80 interaction with the ubiquitin chains generated by the E3 ubiquitin ligases RNF8 and RNF168 (Mailand et al., 2007). However, an earlier H2AX independent (Celeste et al., 2003) and BARD1- and PARylation- dependent (Li and Yu, 2013) recruitment has also been observed, supporting the pleiotropic roles of BRCA1 in different complexes at DSBs. The main function of the BRCA1-A complex is the activation of the G2–M checkpoint and the inhibition of DNA end resection (Hu et al., 2011).

BRCA1–B complex contains TopBP1 and the BRCA1-interacting protein carboxy-terminal helicase 1 (BACH1) and it has a role mainly in DNA replication and S phase checkpoint activation (Huen et al., 2010).

In the BRCA1-C complex BRCA1 interacts with MRN and CtIP. CDK-dependent S327 phosphorylation of CtIP is required for its interaction with BRCA1 (Huertas and Jackson, 2009, Yu and Chen, 2004). This interaction, although dispensable for DNA end resection (Reczek et al., 2013, Polato et al., 2014), increases the efficiency of the process (Cruz-Garcia et al., 2014). Although BRCA1 does not contribute directly to DNA end resection, it has a fundamental role in contrasting its inhibition by resection blockers, including 53BP1, RIF1, and PTIP (Hustedt and Durocher, 2016), as discussed later. Indeed, in the absence of resection barriers (for example, in the case of 53BP1 depletion), CtIP mediated resection is possible even in the absence of BRCA1 (Polato et al., 2014).

The BRCA1-D complex is composed of BRCA1, BRCA2, PALB2, and RAD51 and it has a key function in HR since it mediates the loading of RAD51 on the RPA-covered ssDNA stretches generated upon resection of broken DNA ends. PALB2 bridges the interaction between the coiled-coiled domain of BRCA1 and BRCA2. BRCA2 interacts with RAD51 through different domains, as discussed later, and mediates its loading on resected DNA ends (Prakash et al., 2015).

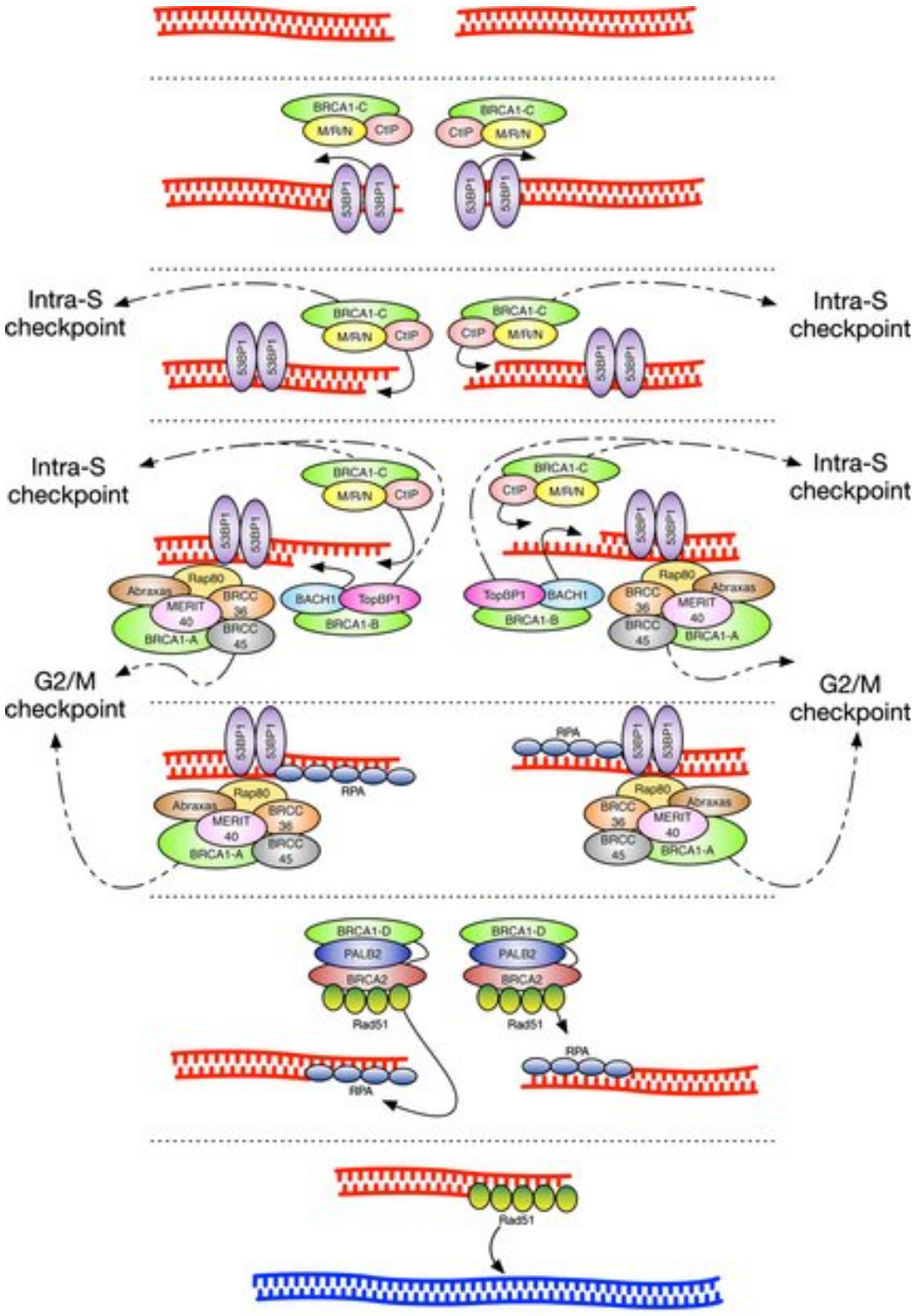

adapted from (Savage and Harkin, 2015)

Figure 1: BRCA1 complexes and their role in DNA damage signaling and repair
BRCA1 associates with MRN and CtIP in the BRCA1-C complex to promote DNA end resection manly by displacing the resection "blockers" such as 53BP1. The BRCA1-B complex, composed of BACH1 and TopBP1, promotes, together with BRCA1-C, extensive resection and the consequent activation of the intra-S checkpoint. The BRCA1–A complex is composed of RAP80, ABRAXAS, BRCC36, BRCC45, and MERIT40. Trough RAP80, BRCA1-A is recruited to flanking chromatin where prevents DNA end resection. Moreover, BRCA1-A participates to the activation of the G2/M checkpoint. BRCA1, PALB2, BRCA2, and RAD51 form the BRCA1-D complex, which facilitates the exchange of RPA with RAD51 on the ssDNA ends generated upon DNA end resection. ssDNA-RAD51-mediated homology search and invasion allows the synthesis of the missing part of the broken DNA end to allow HR completion.

1.1.3 DSB repair pathways

DSBs are the most toxic lesions that, if not properly repaired, can lead to mutations, chromosomal rearrangements and genome instability (Jackson and Bartek, 2009). In order to efficiently repair DSBs, cells have evolved two main pathways that can either use homologous sequences as templates for repair (homology-directed recombination, HDR) (figure 2b) or not (non homologous end joining, NHEJ) (figure 2a). While NHEJ is active throughout the entire cell cycle, the availability of the template sister chromatid during the S and G2 phases restricts HDR to these cell-cycle phases. A key factor in the choice between NHEJ and HDR is the licensing of DNA-end resection (Chapman et al., 2012b).

1.1.3.1 NHEJ

NHEJ is the faster way to repair a DSB since it simply rejoins severed DNA ends, with partial or no processing of them (Chang et al., 2017). The initial step of the classical NHEJ pathway (c-NHEJ) is the loading on the broken ends of the Ku70/Ku80 complex, which tethers DNA ends together and mediates the recruitment and activation of other key proteins with endonuclease, polymerase and DNA ligase activities. Once DSBs have been recognized by the Ku70/80 complex, compatible DNA ends can be directly rejoined by DNA ligase IV, in association with its binding partners X-ray repair cross-complementing protein 4 (XRCC4) and XRCC4-like factor (XLF) (figure 2a). However, 20-50% of IR-induced DSBs need to be processed prior to ligation (Riballo et al., 2004, Kurosawa et al., 2008). In this case, DNA-bound Ku70/80 facilitates the recruitment of the DNA-dependent protein kinase catalytic subunit (DNA-PKcs), which binds both to DNA and to Ku70/80, and mediates its activation. Active DNA-PKcs then contributes to the phosphorylation of several NHEJ factors, including Ku70, Ku80, Artemis, XRCC4, XLF, and LIG4, as well as the histone variant H2AX at DNA breaks (An et al., 2010). Once activated by DNA-PKcs, the nuclease ARTEMIS processes DSBs making the DNA ends compatible for the subsequent ligation step (Chang et al., 2017).

When micro-homology sequences flanking the DSB are present, an alternative NHEJ (a-NHEJ) pathway, also known as micro-homology-mediated end joining (MMEJ), repairs DSBs through the coordinated action of DNA ligase III, XRCC1, and PARP1 (Chang et al., 2017).

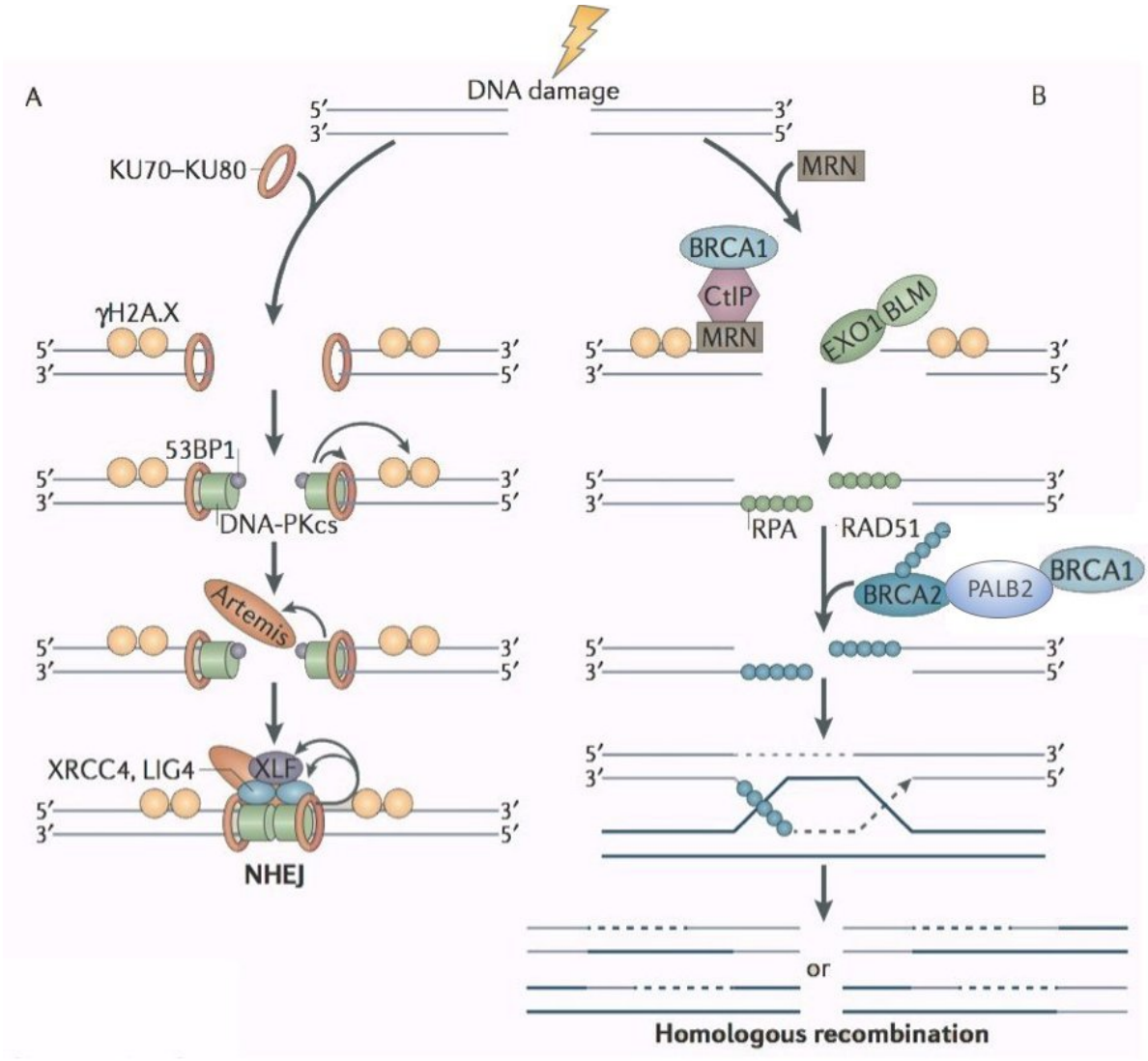

adapted from (Chowdhury et al., 2013)

Figure 2: DSB repair pathways

A DSB can be repaired by either NHEJ (a) throughout the cell-cycle phases or HDR-dependent pathways (b) during S/G2 phase. In NHEJ-mediated repair, the Ku70/80 heterodimer binds to the broken DNA ends and recruits the catalytic subunit of DNA-PK (DNA-PKcs) and 53BP1. DNA-PKcs activation favors Artemis-mediated processing of DNA ends making them suitable for the ligation mediated by the XRCC4/DNA ligase IV complex (a). HDR starts with the resection of the broken DNA ends to generate ssDNA stretches covered by RPA. DNA end resection is initiated by the MRN complex, in the presence of CtIP and it is extended by EXO1 and DNA2/BLM; BRCA1, although not strictly necessary, increases the speed of the process. Next, the BRCA2/PALB2/BRCA1 complex promotes the replacement of RPA with RAD51 on the ssDNA ends. RAD51 nucleofilaments invade the homologous DNA sequences and the invading DNA is extended by DNA polymerase δ and ligated. Once the DNA intermediates structures have been resolved, an exact copy of the original template sequence has replaced the damaged DNA at the DSB site (b).

1.1.3.2 HDR

DNA end resection is a biphasic process. An initial short-tract resection is mediated by the coordinated action of CtIP and the MRE11 subunit of the MRN complex, which has both endo- and exo-nuclease activities. The subsequent long-tract resection requires the additional action of exonuclease 1 (EXO1). The observation that the exo-nucleolytic activity of MRE11 is 3'-5' oriented has been difficult to reconcile with the generation of 3'-protruding ssDNA overhangs. Only recently, a model explaining this apparent controversy has been generated (figure 3). According to this model, DNA end resection starts with MRE11 endo-nucleolytic cleavage of dsDNA few nucleotides away from the DNA end, an event stimulated by CtIP. After endo-nucleolytic cleavage, resection proceeds bi-directionally, with MRE11 and EXO1 respectively resecting in 3′–5′ direction and 5′–3′ resection (Chapman et al., 2012b). The ssDNA filaments generated upon resection are immediately bound by RPA, which protects the ssDNA and avoids the formation of ssDNA secondary structures.

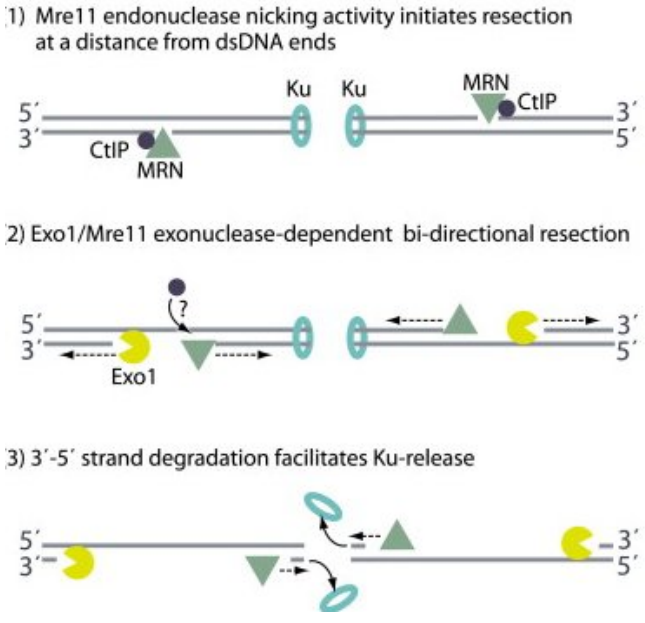

adapted from (Chapman et al., 2012b)

Figure 3: Mechanism of DNA end resection
Mre11 endonuclease nicks the DNA strand few nucleotides away from the DSB, initiating bi-directional resection dependent on the exonuclease activity of Mre11 (3' to 5' oriented) and Exo1 (5' to 3' oriented). This process is facilitated by CtIP and results in the eviction of Ku from the DNA ends

When extensive resection of the broken DNA ends exposes homologous sequences flanking the DSB, the recombinase RAD52 mediates a process known as single-strand annealing (SSA), that anneals the homologous sequences leading to the loss of the genetic information contained on the resected DNA ends. Long range DNA end resection and the associated SSA pathway are inhibited by 53BP1 (Ochs et al., 2016). Recently, an additional role for RAD52 in mediating inverse strand exchange with RNA molecules has been described (Keskin et al., 2014, Mazina et al., 2017). However, the observation that in mammalian cells RAD52 depletion does not affect survival upon IR (Rijkers et al., 1998) and is only lethal in combination with depletion of other HR proteins (Lok et al., 2013), suggests that the RAD52-mediated mechanisms may act as a backup in the absence of canonical HR repair pathway.

More frequently, HDR based mechanism uses homologous sequences located on the sister chromatids to template repair of either one-ended DSBs, generated by broken replication forks (Verma and Greenberg, 2016), or two-ended DSBs, in a process known as HR (Prakash et al., 2015). Since a homologous sequence is used as a template to copy back the information missing at the DSBs site, this is the only way the cell can repair a DSB in an error-free way. Upon resection of the broken DNA ends, the recombinase RAD51 needs to be loaded on the ssDNA ends to mediate homologous pairing and strand invasion. However, RAD51 loading on ssDNA ends is inhibited by RPA and in mammals it is facilitated by the mediator protein BRCA2 (Prakash et al., 2015). BRCA2 binds RAD51 through two unrelated domains: the BRC repeats and the C-terminal domain. While each BRC repeat can bind one single RAD51 monomer, the C-terminal domain (TR2), in its non-phosphorylated form, only binds the oligomeric RAD51. Upon DNA damage, BRCA2-TR2 binds RAD51 oligomers and mediates their assembly on ssDNA ends. Once damage has been repaired, BRCA2-TR2 gets phosphorylated and loses the ability to bind RAD51 oligomers. Consequently, RAD51 oligomers that are not anymore protected by the interaction with BRCA2-TR2 are destroyed by the interaction with the BRC repeats that keep RAD51 in a monomeric form (Davies and

Pellegrini, 2007, Esashi et al., 2007). Additionally, BRCA2 interacts with BRCA1 through PALB2. Interestingly, this interaction is cell-cycle controlled and contributes to DNA repair pathway choice, as discussed in the next section (Orthwein et al., 2015). Once ssDNA-RAD51 nucleoprotein filaments have been formed, homology search and strand invasion generates a D-loop which primes the DNA polymeras δ-mediated extension of the invading DNA. This results in the formation of different DNA intermediates, whose resolution completes the HR process and generates crossover or non-crossover products, the latter process also known as gene conversion (Jasin and Rothstein, 2013) (figure 2b).

1.1.3.2.1 DNA end resection and its role in DSB repair pathway choice

DNA end resection is the key step in DSB repair pathway choice. Once a DSBs has been resected it cannot be repaired anymore via NHEJ. Indeed, DNA end resection not only generates the ssDNA stretches that are essential for HDR, but it also inhibits Ku70/80 binding (Tomimatsu et al., 2012, Shao et al., 2012). Cell-cycle phase strongly influences DSB pathway choice (Hustedt and Durocher, 2016), mainly by impacting on expression and activity of CtIP (Ferretti et al., 2013). CDK-dependent phosphorylation on Thr847 is crucial for CtIP recruitment to DSBs and resection initiation (Huertas and Jackson, 2009), while the CDK-dependent phosphorylation on Ser327 stimulates its binding to BRCA1 (Yu and Chen, 2004), which is not essential for DNA end resection and only increases the rate of the process (Cruz-Garcia et al., 2014). CDK-mediated control of DNA end resection also relies on EXO1 and NBS1 phosphorylation (Ferretti et al., 2013). The CDK-mediated phosphorylation of CtIP also adds a further layer of regulation by promoting the binding of the prolyl isomerase PIN1, which mediates a conformational change that targets CtIP to proteasomal degradation (Steger et al., 2013). In addition, CtIP activity is positively regulated by SIRTUIN 6 (SIRT6)-mediated deacetylation (Kaidi et al., 2010) (figure 4b).

Two key factors in regulating DNA end resection and, therefore, DSB repair pathway choice are BRCA1 and 53BP1. BRCA1 is a key protein in HR, and 53BP1 has been shown to

promote NHEJ of a subset of DSBs, such as at dysfunctional telomeres (Dimitrova et al., 2008). Perturbation of the delicate balance between 53BP1 and BRCA1 at site of damage, resulting from cell-cycle phase (Hustedt and Durocher, 2016) or other factors such as chromatin status (Tang et al., 2013), channels the repair pathway toward either NHEJ or HDR, mainly by licensing or not DNA end resection. Upon DNA damage, ATM-mediated phosphorylation of 53BP1 promotes recruitment of the resection "blockers" PAX transactivation activation domain-interacting protein (PTIP) (Callen et al., 2013) and RAP1-interacting factor 1 (RIF1) (Chapman et al., 2013, Zimmermann et al., 2013), thus inhibiting DNA end resection (figure 4a). In the absence of 53BP1, BRCA1 can still localize to DSBs in G1 phase cells, but it is not able to recruit the BRCA2-PALB2 complex required for HR (Orthwein et al., 2015). The interaction of BRCA1 with the PALB2-BRCA2 complex is indeed cell-cycle regulated through the ubiquitylation of the BRCA1-interacting domain of PALB2 (Orthwein et al., 2015). During the S/G2 phase of the cell cycle the barrier posed by 53BP1 to DNA end resection is neutralized by BRCA1 (Escribano-Diaz et al., 2013). Indeed, the HR deficiency of BRCA1-depleted cells is recued in the absence of 53BP1 (Bunting et al., 2010). Moreover, super-resolution microscopy show a BRCA1-dependent change in the morphology of 53BP1 foci during the S/G2 phase (Chapman et al., 2012a), indicating that BRCA1 may facilitate DNA end resection by repositioning 53BP1 away from the DSB ends (figure 4b).

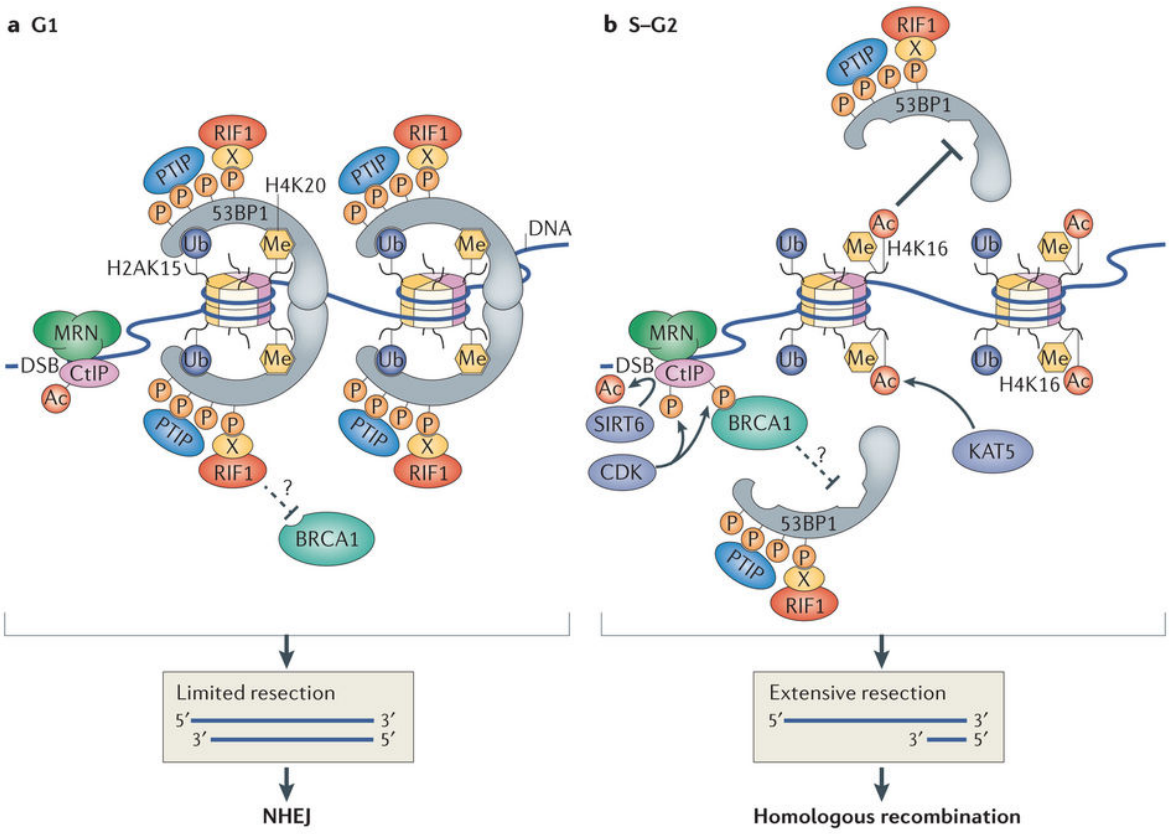

adapted from (Chapman et al., 2012b)

Figure 4: DSB repair pathway choice
(a) In G1 phase, ATM-mediated phosphorylation of 53BP1 allows the binding of the two resection "blockers" RIF1 and PTIP. 53BP1-bound RIF1 prevents the association of BRCA1 with CtIP, therefore inhibiting DNA end resection and favoring NHEJ. The mechanism of PTIP-mediated inhibition of DNA end resection is still not known. (b) During S phase, CDK-mediated phosphorylation of CtIP promotes its binding to BRCA1 and prevents 53BP1–RIF1, and possibly also 53BP1–PTIP, chromatin association. KAT5-mediated acetylation of H4K16 (H4K16ac) further reduces 53BP1 chromatin association. Additionally, CtIP activity is controlled by SIRT6, a deacetylase that removes an inhibitory acetylation mark on CtIP.

1.2 A novel role of RNA in DNA damage signaling and repair

1.2.1 Transcription and DDR

Transcription has been traditionally considered a dangerous process for genome stability (Aguilera and Gaillard, 2014). Collision of the transcription and replication machinery or DNA:RNA hybrids accumulation have been associated with genome instability. Moreover, transcription of damaged genes can lead to the generation of aberrant transcripts that can negatively affect cell viability. In order to avoid this risk, transcription of broken genes is silenced upon DNA damage (Iannelli et al., 2017, Pankotai et al., 2012, Shanbhag et al., 2010). However, transcriptional silencing of damaged genes co-exists with *de novo* transcription of sncRNAs with a function in DNA damage signaling and repair (Rossiello et al., 2017, Francia et al., 2012, Wei et al., 2012, Michalik et al., 2012). Differently from sncRNAs generated at the site of damage, which contribute directly to DNA damage signaling and repair, other RNA species, including miRNA and lncRNA, have also been reported to regulate these processes, for example through modulation of DDR proteins level, thus pointing to an unambiguous role for RNA in DNA damage signaling and repair.

1.2.1.1 DSB-induced transcriptional silencing

Transcription of a damaged gene may result in the production of aberrant transcripts that could be dangerous for the cell. In order to avoid this problem, cells have evolved mechanisms to silence the expression of damaged genes. A DSB within the gene body leads to DNA-PK mediated exclusion of RNA polymerase II (RNA pol II) from the gene body and its promoter (Pankotai et al., 2012). In a different system, in which multiple DSBs are induced upstream of a reporter gene, transcriptional silencing relies on ATM-dependent chromatin condensation associated with RNF8- and RNF168-mediated ubiquitination of the histones H2A/H2AX (Shanbhag et al., 2010). Strengthening the link between ubiquitination and transcriptional repression, reduced *de novo* mRNA synthesis has been observed in ubiquitin-enriched chromatin domains resulting from spontaneous DNA lesions

(Gudjonsson et al., 2012). ATM-mediated gene silencing upon DSB induction in proximity to or within a gene has been further supported by a recent study that combines transcriptome profiling with γH2AX ChIP-seq with a new method for "breaks labelling *in situ* and sequencing" (BLISS) (Yan et al., 2017), which directly labels and amplifies DSBs ends *in situ*, thus allowing a high-resolution genome-wide mapping of DSBs (Iannelli et al., 2017). In summary, transcription does not seem to be inhibited by the lesion *per se*, but by the consequent DDR activation. ATM-dependent transcription inhibition also impacts on RNA Pol I transcription of rDNA (Kruhlak et al., 2007). Damage-induced transcriptional silencing has been observed also in yeast (Lee et al., 2000), where it is due to the resection of both the template and the non-template sequence (Manfrini et al., 2015).

1.2.1.2 Transcription, DNA:RNA hybrids formation and genome instability

It is known since a long time that transcription can induce DNA damage (Skourti-Stathaki and Proudfoot, 2014). DNA damage and recombination may arise upon replication-fork stalling resulting from the collision between the transcription and replication machineries (Branzei and Foiani, 2010, Helmrich et al., 2013). Moreover, pairing of the nascent RNA with the template DNA may generate DNA:RNA hybrids that displace the non-template ssDNA to generate three-stranded nucleic acid structures named R-loops (Reaban et al., 1994). DNA:RNA hybrids form physiologically during DNA replication (Aguilera and Garcia-Muse, 2012) and participate in several physiological processes (Santos-Pereira and Aguilera, 2015), including immunoglobulin gene class-switch recombination (Yu et al., 2003), transcription activation of CpG islands promoters (Ginno et al., 2012), and transcription termination (Skourti-Stathaki et al., 2011). However, several factors, such as G content (Roy and Lieber, 2009), negative supercoiling associated with transcription (Drolet, 2006) in the context of topoisomerases deficiency (Drolet et al., 1995, Tuduri et al., 2009, El Hage et al., 2010), collision between transcription and replication machinery (Helmrich et al., 2011), and pausing of RNA pol II (Grabczyk et al., 2007, Lin et al., 2010,

Reddy et al., 2011), may be responsible for unscheduled R-loops formation and genome instability. On one hand, R-loops expose ssDNA to several assaults that undermine genome stability (Aguilera, 2002). On the other hand, the higher recombination rate observed at highly transcribed genes has been shown to rely on DNA replication (Gottipati et al., 2008), supporting the idea that R-loop-mediated genome instability may arise from replication fork stalling (Wellinger et al., 2006, Tuduri et al., 2009, Gan et al., 2011).

In order to avoid the detrimental effects of DNA:RNA hybrids accumulation, the equilibrium between their formation and resolution must be tightly controlled. This is possible by either preventing DNA:RNA hybrids formation through coating of the nascent RNA with RNA binding proteins (RBPs), or by removing DNA:RNA hybrids already formed (Santos-Pereira and Aguilera, 2015). The key protein responsible for DNA:RNA hybrids resolution are RNase H enzymes (Cerritelli and Crouch, 2009, Wahba et al., 2011), and helicases like Aquarius (Sollier et al., 2014), Senataxin (Skourti-Stathaki et al., 2011, Mischo et al., 2011, Alzu et al., 2012), and Pif1 (Chib et al., 2016, Tran et al., 2017)

1.2.1.2.1 Focus on RNase H enzymes

RNase H are the enzymes responsible for the degradation of the RNA strand of DNA:RNA hybrids (Cerritelli and Crouch, 2009). In eukaryotes two classes of RNAse H exist: the monomeric RNAse H1 (type 1) and the heterotrimeric RNAse H2 (type 2). While RNAse H1 is only able to cleave DNA:RNA hybrids formed of at least four consecutive ribonucleotides embedded in a dsDNA sequence, RNAse H2 can hydrolyze the vast majority of DNA:RNA hybrids in the cell and provides the major RNAse H function in eukaryotes (Cerritelli and Crouch, 2009) (figure 4). However, extended DNA:RNA hybrids can be degraded by either RNase H1 and RNase H2 (Cerritelli and Crouch, 2009). Mammalian RNase H1 has a nuclear isoform with a still unclear function and a mitochondrial isoform with a key role in mitochondrial DNA replication (Cerritelli et al., 2003). RNase H2 is a heterotrimeric complex composed of a conserved catalytic subunit (RNase H2A) and auxiliary subunits (RNase H2B and RNase H2C) (Cerritelli and Crouch, 2009), which form

a soluble stable complex subsequently bound by the subunit A to form the final functional complex. Moreover, the auxiliary proteins can mediate the interaction with other proteins and support other un-known functions. For example, RNase H2B mediates the interaction with PCNA, linking RNase H2 to replication and repair (Chon et al., 2009). Mutations in any of the human RNase H2 subunits can result in Aicardi-Goutieres syndrome (AGS), an neuroinflammatory disease reminiscent of congenital viral infections, possibly caused by the chronic activation of the immune system by excessive accumulation of aberrant forms of nucleic acids (Crow et al., 2006).

RNase H2 activity is crucial for genome stability. First, RNase H2 removes misincorporated ribonucleotides from genomic DNA (Sparks et al., 2012), whose accumulation can interfere with replication fork progression (Watt et al., 2011) and has been associated with DNA damage breakage and mutagenesis (Pizzi et al., 2015). Additionally, RNase H2 is responsible for the resolution of DNA:RNA generated by RNA polymerases during transcription (El Hage et al., 2010, Lin et al., 2010), whose accumulation would otherwise negatively impact on the transcription itself and genome stability. At yeast telomeres, RNase H2 regulates DNA:RNA hybrids levels (Graf et al., 2017). Short telomeres fail to accumulate RNase H2 and the consequent DNA:RNA hybrids accumulation is associated to DNA damage and HR (Graf et al., 2017).

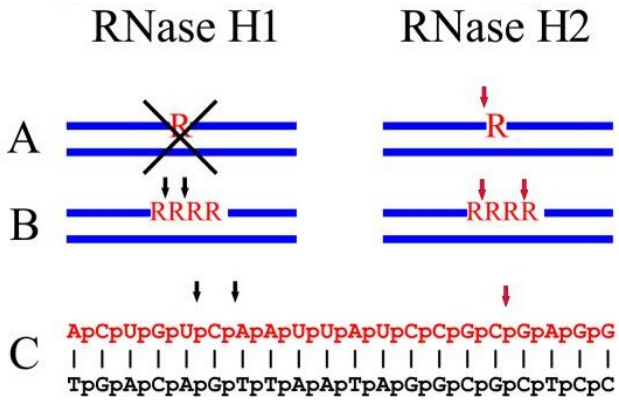

adapted from (Cerritelli and Crouch, 2009)

Figure 4: RNase H substrates and cleavage pattern
RNase H1 and RNase H2 have different substrates and different cleavage patterns on the same substrate. Single ribonucleotides embedded in a duplex DNA are cleaved only by RNase H2, and not by RNase H1 (a) Four consecutive ribonucleotides in a duplex DNA (b) or RNA/DNA hybrids (c) are cleaved differently by RNase H1 and RNase H2

1.2.1.3 A novel link between HR proteins, RNA processing, and DNA:RNA hybrids

As mentioned before, BRCA1 is a multifaceted protein with key roles not only in DNA damage signaling and repair, but also in several other cellular processes. For example, BRCA1 interacts with several transcription and RNA processing factors, including RNA pol II (Scully et al., 1997, Anderson et al., 1998). Upon damage, BRCA1 forms a complex with mRNA splicing factors to mediate the splicing and the stability of a subset of BRCA1 bound promoters, including promoters of genes controlling DNA repair and genome stability (Savage et al., 2014). Moreover, BRCA1 participates in miRNA biogenesis by recognizing miRNAs precursors and promoting their processing through interaction with DROSHA (Kawai and Amano, 2012). Recently, a strong and controversial link between BRCA1, BRCA2, RAD51 and DNA:RNA hybrids has emerged. On one hand, the accumulation of DNA:RNA hybrids and the associated genome instability observed in yeast RNA processing mutants has been attributed to the recombination protein Rad51 (Wahba et al., 2013), introducing a new and unforeseen role for a protein known as a "warden" of genome stability (Tan-Wong and Proudfoot, 2013). Stimulation of DNA:RNA hybrid formation had been also reported in the past for the bacterial Rad51 homologue RecA (Kasahara et al., 2000, Zaitsev and Kowalczykowski, 2000). On the other hand, DNA:RNA hybrids accumulation has been observed in cells depleted for the HR proteins BRCA1 and BRCA2, but not RAD51 (Bhatia et al., 2014, Tan et al., 2017). In line with these results, BRCA1-mediated recruitment of SENX suppresses genome instability induced by DNA:RNA hybrids accumulation at the termination region of the β-actin gene (Hatchi et al., 2015). The link between BRCA2 and DNA:RNA hybrids is less clear. The observation that DNA:RNA hybrids do not accumulate upon RAD51 depletion, together with the cell-cycle independent accumulation of DNA:RNA hybrids in BRCA2-depleted cells, suggests a possible uncoupling between BRCA2 function in DNA:RNA hybrids resolution and its well established role in HR (Bhatia et al., 2014). However, further supporting the connection between BRCA2 and DNA:RNA hybrids, some of the proteins that participate, together with

BRCA2, in the Fanconi Anemia (FA) repair pathway localize to DNA damage sites via DNA:RNA hybrids and suppress DNA:RNA hybrids associated genome instability (Garcia-Rubio et al., 2015, Schwab et al., 2015).

1.2.1.4 The positive impact of transcription on DSB repair

A growing body of evidence supports a role for transcription in DNA damage repair. DSBs are repaired faster in actively transcribed genes compared to inactive genes (Chaurasia et al., 2012) and preferentially via HR (Aymard et al., 2014). In human cells, endonuclease-induced DSBs have been classified in HR- and NHEJ-repair prone, on the bases of the enrichment of RAD51 or XRCC4 proteins, respectively (Aymard et al., 2014). HR-prone DSBs are mainly located in transcriptionally active chromatin, which is enriched in H3K36me3 or H3K9Ac chromatin marks. Recognition of active chromatin by accessory proteins mediates the recruitment of key HR proteins, thus fueling HR (Aymard et al., 2014).

1.2.2 RNA binding proteins and transcription factors recruitment to DNA lesions

In the last years, factors involved in several aspects of RNA metabolism have been found in proteomic and functional DDR screens (Matsuoka et al., 2007, Paulsen et al., 2009, Bennetzen et al., 2010, Bensimon et al., 2010) or have been reported as ATM or ATR substrates (Matsuoka et al., 2007). Moreover, an increasing number of transcription factors and RBPs have been reported to localize to DNA damage sites (Izhar et al., 2015), where they may directly participate in DDR (Dutertre et al., 2014). For example, DNA end resection is stimulated by hnRNPUL1/2 (heterogeneous nuclear ribonucleoprotein U-like), RBPs that control several aspects of RNA maturation (Polo et al., 2012). In particular, hnRNPUL1/2 localize to DSBs in an MRN-dependent way and stimulate DNA end resection by recruiting the helicase BLM. This process can be further stimulated by PRP19, an E3 ubiquitin ligase involved in pre-mRNA splicing, that interacts with and ubiquitylates RPA, favoring the accumulation ATR-ATRIP complex and further amplification of DDR signaling (Marechal et al., 2014). Additionally, components of the exosome, a complex

involved in RNA processing and degradation, have been shown to localize to DSBs, where they promote repair by HR (Marin-Vicente et al., 2015, Manfrini et al., 2015).

1.2.3 The role of RNA in DDR

Transcriptional modulation of DSB repair does not only rely on chromatin status but also on transcription products, either pre-existing or produced upon DNA damage, that can modulate both DDR signaling and repair (d'Adda di Fagagna, 2014). NHEJ proteins have been described to interact with nascent RNAs at DSBs located in actively transcribed genes (Chakraborty et al., 2016). In particular, following DSB induction, RNA pol II co-immunoprecipitates with both the NHEJ proteins Lig IV, XRCC4, Ku-70, Pol μ, DNA-PK and the HR proteins RAD51 and RAD52 (Chakraborty et al., 2016), thus indicating a possible role of the RNA itself in facilitating the recruitment or activation of DDR factors. Moreover, sncRNAs with the sequence of the damaged DNA are generated upon DSB in several organisms (Rossiello et al., 2017, Francia et al., 2012, Wei et al., 2012, Michalik et al., 2012). Our laboratory recently discovered that these damage-induced sncRNAs are generated from DROSHA- and DICER-mediated processing of longer precursor RNAs, which are transcribed from the broken DNA ends (Michelini et al., in press). Although *de novo* transcription and transcriptional inhibition at DSBs may sound as two mutually exclusive events, they could also fit in a unique scenario. Upon DSB induction, chromatin undergoes a first relaxation phase to allow the access of DDR proteins to the site of damage, and then a condensation phase necessary for further amplification of DDR signaling (Price and D'Andrea, 2013). An intriguing hypothesis would be that relaxed and easily accessible chromatin could facilitate the recruitment of transcription factors at DNA damage site. Recruitment of transcription factors might enhance transcription by RNA pol II, whose recruitment could, in turn, be favored by the chromatin relaxation or be the result of a more regulated mechanism. RNA pol II-mediated transcription of small RNA transcripts would then favor DDR activation (Francia et al., 2012) that, in turn, would induce to DNA damage

induced transcriptional silencing.

1.2.3.1 Biogenesis and function of damage-induced sncRNAs

Recent data support the generation of small ncRNAs upon DSB in several organisms (Rossiello et al., 2017, Francia et al., 2012, Wei et al., 2012, Michalik et al., 2012). In Drosophila cells, transfection of a linearized plasmid generates sncRNAs when the linearization truncates a transcribed region (Michalik et al., 2012). The production of these small RNA, with the sequence of the linearized ends, induces the post-translational silencing of the truncated gene, in a process known as endo-siRNA response. This process can be assimilated to a well-known and evolutionary-conserved mechanism known as RNA interference (RNAi), in which small RNA molecules, like siRNA, cause gene silencing (Ghildiyal and Zamore, 2009). Cleavage of a double-stranded precursor by DICER generates siRNAs, that are loaded on Argonaute proteins in the RNA-Induced Silencing Complex (RISC) to repress the expression of target transcripts. microRNA (miRNA) are another class of sncRNAs with a function similar to siRNAs, but slightly different biogenesis. miRNA biogenesis requires the additional cleavage of an hairpin precursor RNA by DROSHA, thus generating the dsRNA substrate for subsequent DICER cleavage. miRNAs are then loaded in the RISC complex and inhibit mRNA translation in a process mediated by the GW-182 family proteins.

In mammalian cells, DSB induction is followed by the production of sncRNAs with the sequence of the damaged locus, known as DNA damage response RNAs (DDRNAs) (Francia et al., 2012). Importantly, DDRNAs are not generated by processing of transcripts already present at the site of damage, rather they are the result of *de novo* transcription from broken DNA ends. Our laboratory recently demonstrated that RNA pol II is recruited to DSBs where it synthesizes damage-induced long non-coding RNAs (dilncRNAs), from and towards the broken DNA ends. DilncRNAs are processed by DROSHA and DICER to generated DDRNAs and they also mediate DDRNAs recruitment to the DSBs via

RNA:RNA pairing (Michelini et al., in press). While in the canonical RNAi pathway, DROSHA and DICER process the precursor transcripts respectively in the nucleus and in the cytoplasm, the exact cellular sub-compartment in which DDRNAs processing takes place is not known yet but it is likely to be nuclear. Indeed, the exclusively cytoplasmic localization of DICER (Billy et al., 2001, Provost et al., 2002, Much et al., 2016) has been recently challenged by several lines of evidence in favor of a nuclear localization and function (Sinkkonen et al., 2010, Ando et al., 2011, Ohrt et al., 2012, Gullerova and Proudfoot, 2012, Doyle et al., 2013, Gagnon et al., 2014, Skourti-Stathaki et al., 2014, White et al., 2014, Matsui et al., 2015, Neve et al., 2016). More conclusively, the laboratory of Monika Gullerova has recently shown that DNA damage-dependent DICER phosphorylation is required for its nuclear localization. Once recruited to the site of damage, two additional phosphorylation events control dsRNA processing, thus contributing to the recruitment of DDR proteins (Burger et al., 2017). It is therefore highly likely that DDRNAs are fully processed at DNA damage sites, where they also mediate DDR activation and DDR foci formation (d'Adda di Fagagna, 2014) (figure 5, right). The observation of DDRNAs production upon damage has been recently extended to an endogenous physiological locus (Rossiello et al., 2017). Our group reported that uncapped/damaged telomeres produce both G-rich and C-rich telomeric dilncRNAs that are processed by DROSHA and DICER to produce short RNAs, named telomeric DDRNAs (tDDRNAs), that are necessary for full DDR activation.

Similar RNA species, named diRNAs (DSB-induced RNAs) (Wei et al., 2012), bind AGO2 and promote HR by mediating the loading of AGO2-bound RAD51 to ssDNA ends (Gao et al., 2014). Moreover, they interact with and mediate the proper localization of the two chromatin modifiers MMSET and TIP60, that in turn favor chromatin relaxation and the recruitment of the HR proteins BRCA1 and RAD51 (Wang and Goldstein, 2016) (figure 5, left).

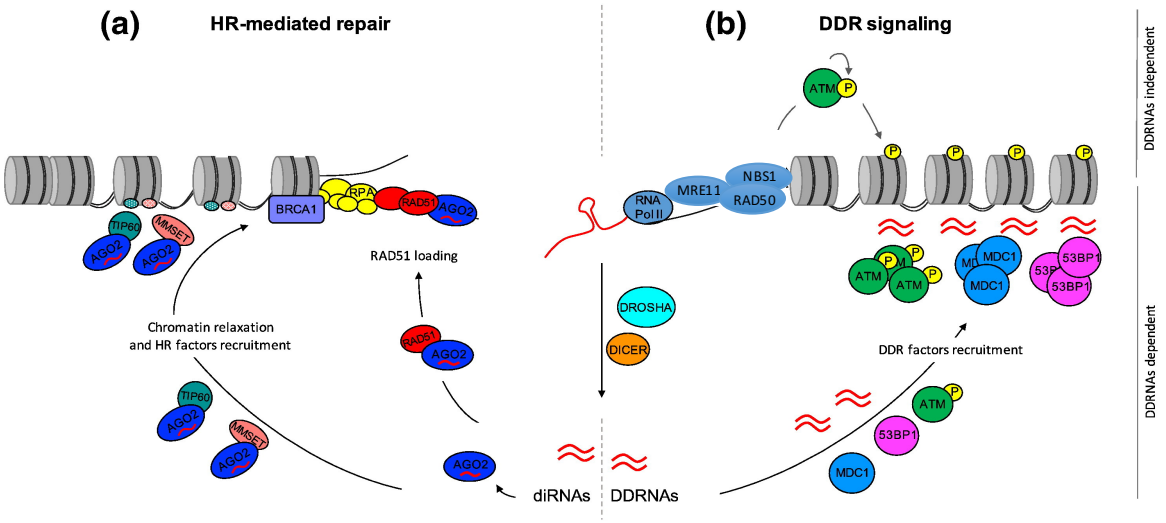

adapted from (D'Alessandro and d'Adda di Fagagna, 2016)

Figure 5: sncRNAs in DNA damage signaling and repair
Upon damage, small RNA species (diRNAs and DDRNAs) are generated by DROSHA- and DICER-mediated processing of a longer RNA transcribed by RNA pol II. DDRNAs contribute to DDR activation by promoting the "secondary recruitment" of DDR proteins, including pATM, MDC1, and 53BP1, to DSBs. "Primary recruitment" of DDR proteins, such as the MRN complex, and H2AX phosphorylation are DDRNAs-independent (b). AGO2-bound diRNAs promote HR by either recruiting the AGO2–RAD51 complex to DNA lesions, or by recruiting the chromatin remodeler MMSET and TIP60, which induce a permissive chromatin status for BRCA1 and RAD51 loading and HR-mediated repair.

1.2.3.2 DNA:RNA hybrids in DSB repair

A growing body of evidence suggests that DNA:RNA hybrids form at nicks (Roy et al., 2010) and DSBs (Ohle et al., 2016, Li et al., 2016, Li et al., 2008, Britton et al., 2014) and that they have a role in DNA repair. DNA:RNA hybrids formation upon damage is supported by the observation of transcription-dependent accumulation of the catalytically inactive *Escherichia coli* RNase H at laser micro-irradiation sites in human cells (Britton et al., 2014). Moreover, the human RNA-unwinding protein DEAD box 1 (DDX1) has been shown to localize to IR-induced DSBs. Damage induced localization of DDX1 at DSBs is depended on transcription and DNA end resection and it is abrogated by treatment with recombinant RNase H (Li et al., 2008, Li et al., 2016). Moreover, DNA:RNA hybrids accumulation upon DDX1 depletion impairs HR-mediated repair (Li et al., 2016). In *Schizosaccharomyces pombe*, RNA pol II localization and DNA:RNA hybrids formation at DSBs has been observed (Ohle et al., 2016). In particular, DNA:RNA hybrids formation is facilitated by DNA end resection and modulates HR by impacting on RPA loading on ssDNA stretches.

HR is only proficient in the presence of RNase H activities. Interestingly, either lack of both RNase H1 and RNase H2 or RNase H overexpression hampers DSB repair capacity. In particular, while RNase H depletion is associated with reduced RPA loading on ssDNA ends, upon RNase H overexpression RPA loading spreads further away from the DSBs, indicating an over-resection possibly causing the choice of other DNA repair pathways, such as SSA, rather than HR. Therefore, only a certain level of DNA:RNA hybrids favors DSB repair: an excessive level impedes RPA loading, while an insufficient level allows over-resection and the choice of pathways alternative to HR. At telomeres, DNA:RNA hybrids positively modulate HR-mediated repair (Graf et al., 2017, Balk et al., 2013, Arora et al., 2014, Pfeiffer et al., 2013, Yu et al., 2014). In yeast and mammalian telomerase negative cells, elongation of damaged telomeres is controlled by DNA:RNA hybrids formed upon hybridization of long noncoding telomeric repeat-containing RNA (TERRA) with the template DNA (Graf et al., 2017, Balk et al., 2013, Arora et al., 2014, Pfeiffer et al., 2013, Yu et al., 2014). In particular, TERRA and the associated DNA:RNA hybrids levels increase at the G1/S transition, before being degraded during progression from the S to the G2 phase (Graf et al., 2017). Recent data show that RNase H2, which is the major source of DNA:RNA hybrid nucleolytic activity in eukaryotic cells (Cerritelli and Crouch, 2009), is recruited to telomeres where it mediates DNA:RNA hybrids degradation. However, when telomeres become critically short, RNase H2 does not localize anymore to shortened telomeres and DNA:RNA hybrids accumulate. This leads to HR possibly due to collision between DNA:RNA hybrids and the replication machinery.

DNA:RNA hybrids are also intermediates of a newly discovered repair pathway known as RNA-templated repair. While it was already known that exogenous RNA oligonucleotides could template DSBs repair in yeast and human cells (Storici et al., 2007, Shen et al., 2011), only recently a role for endogenous RNA molecules in templating HR-mediated DSBs has been demonstrated (Keskin et al., 2014). Endogenous transcripts can either template the synthesis of cDNA molecules or be directly used as templates for HR, by forming

DNA:RNA hybrids intermediates. Key player in the RNA-templated DNA is the HR protein Rad52 (Keskin et al., 2014, Mazina et al., 2017) , that has been shown to catalyze *in vitro* the annealing of RNA to DNA (Keskin et al., 2014), mediating the formation of DNA:RNA hybrids. More recently, it has been also shown that yeast and human RAD52 catalyze *in vitro* an inverse strand-exchange reaction with DNA or RNA (Mazina et al., 2017). In the same setting no RAD51 mediated stimulation of RNA inverse strand exchange has been observed, although DNA:RNA hybrids formation has been also associated with Rad51 in yeast (Wahba et al., 2013) and RecA, the bacterial Rad51 orthologue, has been reported to promote paring between duplex DNA and ssRNA *in vitro* (Zaitsev and Kowalczykowski, 2000). Interestingly, inverse RNA strand exchange is stimulated by RPA, possibly via protein-protein interaction with RAD52, but it is still efficiently mediated by the Rad52 N-terminal domain (NTD), which lacks the RAD51 and RPA binding domains, pointing out to a unique role for Rad52 in this process (Mazina et al., 2017). The formation of DNA:RNA hybrids during this process is further supported by the observed stimulation of RNA-templated repair in the absence of RNase H functions (Keskin et al., 2014).

2 Materials and Methods

2.1 Cell culture

All the cell lines used were grown under standard tissue culture conditions (37°C, 5% CO_2). HeLa and U2OS cells were used to study DDR foci formation and were grown respectively in MEM supplemented with 10% fetal bovine serum (FBS), 1% L-glutamine, 1% penicillin/streptomycin, and McCoy supplemented with 10% FBS, 1% L-glutamine, and 1% penicillin/streptomycin. HeLa-FUCCI (RIKEN BioResource Center cell bank) (Sakaue-Sawano et al., 2008) were used to perform cell cycle studies and were grown in DMEM supplemented with 10% FBS, 1% L-glutamine, and 1% penicillin/streptomycin.

Dox-inducible I-SceI/DR-GFP (TRI-DR-U2OS) (kind gift from P. Oberdoerffer) are U2OS cells containing the DR-GFP reporter system and a doxyciclin-inducible I-SceI expressing vector. When I-SceI expression is induced (by adding 5 μg/ml doxycycline to the cell medium) I-SceI target sequence is cut and a recombination event between two mutated GFP cassettes generates the correct GFP sequence which is translated into a functional GFP that confers the green color to the cells. TRI-DR-U2OS cells were grown in DMEM supplemented with 10% FBS, 1% L-glutamine, and 1% penicillin/streptomycin.

DIvA cells (AsiSI-ER-U20S) (kind gift from G. Legube) were cultured in DMEM without phenol red supplemented with 10% FBS, 1% L-Glutamine, 1% pyruvate, 2.5% HEPES, 1% penicillin/streptomycin, and 1 μg/ml puromycin as a selection marker. AsiSI-dependent DSBs induction was obtained by treating the cells with 300 nM 4OHT (Sigma-Aldrich) for 4 hours.

U2OS19ptight (kind gift from E. Soutoglou) were grown in DMEM without phenol red supplemented with 10% FBS Tetracycline tested, 1% L-glutamine and G418 (800μg/mL). I-SceI expression was induced by adding 1μg/mL doxycycline for 16 hours.

U2OS D210N-GFP were provided by our collaborator Pavel Jansack. These are U2OS cells in which the expression of an shRNA against the endogenous RNase H1 and the overexpression of a catalytically inactive RNase H1 mutant (D210N) is induced by adding doxycycline (1 μg/ml) to the cell media. U2OS D210N-GFP were grown grown in DMEM

without phenol red supplemented with 10% FBS Tetracycline tested, 1% L-glutamine, and 1% penicillin/streptomycin. In general, medium without Phenol Red was used to avoid leakiness in the expression of the plasmids constitutively expressed or transfected in cells (i.e. upon I-PpoI transfection).

U2OS cell synchronization for super-resolution imaging experiments was obtained by serum starvation. Briefly, cells were plated on glass coverslips for 24 hours. G0/G1 phase synchronization was achieved by replacing complete medium with serum free medium for 72 hours. A mid-S phase cell population was obtained after 16 hours release into complete medium. Double strand breaks (DSBs) were generated by using the radiomimetic drug Neocarzinostatin (NCS) (Sigma-Aldrich).

2.2 Ionizing radiation (IR)

Ionizing radiation (IR) is a radiation able to ionize the target. The Gray (Gy) is the International System of Units of absorbed radiation dose, where 1 Gy is the absorption of 1 joule of radiation energy by 1 kilogram of matter. When DNA is targeted by IR DSBs and several other types of DNA damage are generated. Here, DSBs were generated by using X-rays, an electromagnetic type of IR, generated by a high-voltage X-rays generator tube (Faxitron X-Ray Corporation).

2.3 Plasmid transfection

For immunoprecipitation experiments, HEK293T cell were transfected with the calcium phosphate transfection method, that is based on the formation of calcium phosphate-DNA precipitates that bind the cell surface and enter the cell by endocytosis. Precipitates are obtained by slowly mixing a solution containing calcium chloride and DNA with a HEPES-buffered saline solution containing sodium phosphate. In details, for a 10 cm dish, 10 μg of DNA was resuspended in 439μl of H2O with 61μl of $CaCl_2$ (2M) and subsequently this solution was added to 500 μl of 2xHBS, constantly mixing. The mixture was added to the cells after 10 minutes incubation at RT.

For all the other experiments, plasmid transfection was performed by lipofection, a technique based on the formation of complexes between cationic synthetic lipids and negatively charged nucleic acids, that are then internalized in the cell. In particular, 90% confluent cells were transfected with Lipofectamine 2000 transfection reagent (Life Technologies). For each transfection reaction (in one well of a 6-well), 250 µl of serum-free medium (Opti-MEM) were mixed with plasmidic DNA (usually 1 µg final concentration) and 250 µl of Opti-MEM were mixed with 6 µl Lipofectamine 2000 transfection reagent. The two solutions were incubated 5 minutes at RT, then mixed and incubated for 20 minutes at RT to allow the formation of lipid complexes. The mix was added to the cells for 6 hours and then fresh culture medium was added.

Where indicated, 2 µg of mammalian RNase H1 expressing plasmid or HB-GFP (kind gift from A. Aguilera) or GFP-RNaseH1 (kind gift from N. Proudfoot) and their related control were transfected and experiments were performed 24 h after transfection. Where indicated, 1 µg of Cherry-LacR (kind gift from E. Soutoglou) and 1 µg of RNase H2A (kind gift from M. Lee-Kirsch) were used. I-PpoI expression was obtained by transfection of 1 µg of mammalian ER-I-PpoI expressing plasmid (kind gift from M. Kastan). 24 h after transfection, nuclear translocation of ER-I-PpoI was induced by adding 4-OHT (Sigma-Aldrich) at 2 µM final concentration for the indicated time.

2.4 RNA interference

Gene silencing was obtained by RNA interference, using short interfering RNAs (siRNAs). siRNA transfection was usually performed in 6-wells dishes on 30-50% confluent cells; for bigger plates volumes were scaled-up. For each transfection reaction 250 µl of serum-free medium (Opti-MEM) were mixed with siRNA oligo (5 to 20nM final concentration) and 250 µl of Opti-MEM were mixed with 4 µl Lipofectamine RNAiMAX transfection reagent (Life Technologies). Lipid complexes formation was obtained by mixing and incubating the two solutions for 20 minutes at RT. The 500 µl mix was added to 1.5 ml of cell media and

72 hours later knockdown efficiency was tested and cells were used for further analysis. Sequences of the siRNA used are listed in table 1.

Name	Sequence
LUCIFERASE	GCCAUUCUAUCCUCUAGAGGAUG
GFP	AACACUUGUCACUACUUUCUC
BRCA2	
1	GAAACGGACUUGCUAUUUA
2	GGUAUCAGAUGCUUCAUUA
3	GAAGAAUGCAGGUUUAAUA
4	UAAGGAACGUCAAGAGAUA
CtIP	
1	GGAGCUACCUCUAGUAUCA
2	GAGGUUAUAUUAAGGAAGA
3	GAACAGAAUAGGACUGAGU
4	GCACGUUGCCCAAAGAUUC
RAD51	
1	UAUCAUCGCCCAUGCAUCA
2	CUAAUCAGGUGGUAGCUCA
3	GCAGUGAUGUCCUGGAUAA
4	CCAACGAUGUGAAGAAAUU
RNase H1	
1	GACAGUAUGUUUACGAUAA
2	GAGCACAGGUGGACCGGUU
3	ACAAGAAUCGGAGGCGAAA
4	GAGCAGGAAUCGGCGUUUA
RNase H2	
1	CGGGAAAGGCUGUUUGCGA
2	AAAUGGAGGACACGGACUU
3	AUGCAUUGGACCAGGGCGU
4	AGACCCUAUUGGAGAGCGA

Table 1: siRNA list

2.5 LNA transfection

Locked Nucleic Acid (LNA) are nucleic acids analogues in which a bridge between the 2' oxygen and 4' carbon "locks" the ribose in an ideal conformation for Watson-Crick binding. This peculiarity makes LNA highly thermally stable and increases their binding affinity for a complementary sequence. For this reason, LNAs are used as Antisense Oligonucleotides (ASOs) that bind the target nucleic acids and inhibit their further processing and/or function. DR-GFP cells were transfected with 20 nM LNA oligos following the procedure already described for siRNA (see "RNA interference" section). Before transfection, LNA solution was incubated at 95°C for 5 minutes and chilled on ice for 5 minutes, to prevent the formation of secondary structures of the oligos. Concomitantly with LNA transfection, I-SceI expression was induced by adding doxycycline to the cell media. 72 h after the HR events were evaluated by amplification of the recombination products by PCR on genomic DNA (see section "DR-GFP reporter assay") and by monitoring the percentage of GFP positive cells by FACS analysis (see section "Fluorescence-activated cell sorting"). LNA sequences are listed in table 2.

2.6 Inhibition of RNA polymerase II transcription

In order to specifically inhibit RNA polymerase II (RNA pol II) transcription, HeLa and U2OS cells were treated with α-amanitin (50 μg/mL) or 5,6-dichloro-1-β-D-ribofuranosylbenzimidazole (DRB, 50 μM), respectively dissolved in deionized water and DMSO. α-amanitin is a toxin extracted from the mushroom *Amanita phalloides* that binds to RNA pol II, blocks RNA synthesis, and triggers RNA pol II degradation (Bushnell et al., 2002, Nguyen et al., 1996). DRB inhibits RNA pol II elongation by targeting CDK9 and inhibiting CDK9-mediated phosphorylation of RNA pol II C-terminal domain (CTD) during transcription.

Once the drugs were added, cells were irradiated and then fixed 6 hours later. For α-amanitin treatment, before adding the drug to the medium, cells were mildly permeabilized with 2% (HeLa cells) or 0.2% (U2OS cells) Tween 20 in PBS for 10 min at room temperature. RT-

qPCR analysis of the the levels of c-fos RNA, a short-lived RNA specifically transcribed by RNA pol II, was used to monitor the efficacy and specificity of the drugs.

Name	Sequence
CTRL	AGAGAAAAGTGAAAGTCGAGT
A1	TCGGGGTAGCGGCTGAAGCA
A2	CGCCGTAGGTCAGGGTGGTC
A3	GCCAGGGCACGGGCAGCTTG
A4	CCGGTGGTGCAGATGAACTT
A5	TCAGCTTGCCGTAGGTATTA
B1	GGATCCACCGGTCGCCAC
B2	AGCAAGGGCGAGGAGCTGTT
B3	ACCGGGGTGGTGCCCA
B4	GAGCTGGACGGCGACGTAAA
B5	TTCAGCGTGTCCGGCTAGGG
RA 1	TAATACCTACGGCAAGCTGA
RA 2	CTGAAGTTCATCTGCACCAC
RA 3	CAAGCTGCCCGTGCCCT
RA 4	TCGTGACCACCCTGACCTA
RA 5	TGCTTCAGCCGCTACCCCGA
RB 1	GGATCCACCGGTCGCCAC
RB 2	AGCAAGGGCGAGGAGCTGTT
RB 3	ACCGGGGTGGTGCCCA
RB 4	GAGCTGGACGGCGACGTAAA
RB 5	TTCAGCGTGTCCGGCTAGGG

Table 2: ASOs sequence

2.7 RNase A and RNase H treatment

U2OS cells were plated on coverslips and irradiated (2Gy). 1 hour later cells were permeabilized with 0.2% Tween 20 in PBS for 10 minutes at RT. After 2 washes in PBS, each coverslip was incubated for 30 minutes at RT with 0.1 mg RNase A (USB corporation) or 15 U RNase H (USB corporation) diluted in 200 µl PBS with 5 mM $MgCl_2$. Next, coverslips were washed twice in PBS and fixed and stained as described in the "immunofluorescence" section.

2.8 RNA extraction and retro-transcription

Total RNA from cultured cells was extracted with Maxwell® RSC simplyRNA Tissue Kit with the Maxwell® RSC Instrument (Promega), according to manufacturer instructions. 1 µg of RNA was retro-transcribed using SuperScript VILO cDNA Synthesis Kit (Life Technologies), according to manufacturer instructions, and used as template in qRT-PCR analysis.

2.9 Quantitative PCR (qPCR)

A SYBR-green based system was used to perform qPCR. SYBR-Green is a fluorescent dye that binds the double-stranded DNA species produced during the PCR reaction, generating a fluorescent signal that is detected in real time by the real time qPCR machine.

The low fluorescence detected during the initial PCR cycles defines the baseline fluorescence, above which a fixed fluorescence threshold is set. The cycle number at which the fluorescence is higher than the fixed threshold is the threshold cycle (Ct).

For knock-down experiments, usually 10 ng of cDNA was used for RT-qPCR. The relative change in the level of the target molecule was calculated using the comparative CT method (i.e. $2^{\Delta\Delta CT}$ method) (Livak, 2001). This method is based on the calculation of ΔCt between the target gene and reference (housekeeping) in the sample analysed (ΔCt_{sample}) and the control sample ($\Delta Ct_{control}$). $2^{\Delta\Delta Ct}$ (with $\Delta\Delta Ct = \Delta Ct_{sample} - \Delta Ct_{control}$) is the value indicating the level of expression of the target gene.

In case of ChIP and DRIP experiments, same volumes of immunoprecipitated chromatin were used for RT-qPCR analysis of different loci (see table 3 for primers). ChIP and DRIP data were normalized on the input.

SYBR-Green based RT-qPCR experiments were performed on a Roche LightCycler 480 machine using Roche SYBR and the following program:

1. Denaturation: 95°C 15 min, 1 cycle

2. Denaturation/Annealing/Extension: 95°C 15 sec > 60°C 20 sec > 72°C 30 sec, 50 cycles

3. Melting curve: 40°C > 90°C > 40°C, 1 cycle

NAME	SEQUENCE
qRT-PCR	
BRCA1_Fw	5'-ATCATTCACCCTTGGCACA-3'
BRCA1_Rev	5'-ATGGAAGCCATTGTCCTCT-3'
BRCA2_Fw (start)	5'-AGCTTACTCCGGCCAAAAA-3'
BRCA2_Rev (start)	5'-TTCCTCCAATGCTTGGTAAATAA-3'
BRCA2_Fw (middle)	5'-CCTGATGCCTGTACACCTCTT-3'
BRCA2_Rev (middle)	5'-GCAGGCCGAGTACTGTTAGC-3'
BRCA2_Fw (end)	5'-TCCAAATCAGGCCTTCTTACTT-3'
BRCA2_Rev (end)	5'-GCTTGTTTTCTGCTTCATTGC-3'
c-FOS_Fw	5'-ACTACCACTCACCCGCAGAC-3'
c-FOS_Rev	5'-CCAGGTCCGTGCAGAAGT-3'
CtIP_Fw	5'-GGAAGAAAATAAAAAGCTTTCTGAAC-3'
CtIP_Rev	5'-TGCTTGATGCTGTTGATCATT-3'
RAD51_Fw	5'-TGAGGGTACCTTTAGGCCAGA-3'
RAD51_Rev	5'-CACTGCCAGAGAGACCATACC-3'
RNase H2A_Fw	5'-GAGAAAGAGGCGGAAGATGTTA-3'
RNase H2A_Rev	5'-TCTTCCTGAGTCCCTCCTGA-3'
RPP0_Fw	5'-TTCATTGTGGGAGCAGAC-3'
RPP0_Rev	5'-CAGCAGTTTCTCCAGAGC-3'
ChIP qPCR	
Rev	5'-ATCACATGGTCCTGCTGGAGTT-3'
Fw	5'-TGGCTGATTATGATCTAGAGTCGCGG-3'

DRIP-qPCR	
DAB1_Right_1000_Fw	5’-TGGCCTCTAATGAGATGGAATCCC-3’
DAB1_Right_1000_Rev	5’-TTGGAGTCTAACAGCCCAGTCA-3’
DAB1_Right_1500_Fw	5’-GGTGATACTCACCACTATGCCT-3’
DAB1_Right_1500_Rev	5’-TCTGGGATGGGTGTTGAAGTGT-3’
DAB1_Right_2000_Fw	5’-TGC CTGTTTGCTTGATTTCCAC-3’
DAB1_Right_2000_Rev	5’-TGAGCTGGGGTCATGTTCTTGAG-3’
DAB1_Right_3000_Fw	5’-ATGCTGGTCCCATATAATCAGGC-3’
DAB1_Right_3000_Rev	5’-CTTCTGGGATTGTCTTGCTGGAGT-3’
DAB1_Right_3800_Fw	5’-GGCATTGTTCTGGGGATAAA-3’
DAB1_Right_3800_Rev	5’-TTGCCCAGGAGGTGACTC-3’
DAB1_Left_100_Fw	5’-TGTGCTCTTTCCACTGTGGT-3’
DAB1_Left_100_Rev	5’-ATCACACTCTGCCACGTATG-3’
DAB1_Left_1000_Fw	5’-GCAGCCACAATGGACTAAGA-3’
DAB1_Left_1000_Rev	5’-AGCCTTCAGTTCTGTTTCAC-3’
DAB1_Left_1500_Fw	5’-TTGCTCAGCTCTGCCCTCAAC-3’
DAB1_Left_1500_Rev	5’-AGTCAAGGCTAGGTGATTCC-3’
DAB1_Left_2000_Fw	5’-CCAACTTCTGTGCCTAGAAC-3’
DAB1_Left_2000_Rev	5’-GACTCCAGTGTGGCTAATC-3’
DAB1_Left_3000_Fw	5’-GCAGCCTAATTACTCATAGGG-3’
DAB1_Left_3000_Rev	5’-GCCTCCAAATTCTAGATCTC-3’
DAB1_Intergenic_Fw	5’-GATTCCACCAACCCCATTC-3’
DAB1_Intergenic_Rev	5’-GAGATTCCCACTGTCCCTAC-3’
AsiSI_Intergenic_Fw	5’-GCTGGAAGCTTCTGGAATCGTA-3’
AsiSI_Intergenic_Rev	5’-TTGTCAGTGCCCACCCTATGTT-3’
PCR	
ACTIN_Fw	5’-GATCATTGCTCCTCCTGAGC-3’
ACTIN_Rev	5’-AAAGCCATGCCAATCTCATC-3’
P1	5’-GAGGGCGAGGGCGATGCC-3’
P2	5’-TGCACGCTGCCGTCCTCG-3’
F1	5’-TTTGGCAAAGAATTCAGATCC-3’
F2	5’-CAAATGTGGTATGGCTGATTATG-3’

Table 3: primer list

2.10 Immunofluorescence and imaging analysis

Immunofluorescence technique was mainly used to study DDR foci formation. Cells grown on coverslips were washed twice for 5 minutes with PBS and fixed with 4% PFA for 10 minutes at RT. Then, cells were permeabilized with 0.2% Triton X-100 for 10 minutes at RT. In order to reduce the aspecific binding of the antibodies, 1 hour blocking in PBG (0.5% BSA, 0.2% gelatin from cold water fish skin in PBS 1X) was performed. After blocking, cells were stained with primary antibodies diluted in PBG for 1 hour at RT in a humidified chamber (primary antibodies used are listed in table 4). Next, cells were washed 3 times for 5 minutes with PBG and incubated with secondary antibodies conjugated with different sets of fluorophores diluted in PBG for 45 minutes at RT in a dark humidified chamber. Secondary antibodies used were: goat anti-rabbit or anti-mouse Alexa 405 IgG (Life Technologies, 1:100, excitation wavelength 401 nm, emission wavelength 421 nm); donkey anti-mouse or anti-rabbit Alexa 488 IgG (Life Technologies, 1:100, excitation wavelength 495 nm, emission wavelength 519 nm); donkey anti-mouse or anti-rabbit Cy3 IgG (Jackson Immuno Research, 1:400, excitation wavelength 550 nm, emission wavelength 570 nm), donkey anti-mouse or anti-rabbit Alexa 647 IgG (Life Technologies, 1:100, excitation wavelength 650 nm, emission wavelength 665 nm). After incubation with secondary antibodies, cells were washed twice for 5 minutes with PBG, twice for 5 minutes with PBS and incubated with 4'-6-Diamidino-2-phenylindole (DAPI, 1 μg/ml, Sigma-Aldrich, excitation wavelength 358 nm, emission wavelength 461 nm) for 2 minutes at RT. After DAPI staining, cells were washed once in PBS and once in water and coverslips were then mounted with mowiol mounting medium (Calbiochem), which is a polyvinyl alcohol solution containing an "anti-fade" agent, capable of reducing light-induced fading (photobleaching) of the fluorophore. Coverslips were air dried before microscope analysis.When ssDNA was visualized by BrdU native staining, cells were incubated with BrdU (Sigma-Aldrich, 10 μg/ml) for 24 h, in order to allow almost all the cells to incorporate the nucleotide analogue, and stained as described above.

For DNA:RNA hybrids detection, cells were fixed in ice-cold methanol for 10 minutes and then blocked and incubated with the S9.6 antibody (kind gift from M. Foiani) as described above.

Immunofluorescence images were acquired using a widefield Olympus Biosystems Microscope BX71 and the MetaMorph software (Soft Imaging System GmbH). Confocal sections were obtained with a Leica TCS SP2 or AOBS confocal laser microscope by sequential scanning. Comparative immunofluorescence analyses were performed in parallel with identical acquisition parameters. Images were analysed software CellProfiler 2.1.1. (Carpenter et al., 2006).

2.11 Super-Resolution (SR) imaging

SR experiments were performed on U2OS cells seeded on coverslips and synchronized as described in the section "Cell culture". Upon DNA damage induction, cells were pre-extracted at RT for 3 minutes in CSK buffer (10 mM Hepes, 300 mM Sucrose, 100 mM NaCl, 3 mM MgCl2, and 0.5% Triton X-100, pH = 7.4) and fixed for 15 minutes in paraformaldehyde (3.7% from 32% EM grade, Electron Microscopy Sciences, 15714) and glutaraldehyde (0.3% from 70% EM grade, Sigma-Aldrich, G7776) in PBS. Blocking was performed in blocking buffer (2% glycine, 2% BSA, 0.2% gelatin, and 50 mM NH4Cl in PBS) for 1 hour at RT. Primary and secondary antibodies used are listed in table 4. Immediately before imaging analysis, coverslips were mounted onto a microscope microfluidics chamber and freshly prepared SR imaging buffer, comprising an oxygen scavenging system (1 mg/mL glucose oxidase (SigmaAldrich, G2133), 0.02 mg/mL catalase (SigmaAldrich, C3155), and 10% glucose (SigmaAldrich, G8270) and 100 mM mercaptoethylamine (Fisher Scientific, BP2664100) in PBS, was added to the imaging chamber. Images were acquired with a custom-built SR microscope based on a Leica DMI 3000 inverted microscope. For each field 2000 sequential frames of single molecule emissions at 40 Hz were collected and imaged on a Prime 75B CMOS camera (Photometrics) using MicroManager. Each raw image stack was processed for single molecule localization

and rendered using 20 nm pixels via rapidSTORM. Monte Carlo simulations were used to randomly rearrange the clusters within an ROI to calculate a baseline level of random colocalization. Using this approach, 20 random simulations were generated for each nucleus in a pair-wise fashion, examining Red/Green, Red/Blue, and Green/Blue overlap. The total number of overlaps detected in each nucleus (typically 15-100) was normalized to the determined random level of overlap by dividing the number of real overlaps by the average number of overlaps in the same randomly-simulated nucleus. For display purposes, images were smoothed by applying a Gaussian blur filter and colors were thresholded to best produce a clear picture of the single foci.

2.12 Proximity Ligation Assay (PLA)

Proximity Ligation Assay (PLA) is a technique that can be used to assess the proximity (<40nm) of two candidate proteins by using DNA oligonucleotide conjugated-antibodies (PLA probes). Briefly, once epitopes have been recognized by primary antibodies raised in different species, DNA oligonucleotide-conjugated secondary antibodies are added. Ligation of the antibodies-conjugated oligos with connector oligonucleotides allows the formation of a close DNA circle. In the following amplification step, one of the two oligos is used as primer for a rolling circle amplification (RCA). Fluorescent-tagged oligonucleotides complementary to the amplified DNA allow the visualization of the signal with a fluorescence microscope. Duolink in Situ FarRed Starter Kit Mouse/Rabbit (Sigma-Aldrich) was used according to the manufacturer's instructions.

Briefly, cells were fixed in 4%, permeabilized in 0.2% Triton-X 100, and blocked in PBG1X, as described in the section "immunofluoresce and imaging analysis". Incubation with primary antibodies was performed overnight at 4°C. After washing the primary antibodies (3 times in PBG1X), cells were incubated with PLA probes for 1 h at 37°C in a humid chamber. Cells were washed twice in Buffer A (supplied with the kit) and the ligation reaction was carried out at 37°C for 30 min in a darkened humidified chamber. After washing with Buffer A, cells were incubated with the amplification mix for 1.5 hours at 37°C in a

darkened humidified chamber. After washing with Buffer B (supplied with the kit), cells were incubated with DAPI 0.2 µg/mL (Sigma-Aldrich) and mounted. Images were acquired using a widefield epifluorescent microscope (Olympus IX71) equipped with 40X objective. Quantification of nuclear PLA dots was performed with the automated image-analysis software CellProfiler 2.1.1. (Carpenter et al., 2006).

Antibody	Company and product ID	Host	Applications			
			IF	PLA	WB	ChiP
BRCA1	Santa Cruz, D-9	Mouse	1:400			2 µg/IP
BRCA2	Calbiochem, OP-95	Mouse	1:400		1:1000	
BrdU	GE Healthcare, RPN202	Mouse	1:800			
CENP-F	Abcam, ab-5	Rabbit	1:400			
Cyclin A	Santa Cruz, sc-751	Rabbit	1:200		1:1000	
Cyclin A	BD transduction laboratories, 611268	Mouse	1:400			
CtIP	Bethyl, A300-488A	Rabbit			1:6000	
PALB2	Gift of Xia Bing	Rabbit				
RAD51	Abcam, Ab213	Mouse	1:200			
RAD51	Santa Cruz, sc-8349	Rabbit				1 µg/IP
RAP80	Novus biological,NBP1-87156	Rabbit			1:6000	
RPA	Calbiochem, NA18	Mouse	1:1000		1:1000	
RPA P-S4/8	Bethyl, A300-245A	Rabbit	1:2000		1:2000	
RNase H1	Novus biological, NBP2-20171	Rabbit			1:1000	
RNase H2A (ab-1)	Abcam, ab83943	Rabbit	1:1000	1:1000	1:1000	
RNase H2A (ab-2)	Proteintech, 16132-1-AP	Rabbit	1:1000	1:1000	1:1000	
RNase H2B	Proteintech	Rabbit	1:1000	1:1000	1:1000	
RNase H2C	Proteintech	Rabbit	1:1000	1:1000	1:1000	
S9.6	From M. Foiani's lab	Mouse	1:500			
Tubulin	Sigma-aldrich T5168	Mouse			1:5000	
Vinculin	Sigma-aldrich V9131	Mouse			1:5000	

γH2AX	Millipore 05-636	Mouse	1:1000	1:1000		
γH2AX	Abcam, ab2893	Rabbit	1:1000			

Table 4: Antibodies list

2.13 DR-GFP reporter assay

TRI-DR-U2OS cells were used to study homologous recombination. I-SceI expression was induced by adding 5 μg/ml Doxycycline. 72 h after induction, the HR efficiency was determined by quantifying GFP-positive cells (product of successful HR) by flow cytometry, as described in the section "Fluorescence-activated cell sorting (FACS)". A PCR method was also used to monitor HR and SSA. DNA was extracted with the DNeasy Blood & Tisue Kit (Qiagen) and PCR was performed with the GoTaq® DNA Polymerase (Promega). HR was monitored by measuring the intensity of the amplicon generated by the primers P1 and P2 (Weinstock et al., 2006). SSA was monitored by measuring the intensity of the amplicon generated by amplification with primer F and R2 (Ochs et al., 2016, Weinstock et al., 2006). Both the measurements were normalized on the actin amplicon. Sequences of the primers are listed in table 3. Amplifications were performed using the following program and were determined to be in the linear range.:

For P1-P2 primers (443-bp amplified fragment): 98 °C /5 min × 1 cycle; 98 °C /45 s, 70 °C /30 s, and 72 °C /30 s × 30 cycles; 72 °C/10 min × 1 cycle.

For F-R2 primers: 98 °C /45 s × 1 cycle; 98 °C /10 s, and 50°C /30 s, 72 °C /60 s × 25 cycles; 72 °C/2 min × 1 cycle.

For Actin primers: 95 °C /5 min × 1 cycle; 95 °C /30 s, 62°C /30 s, and 72°C /30 s × 25 cycles; 72 °C/10 min × 1 cycle.

10 μl of the PCR products was loaded on a 1% agarose gel and visualized by Gel Red staining. Images were acquired with Chemidoc imaging system (Bio-Rad) and densitometric analysis was performed using the Image Lab 5.2 software.

2.14 Immunoblotting

Cells were lysed in Laemmli sample buffer (2% sodium dodecyl sulphate (SDS), 10% glycerol, 60 mM Tris HCl pH 6.8). SDS is an anionic detergent that denatures proteins secondary and tertiary structures and confers a uniform negative charge to the polypeptide allowing electrophoretic separation of the proteins based on the molecular weight. Protein concentration was determined by the biochemical Lowry protein assay and the desired amount of protein was mixed with bromophenol blue, a dye that allows proteins tracking during electrophoresis. Disulfide linkages were reduced by adding Dithiothreitol (DTT) and proteins were further denatured by heating at 95°C for 5 minutes. Usually, 30/50 μg of whole cell extracts were resolved by SDS polyacrylamide gel electrophoresis (SDS-PAGE). Next, proteins were transferred on a nitrocellulose membrane (0,45mm) (400mA; 1h) in transfer buffer (25 mM Tris HCl, 0.2 M Glycine, 20% methanol). Transfer efficiency was checked by temporary staining with Ponceau. After blocking with 5% skim milk in TBS-T buffer (Tween20 0.1%) for 1 hour at RT, membranes were incubated overnight at 4^{o}C with primary antibodies diluted in in 5% milk in TBS-T (see table 4). Next, membranes were washed with TBS-T 3 times for 10 minutes and incubated with secondary horseradish peroxidase (HRP)-conjugated antibodies (Bio-rad) diluted in 5% milk in TBS-T. After 3 more washes with TBS-T, HRP activity was detected using a Chemidoc imaging system (Bio-Rad) machine after adding the substrate for the enhanced chemiluminescent reaction ECL (GE Healthcare).

2.15 Immunoprecipitation

HEK293T cells were collected and lysed in TEB150 lysis buffer (50 mM HEPES pH 7.4, 150 mM NaCl, 2 mM $MgCl_2$, 5 mM EGTA pH 8, 1 mM dithiothreitol (DTT), 0.5% Triton X-100, 10% glycerol, protease inhibitor cocktail set III (Calbiochem) and Benzonase 1:1000 (Sigma) for 45 minutes at 4^{o}C. Next, samples were centrifuged for 15 minutes at $16x10^{3}$ g at 4^{o}C and supernatant were collected. Protein concentration was determined by using the Bradford assay (Bio-rad). Usually, 1mg of the protein lysate was used per each immunoprecipitation in a reaction volume of 500 μl. As input, 1% of the immnoprecipitation

reaction was collected and denatured in the sample buffer (50 mM Tris-HCl pH 6.8; 2% SDS; 10% glycerol; 12.5 mM EDTA; 0,02 % bromophenol blue; 100 μM DTT) for 10 minutes at 95°C. Unspecific binding of proteins to the beads was reduced by incubating samples with Protein G beads (50 μl) (Zymed Laboratories) for 1 hour at 4°C (pre-clearing). Pre-cleared samples were incubated with the indicated antibodies (see table 4) overnight at 4°C. Next, samples were incubated with 40 μl of Protein G beads for 2h in order to allow antibodies binding to the beads. After 3-6 washes with lysis buffer, immunoprecipitated proteins were released by the addition of sample buffer and incubation at 95°C for 10 minutes.

2.16 Purification of Glutathione S-transferase (GST)-tagged proteins

Purification of GST-tagged proteins exploits the affinity of GST for the glutathione ligand coupled to a matrix, a sepharose one for our experiments. GST-RAD51 fragments (Buisson et al., 2010) were transformed in *Esherichia Coli* BL21 and protein expression was induced with isopropyl β-D-1-thiogalactopyranoside (IPTG) (0,4 mM) during bacterial exponential growth phase (cell density 0,6-0,8 at 600nm). Upon induction, bacteria were incubated overnight at 20°C. Next, bacteria were collected by centrifugation for 25 minutes at 4°C and resuspended in lysis buffer (50mM Tris-HCl pH 7,9, 300mM KCl, 1% Triton X-100, 2mM DTT and protease inhibitor cocktail set III (Calbiochem) 1:200). Cells were sonicated 3 times for 20 seconds at the amplitude of 5 impulses and power of 75%. After centrifugation at $20x10^3$g at 4°C for 90 minutes, supernatants were collected and incubated with glutathione sepharose beads (GE Healthcare) for 2 hours at 4°C. Next, lysates were washed for 30 minutes at 4°C with Buffer I (PBS, 1% Triton X-100, 2mM DTT and protease inhibitor cocktail set III (Calbiochem) 1:200), Buffer II (300mM KCl, 50mM Tris-HCl pH 8, 2mM DTT and protease inhibitor cocktail set III (Calbiochem) 1:200) and Buffer III (100mM KCl, 50mM Tris-HCl pH 8, 2mM DTT, 10% glycerol and protease inhibitor cocktail set III (Calbiochem) 1:200). Next, sepharose-bound proteins were aliquoted, flash-frozen in liquid nitrogen, and stored until use.

2.17 GST-pulldown

GST-RAD51 fragments bound to sepharose beads, generated as described in section "Purification of Glutathione S-transferase (GST)-tagged proteins purification", were used for GST-pulldowns. 1-2µg of recombinant HEK293T cells were transfected with RNase H2A-YFP construct (see section "plasmid transfection") and subsequently lysed in TEB150 buffer. Next, purified GST-RAD51 fragments were incubated with 1 mg of HEK293T cell lysate for 2h at 4°C. After incubation, beads were washed 4 times with TEB150 buffer, then resuspended in sample buffer and subjected to immunoblot analysis.

2.18 Chromatin Immunoprecipitation (ChIP)

Cells were cross-linked for 5.5 minutes at room temperature with Fixation Buffer (1% formaldehyde; 100 mM NaCl; 1 mM EDTA; 0.5 mM EGTA; 50 mM HEPES pH 7.4). Cross-linking was quenched by addition of glycine (125 mM). Fixed cells were rinsed twice in 1X PBS, collected by scraping and centrifuged at 2000 rpm for 5 min at 4°C. Pellets were re-suspended in cold B1 Buffer (0.25% Triton X-100; 1 mM EDTA; 0.5 mM EGTA; 10 mM Tris pH 8; Proteases inhibitors (Roche); Microcystin (Enzo Life Sciences)) by mixing for 10 minutes on a rotating wheel at 4°C and then centrifuged at 2000 rpm for 5 minutes at 4°C. The same steps were repeated with cold Buffer B2 (200 mM NaCl; 1 mM EDTA; 0.5 mM EGTA; 10 mM Tris pH 8; Proteases inhibitors (Roche); Microcystin (Enzo Life Sciences)). Finally, pellets were re-suspended in a suitable volume of cold Buffer B3 (TE 1X; EGTA 0.5 mM). Pellets were sonicated using a Focused- Ultrasonicator Covaris (duty: 5.0; PIP: 140; cycles: 200; amplitude: 0; velocity: 0; dwell: 0; microTUBEs with AFA fiber). Sonicated chromatin was diluted in RIPA buffer (1% TritonX-100; 0,1% Na- Deoxycholate; 0,1% SDS; 64 mM NaCl; 10 mM Tris HCl pH 8.0). Samples were pre-cleared for 2 hours on rotating wheel at 4°C by incubation with 20 µl of magnetic beads (Dynabeads® Protein G, LifeTechnologies). Sample were then incubated overnight rotating at 4°C with specific antibodies (see table 4) or no antibody (mock). The bound material was recovered by 2 hours incubation with 20 µl of magnetic beads per ChIP. Beads were then washed, rotating at 4°C

for 10 min, four times in RIPA buffer, once in LiCl buffer (250 mM LiCl; 0.5% NP-40; 0.5% Na Deoxycholate; 1 mM EDTA; 10 mM Tris-HCl pH 8) and finally in 1X TE. ChIPed material was eluted by 15 min incubation at 65°C with 150 µl Elution Buffer (1% SDS; 10 mM EDTA; 50 mM Tris HCl pH 8). Samples were reverse-crosslinked by incubation with proteinase K (Invitrogen) at 37°C for 5 hours and then at 65°C overnight. DNA was cleaned up by QIAquick PCR purification column (Qiagen) according to the manufacturer's instructions and eluted in 30 ul of elution buffer (EB).

2.19 DNA:RNA hybrids immunoprecipitation (DRIP)

DRIP is a technique used to detect and map DNA:RNA hybrids. 5×10^6 HeLa cells were collected, washed with cold PBS, resuspended in 1.6 ml of Tris-EDTA (TE) buffer and incubated overnight with 41.5 ul of 20% SDS and 5 ul of proteinase K (Roche) at 37°C. DNA was extracted gently with phenol–chloroform. Briefly, after adding one volume of phenol-chloroform, samples were centrifuged at maximum speed for 10 minutes and the upper layer containing nucleic acids was precipitated by adding 1/10 volume of sodium acetate, 2.4 volumes of ethanol and 1 ul of glycogen. After 1 hour centrifugation at maximum speed at 4°C, pellets were washed twice with 70% ethanol, gently resuspended in TE1X and digested overnight with 50 U of *Hind*III, *Eco*RI, *Bsr*GI, *Xba*I and *Ssp*I, 2 mM spermidine and BSA. After checking digestion, the nucleic acids were purified again with phenol–chloroform extraction and next, as negative control, half of the DNA was treated overnight with RNase H (M0297; New England BioLabs). In the meantime, serum-free medium containing the S9.6 antibody was mixed with protein A and protein G Dynabeads (Invitrogen) at 4°C ON.

Samples were purified again with phenol-chloroform extraction and 4 ug of DNA was used for each IP in 450 ul of TE1X and 51 ul of 10X binding buffer (10 mM NaPO4, 140 mM NaCl, 0.05% Triton X-100). Samples were incubated with the antibody overnight on a rotating wheel at 4°C. DNA–antibody complexes were washed twice with binding buffer

1X. DNA was eluted with 50 mM Tris-HCl pH 8.0, 10 mM EDTA, 0.5% SDS, then treated for 45 min with 10 ul of proteinase K at 55 °C and cleaned up with QIAquick PCR purification column (Qiagen) according to the manufacturer's instructions. The indicated regions were amplified by RT-qPCR (see table 3 for primers sequence). The signal intensity plotted is the relative abundance of DNA–RNA hybrid immunoprecipitated in each region, normalized to input values.

2.20 Fluorescence-activated cell sorting (FACS)

For GFP analysis, 10^6 cells were fixed in 1% formaldehyde for 20 minutes on ice. Next, cells were washed in PBS 1% BSA and fixed in 75% ethanol. Fixed cells were washed again in PBS 1% BSA and stained with Propidium Iodide (PI) (Sigma-Aldrich, 50 μg/ml) in PBS supplemented with RNase A (Sigma-Aldrich, 250 μg/ml).

For cell cycle analysis, 10^6 cells were directly fixed in 75% ethanol, as described above. Samples were acquired on an Attune NxT machine and analyzed with FlowJo_V10 software. At least 10^4 events were analyzed per sample.

For sorting of HeLa-FUCCI cells, cells were collected in PBS with 2% FBS and the G1 and S/G2 population were sorted with a MofloAstrios (Beckman Coulter) in PBS supplemented with RNaseOUT (Thermo Fisher). Sorted samples were processed for DRIP as described in the section "DNA:RNA hybrids immunoprecipitation (DRIP)".

2.21 Electrophoretic mobility shift assay

Recombinant BRCA1 and BARD1 were expressed and purified as a complex in insect cells by co- infection with baculoviruses. The 50 bp-long dsDNA substrate was prepared by annealing oligonucleotides X12-3 (5' GACGTCATAGACGATTACATTGCTAGGACATGCTGTCTAGAGACTATCGC3') and X12-4C (5' GCGATAGTCTCTAGACAGCATGTCCTAGCAATGTAATCGTCTATGACGTC 3') as previously described (Cejka and Kowalczykowski, 2010). The 50 bp-long DNA:RNA hybrid substrate was prepared by annealing X12-3 DNA and X12-4C RNA. Proteins were

incubated for 30 minutes at 37º C with 10 nM dsDNA or DNA:RNA hybrid substrate in a reaction buffer containing Tris HCl (pH 7.5), 25 mM; KCl, 90 mM; EDTA (ph 8.0), 1 mM; DTT, 1 mM; BSA (NEB), 0.1 mg/mL; RNaseOUT (Invitrogen), 1X. Loading dye (5 µL; 50% glycerol; Tris HCl (pH 7.5), 20 mM; EDTA, 0.5 mM; bromophenol blue) was added to reactions and products were separated by 6% non-denaturing polyacrylamide gel electrophoresis at 4 C. The gels were dried on 17CHR filter paper (Whatman), exposed to storage phosphor screens, and scanned by a Typhoon Phosphor imager (FLA 9500, GE Healthcare). Quantification of protein-bound substrates was done using Imagequant software.

2.22 Statistical analysis

Statistical analysis was performed with the unpaired two tailed Student's t-test and represented as a mean ±SEM. Asterisk in the figures indicates p value <0.05.

3 Results

3.1 DNA:RNA hybrids are produced at DSBs

We recently reported that RNA polymerase II (RNA pol II) is recruited to DSBs where it transcribes long non-coding RNA species, named dilncRNAs (Michelini et al., in press). Here, I wanted to investigate whether dilncRNAs generated at DSBs could form DNA:RNA hybrids and study the potential role of these hybrids in DSB repair modulation. In order to address this, I performed DNA:RNA hybrids immunoprecipitation (DRIP) followed by quantitative PCR (DRIP-qPCR) by the use of the S9.6 antibody, which specifically recognizes DNA:RNA hybrids. I transfected HeLa cells with the I-PpoI nuclease (Pankotai et al., 2012) and I monitored by DRIP-qPCR the formation of DNA:RNA hybrids upon damage at the I-PpoI site within the DAB1 gene, which is efficiently cut and very weakly transcribed in untreated HeLa cells. I observed that DSB generation induced the formation of DNA:RNA hybrids, within 2-4 Kb from the DSB, at both the left (figure 6b) and the right (figure 6c) sides of the DSB. As a specificity control, the observed signal is lost upon *in vitro* treatment with RNase H.

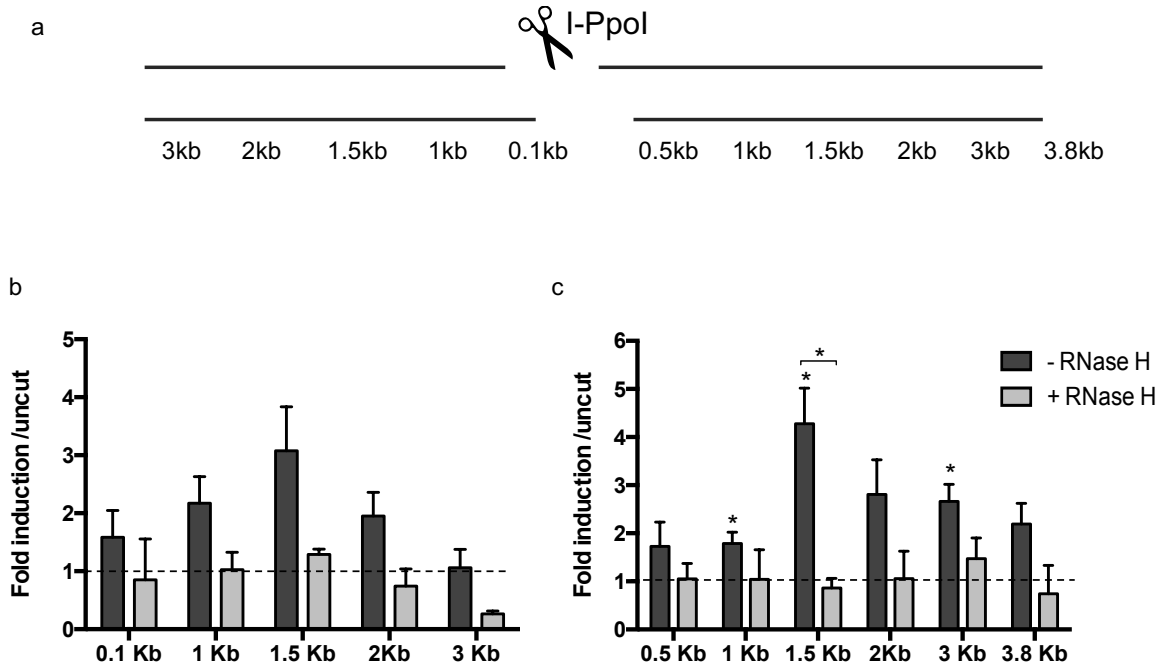

Figure 6: DNA:RNA hybrids formation at the I-PpoI cleavage site within the DAB1 gene
a) Schematic representation of the loci within the DAB1 gene tested for DNA:RNA hybrids formation upon I-PpoI-mediated DSB generation b) DRIP-qPCR with the S9.6 antibody was used to monitor DNA:RNA hybrids accumulation in HeLa cells transfected with the nuclease I-PpoI at either the left (b) or the right (c) side of I-PpoI cleavage site in DAB1 gene. The bar graph represents fold induction of cut samples relative to uncut. RNase H treatment (RH) was performed on cut samples to show specificity of the signal. Error bars represent s.e.m of 3 biological replicates.

Moreover, in order to exclude any contribution of pre-existing genic transcription, damage-induced DNA:RNA hybrids formation was determined by DRIP-qPCR also at a distinct intergenic site cut by I-PpoI (figure 7), thus ruling out the possibility that DNA:RNA hybrids formation is the result of the annealing of a pre-existing transcript to the template genomic DNA.

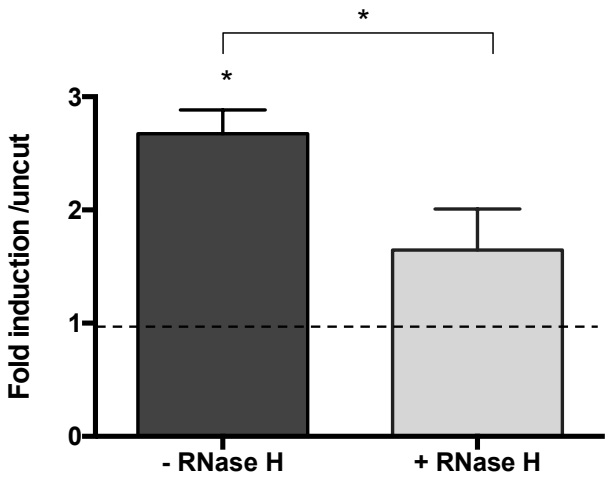

Figure 7: DNA:RNA hybrids formation at an intergenic I-PpoI cleavage site
HeLa cells were transfected with the nuclease I-PpoI and DNA:RNA hybrids accumulation was monitored by DRIP-qPCR with the S9.6 antibody at an intergenic I-PpoI cleavage site. The bar graph represents fold induction of cut samples relative to uncut. RNase H treatment (RH) was performed on cut samples to show specificity of the signal. Error bars represent s.e.m of 3 biological replicates.

To further strengthen these results, we exploited the DIvA (DSB inducible via AsiSI) cellular system, a clonal U2OS cell line that stably expresses the AsiSI restriction enzyme fused to a modified oestrogen receptor (ER) hormone-binding domain responsive to 4-hydroxy tamoxifen (4OHT) (Iacovoni et al., 2010). Upon treatment with 4OHT, AsiSI-ER enzyme translocates to the nucleus and generates DSBs at multiple genomic loci (Iannelli et al., 2017). Only 10 to 20% of the genomic AsiSI sites are cut and the cleavage efficiency for each site is heterogeneous and generally lower than 50% (Iacovoni et al., 2010). DSBs generation upon treatment of DIva cells with 4OHT is demonstrated by representative images (figure 8a) and relative quantification (figure 8b) of immunofluorescence staining of the DDR marker γH2AX. All the quantifications of the "number of foci per cell" shown are generated with the automated software CellProfiler (Carpenter et al., 2006), applying an ad

hoc designed pipeline which recognizes and counts the number of foci in each nucleus, according to their size and fluorescence intensity compared to the background signal.

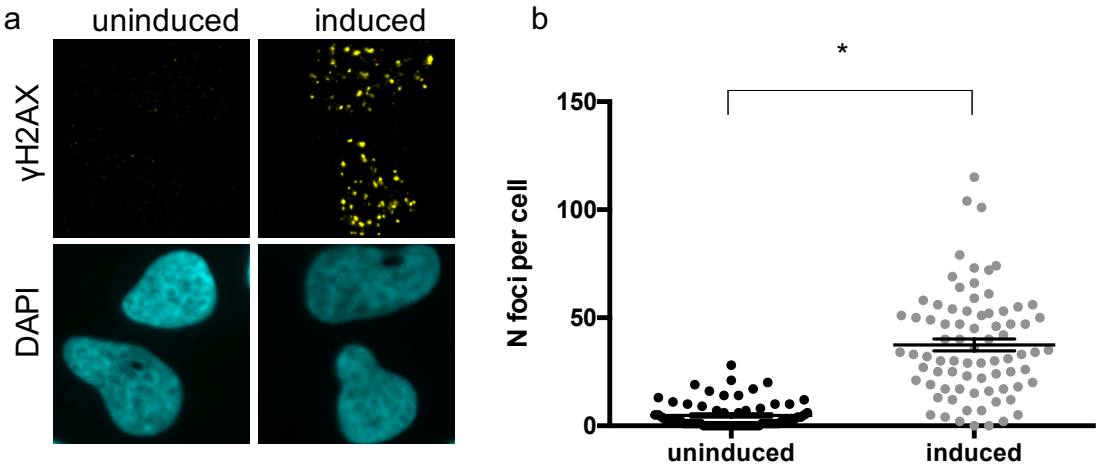

Figure 8: Treatment of DIvA cells with 4OHT induces DSBs generation
Treatment of DIvA cells with 4OHT induces AsiSI-ER nuclear localization and DSB generation. a) Representative images of DIvA cells co-stained with γH2AX and DAPI before and after 4 hours treatment with 4OHT. b) Dot plots show the number of γH2AX foci measured using Cell Profiler software. Error bars indicate s.e.m. (n = 2).

By exploiting DIvA cells, I observed DNA:RNA hybrids accumulation at non-genic DSBs (figure 9), thus confirming my results also in an unrelated cellular system at an additional genomic site. In particular, the detection of damage-induced DNA:RNA hybrids at non-genic sites confirms that DNA:RNA hybrids formation upon damage is the result of *de novo* transcription.

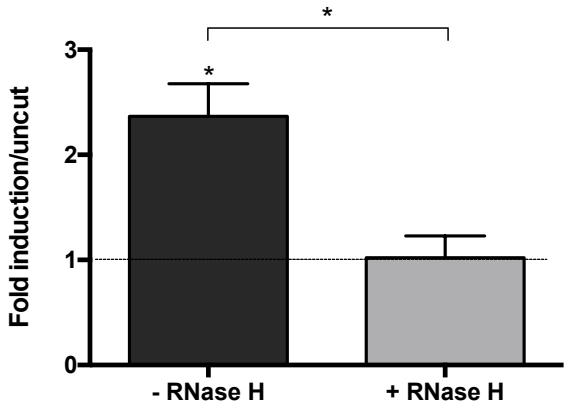

Figure 9: DNA:RNA hybrids formation at an intergenic AsiSI cleavage site
DNA:RNA hybrids accumulation was monitored by DRIP-qPCR with the S9.6 antibody in DivA cells before and after 4 hours treatment with 4OHT. DNA:RNA hybrids formation is shown at a non-genic AsiSI-ER induced DSBs. The bar graph represents fold induction of cut sample relative to uncut. RNase H treatment (RH) was performed on cut samples to show specificity of the signal. Error bars represent s.e.m of 3 biological replicates.

Next, I attempted to recapitulate my results with imaging techniques in other cellular systems. First, I studied DNA:RNA hybrids formation at a specific locus in U2OS19 cells, a human cell line carrying an integrated plasmid containing an array of Lac- and Tet-operator sequences flanking the I-SceI endonuclease target site (Lemaitre et al., 2014). Binding of the fluorescently-tagged Lac or Tet repressor protein to the operator sequences and expression of the I-SceI nuclease allows visualization of the DSB site in the nucleus (figure 10a). I induced I-SceI expression in U2OS19 cells and I immunostained for γH2AX and DNA:RNA hybrids with the S9.6 antibody. As shown in figure 10b, upon I-SceI expression, γH2AX signal is observed at the DSB detected by focal accumulation of Cherry-LacR proteins. Moreover, 70% of the sites that are efficiently cut, as monitored by γH2AX signal, accumulate DNA:RNA hybrids (figure 10b).

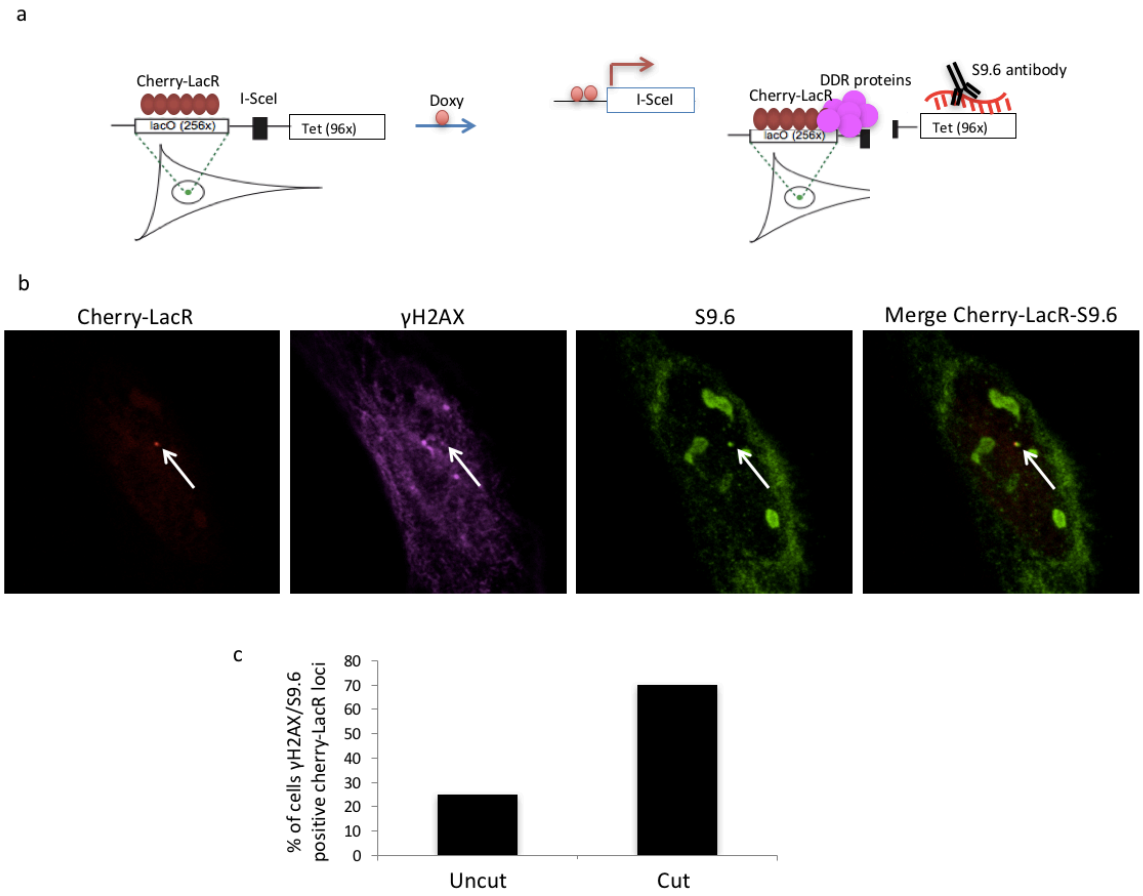

Figure 10: Immunofluorescence with the S9.6 antibody shows DNA:RNA hybrids formation at a site specific DSB

a) Schematic representation of the U2OS19 cellular system. U2OS19 cells contain an array of Lac and Tet repeats flanking the I-SceI recognition site. Expression of I-SceI and of a fluorescently tagged Lac repressor protein (cherry-LacR) allows DSB visualization in the nucleus. b) representative images of γH2AX and S9.6 staining in U2OS19 cells. c) Bar graph represent the % of colocalization of γH2AX and S9.6 with cherry-LacR (n=1)

I also monitored DNA:RNA hybrids accumulation upon DSB induction by using RNH1(D210N)-GFP, a cellular system developed in Pavel Jansak's lab, in Zurich. RNH1(D210N)-GFP cells express a catalytically inactive RNase H1 that binds DNA:RNA hybrids but does not cut them, and it is therefore a useful tool for their detection. Moreover, endogenous RNase H1 levels are partially reduced by inducible expression of an shRNA against it. Upon irradiation, RNH1(D210N)-GFP cells accumulate γH2AX foci (figure 11a) and DNA:RNA hybrids, as detected by the increase in the GFP dotted pattern (figure 11a and b), thus confirming the results obtained with the other cellular systems.

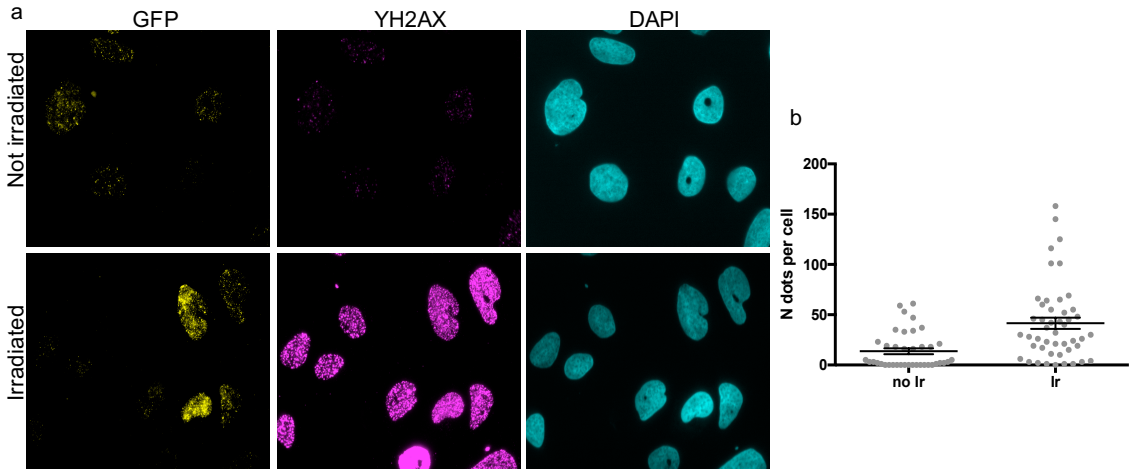

Figure 11: DNA:RNA hybrids form upon IR
a) Representative images of γH2AX and GFP signal in RNH1(D210N)-GFP cells exposed or not to IR. b) dot plots represents the number of GFP foci per cell. Error bars represent the s.d. of 1 single experiment.

Since dilncRNA production was shown to be dependent on RNA pol II (Michelini et al., in press), I next monitored whether treatment with the RNA pol II inhibitor 5,6-dichloro-1-β-D-ribofuranosylbenzimidazole (DRB) affected DNA:RNA hybrids generation. To test this hypothesis, I performed DRIP-qPCR at the I-PpoI cleavage site within the DAB1 gene in HeLa cells treated with DRB or with vehicle prior to DSB induction. While DNA:RNA hybrids formed upon damage in vehicle-treated cells, they did not accumulate at the damaged locus when RNA pol II activity was inhibited by treatment with DRB (figure 12), thus confirming that DNA:RNA hybrids formation upon damage requires RNA pol II activity.

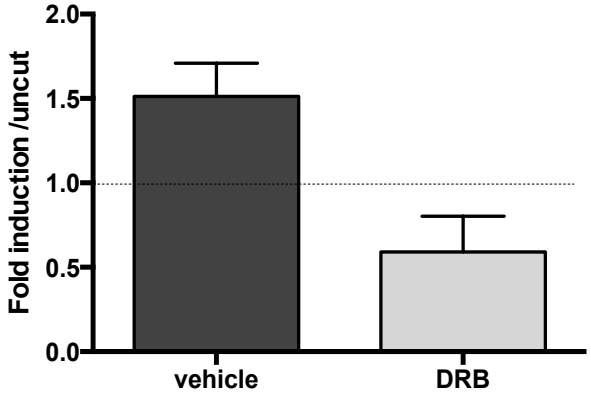

Figure 12: DNA:RNA hybrids formation depends on RNA pol II activity
HeLa cells were treated with DMSO or DRB for 2 hours and next I-PpoI induction was induced for 1.5 hours. DNA:RNA hybrids accumulation was measured by DRIP-qPCR with the S9.6 antibody at the I-PpoI cleavage site within the DAB1 gene. The bar graph represents fold induction of cut samples relative to uncut. Error bars represent s.e.m of 3 biological replicate.

Altogether these results show, in different cellular systems and by different techniques, that DNA:RNA hybrids accumulate at DSBs and that their formation is dependent on RNA pol II transcription.

3.1.1 Damage-induced DNA:RNA hybrids form preferentially during the S/G2 cell cycle phase

Once established that DNA:RNA hybrids are formed at DSBs in different cellular systems and at different genomic locations, I wanted to test whether DNA:RNA hybrids form preferentially during a specific cell-cycle phase. For this purpose, I took advantage of HeLa cells expressing the fluorescent ubiquitination-based cell cycle indicator (FUCCI) (Sakaue-Sawano et al., 2008). The FUCCI sensor consists of a fluorescent protein-based system that employs a green (GFP) and a red (RFP) fluorescent protein, respectively fused to the cell cycle regulators GEMININ and CDT1. Temporal regulation of GEMININ and CDT1 ubiquitylation determines their selective proteasomal degradation. Therefore, nuclei appear red when GEMININ-GFP is degraded (G1 phase) and green when CDT1-RFP is degraded (S/G2 phase). I sorted the G1 and S/G2 populations and I monitored in each one of them the accumulation of DNA:RNA hybrids at the I-PpoI cleavage site within the DAB1 gene. I observed that upon DSB induction, DNA:RNA hybrids accumulate preferentially in the

S/G2 phase of the cell cycle (figure 13). The complete loss of signal upon *in vitro* treatment with RNase H demonstrates its specificity.

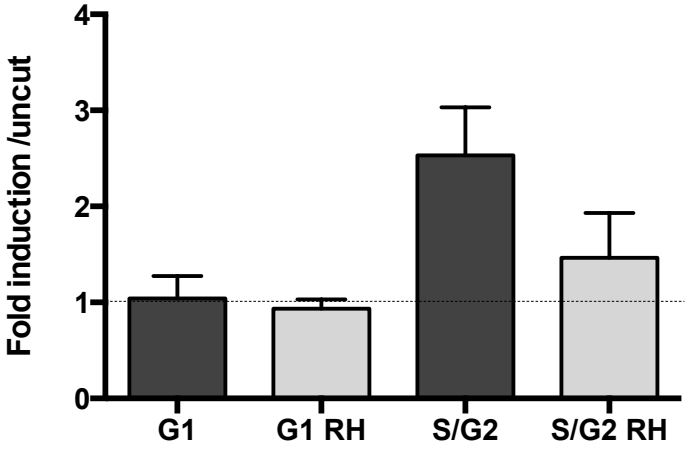

Figure 13: DNA:RNA hybrids form preferentially during S/G2 cell cycle phase
G1 and S/G2 phase I-PpoI transfected HeLa-FUCCI cells were sorted and DRIP-qPCR analysis was performed with the S9.6 antibody. The bar graph represents fold induction of cut samples relative to uncut. RNase H treatment (RH) was performed on cut G1 and S/G2 samples to show specificity of the signal. Error bars represent s.e.m of 3 biological replicate.

Next, I tried to recapitulate this result at the site-specific DSB inducible in U2OS19 cells as described above. As already mentioned, U2OS19 cells contain an array of Lac and Tet repeats flanking the I-SceI target site. Accumulation of a fluorescently-tagged Lac repressor protein and I-SceI expression allows DSB site visualization. Since the S9.6 staining could not be coupled with staining for cyclin A, which is the marker of S/G2 phase cells, I used as a tool for DNA:RNA hybrids detection the HB-GFP, which is the GFP-tagged DNA–RNA hybrid-binding (HB) domain of the RNase H1, that only binds DNA:RNA hybrids but does not cut them (Bhatia et al., 2014). I induced I-SceI expression in U2OS19 cells transfected with HB-GFP and I immunostained for γH2AX and cyclin A, to detect S/G2 phase cells. As shown in figure 14, DNA:RNA hybrids levels at the locus studied decrease upon damage in G1 phase cells, while they increase in S/G2 cells, thus confirming DNA:RNA hybrids accumulation at DSBs specifically in S/G2 phase cells.

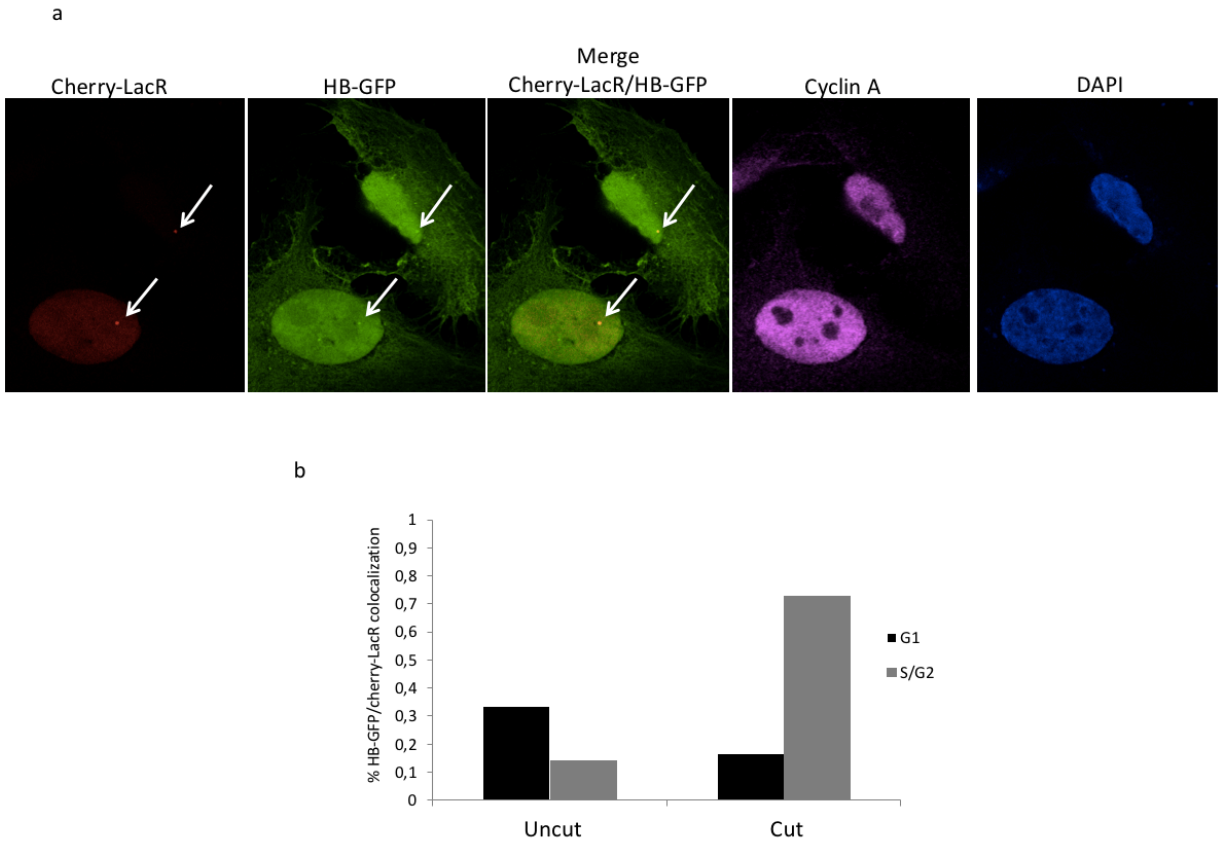

Figure 14: Imaging analysis confirms DNA:RNA hybrids formation at a site-specific DSB in S/G2 phase cells
a) Representative images of cherry-LacR and HB-GFP fluorescent signal and cyclin A staining of U2OS19 cells. b) Bar graph represent the % of colocalization of HB-GFP with cherry-LacR (n=1)

In order to strengthen these results, we established a collaboration with Eli Rothenberg's group at NYU and his postdoc Donna Whelan, who performed super-resolution imaging analysis on G1- and S/G2-synchronized U2OS cells treated with the radiomimetic drug Neocarzinostatin (NCS), which generates DSBs by free radical attack on DNA. We monitored the colocalization of DNA:RNA hybrids, visualized with the S9.6 antibody, with the DSB marker γH2AX in G1 and S phase NCS-treated U2OS cells. An increase in the colocalization events in S phase cells compared to G1 phase cells was observed (figure 15).

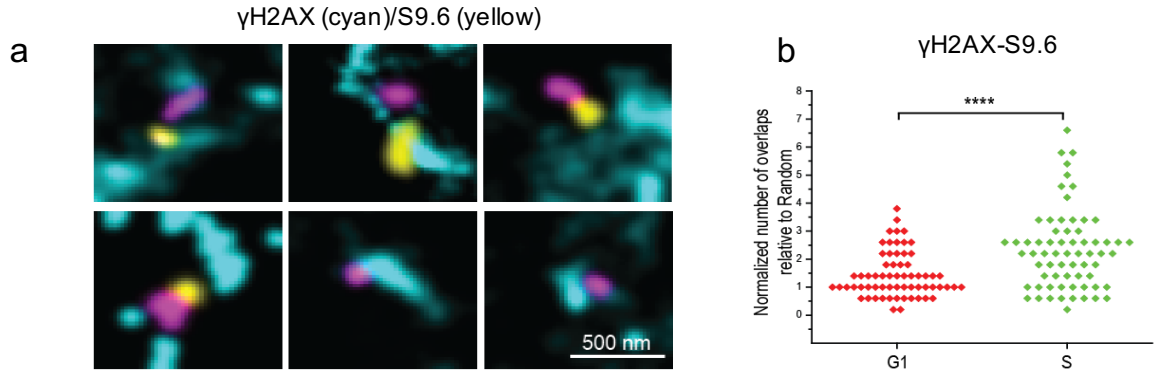

Figure 15: DNA:RNA hybrids and γH2AX colocalize preferentially in NCS-treated S phase cells
a) Representative images of γH2AX (cyan) –DNA:RNA hybrids (magenta) colocalization in NCS treated S phase U2OS cells. b) dot plot represents the number of γH2AX and DNA:RNA hybrids colocalization in G1 and S phase cells relative to random (>50 cells, n=3).

Next, under the same super-resolution settings, DNA:RNA hybrids were studied for their colocalization with the HR proteins BRCA1 and RAD51. Indeed, we observed an increase in the colocalization of DNA:RNA hybrids with BRCA1 and RAD51 in NCS-treated S phase cells (figure 16).

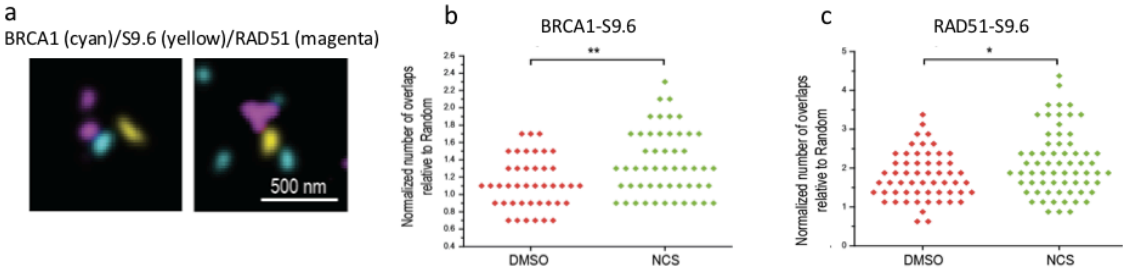

Figure 16: DNA:RNA hybrids colocalize with BRCA1 and RAD51 in NCS-treated S phase cells
a) Representative images of BRCA1 (cyan), DNA:RNA hybrids (yellow), RAD51 (magenta) colocalization in NCS treated S phase U2OS cells. Dot plot represents the number of DNA:RNA hybrids and either BRCA1 (b) or RAD51 (c) colocalization in DMSO or NCS-treated S phase U2OS cells relative to random (>50 cells, n=3).

Altogether, my data and data generated in a different lab with an independent experimental setup (super-resolution microscopy on NCS-treated cells) confirm that DNA:RNA hybrids form at DSBs preferentially during the S/G2 cell cycle phase.

3.1.2 DNA end resection favors the formation of damage-induced DNA:RNA hybrids

In the light of the preferential accumulation of damage-induced DNA:RNA hybrids at DSBs during the S/G2 phase of the cell cycle, I tested the impact of DNA end resection on DNA:RNA hybrids formation. To test this hypothesis I knocked-down CtIP in HeLa cells

and I monitored DNA:RNA hybrids accumulation at the I-PpoI cleavage site within the DAB1 gene at three time-points after cut. I observed that impairment of DNA end resection prevented DNA:RNA hybrids formation in all the time-points analysed (figure 14).

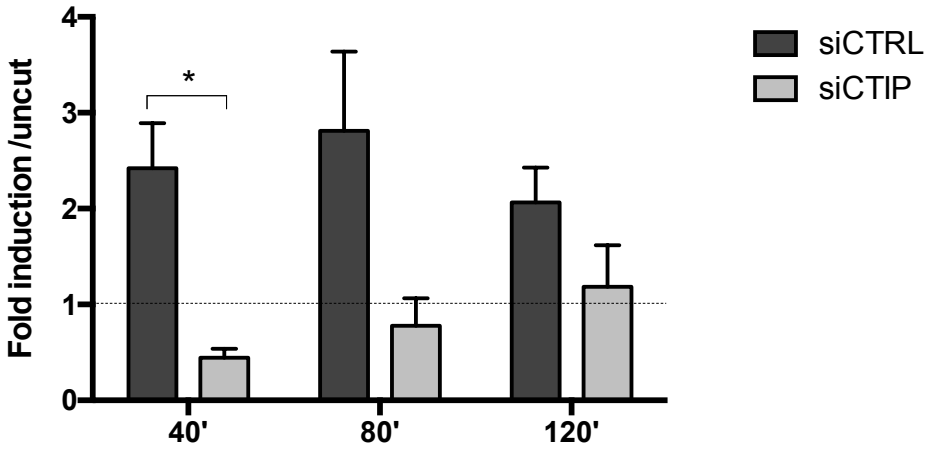

Figure 14: DNA end resection facilitates DNA:RNA hybrid formation at DSBs
HeLa cells were depleted for CtIP by RNAi. 48 hours later, I-PpoI was transfected and DSB generation was induced the day after for 40, 80 and 120 minutes. DRIP experiment was performed with the S9.6 antibody. The bar graph represents fold induction of cut samples relative to uncut. RNase H treatment (RH) was performed on cut samples to show specificity of the signal. Error bars represent s.e.m of 3 biological replicate

Importantly, I observed that CtIP knock-down, whose extent is shown in figure 15a, did not strongly alter cell cycle distribution (figure 15b), a parameter that could affect my analyses, being DNA:RNA hybrids accumulation restricted to the S/G2 cell cycle phase, as previously shown.

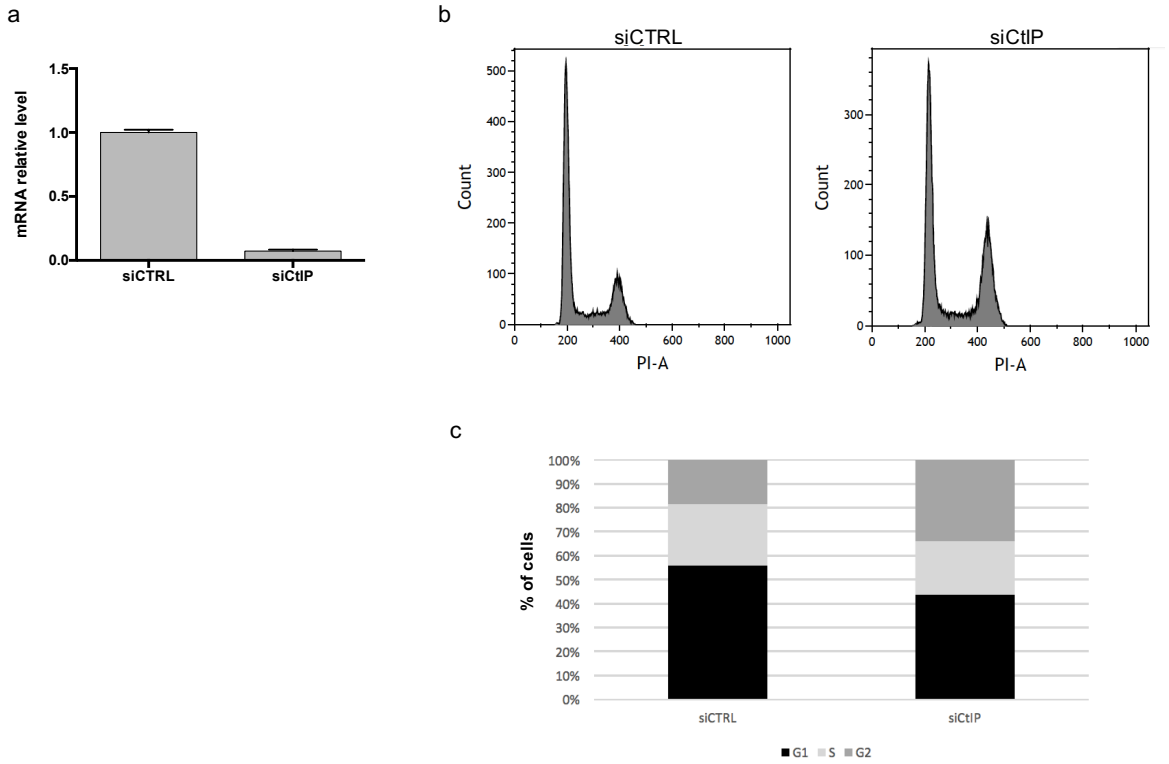

Figure 15: CtIP depletion does not affect cell cycle distribution
qPCR analysis of CtIP mRNA levels in HeLa cells transfected with siRNAs against CtIP for 72 hours (a). FACS analysis (b) and relative quantification (c) of cell cycle distribution of HeLa cells untreated or depleted for CtIP.

Next, I wanted to test whether proteins involved in HR also affected damage-induced DNA:RNA hybrids accumulation. For this reason, I depleted by RNAi BRCA2 and RAD51 in HeLa cells (figure 16a) and I first monitored the impact of the knock-down on the cell cycle. Cell cycle profiling of BRCA2 and RAD51 depleted HeLa cells revealed cell cycle changes that discouraged me from using this setup for these analysis (figure 16b) and prevented me to obtain conclusive results.

Altogether, this set of results shows that RNA pol II transcripts, most likely dilncRNAs, form DNA:RNA hybrids at DSBs, preferentially on resected DNA ends generated during the S/G2 phases of the cell cycle.

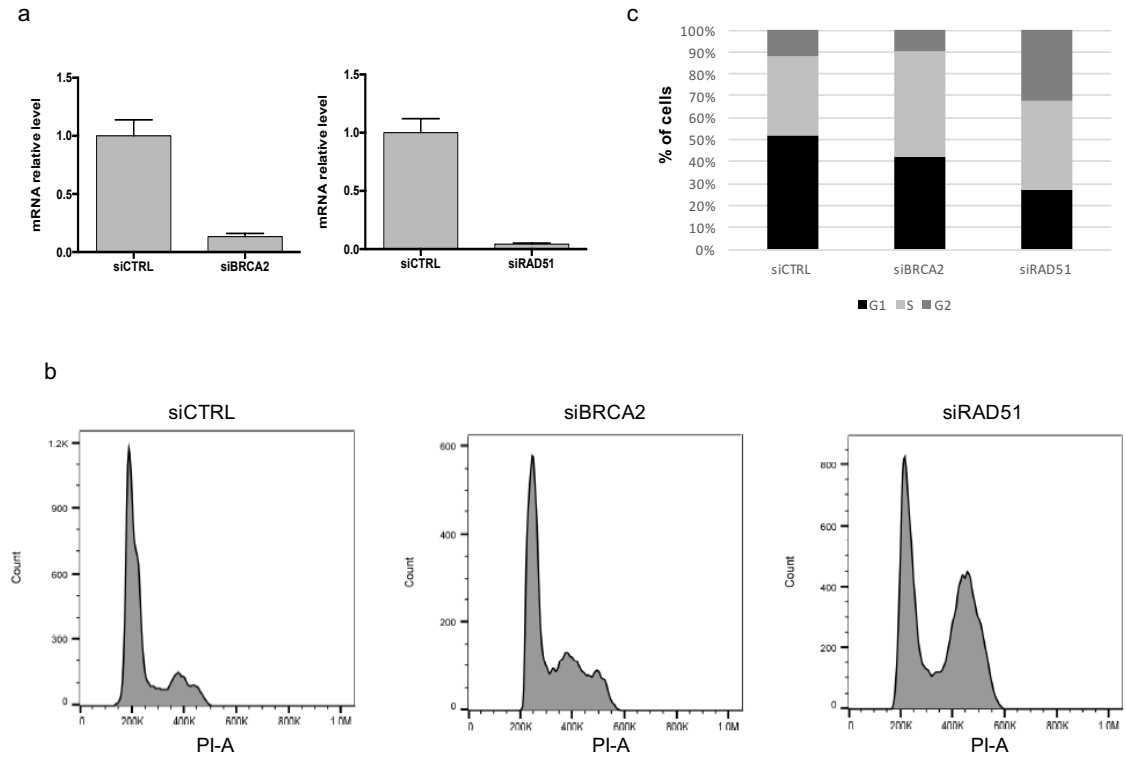

Figure 16: BRCA2 and RAD51 depletion affect cell cycle distribution
qPCR analysis of BRCA2 or RAD51 mRNA levels in HeLa cells transfected with siRNAs against BRCA2 or RAD51 for 72 hours (a) FACS analysis (b) and relative quantification (c) of cell cycle distribution of HeLa cells untreated or depleted for BRCA2 or RAD51.

3.2 RNA participates in HR proteins recruitment to DSB

3.2.1 Inhibition of RNA pol II transcription impairs HR proteins foci formation

Once demonstrated that DSB-induced RNA pol II-mediated *de novo* transcription generates DNA:RNA hybrids at DSBs in S/G2 phase, I proceeded to study the impact of transcriptional inhibition on focal accumulation of HR proteins. In order to test this, I took advantage of two drugs, α-amanitin and DRB, that inhibit RNA Pol-II transcription in two different ways: α-amanitin binds RNA pol II, blocks RNA synthesis and triggers RNA pol II degradation; DRB inhibits RNA pol II elongation by targeting mainly CDK9 and inhibiting CDK9-mediated phosphorylation of RNA pol II C-terminal domain (CTD) during transcription (Bushnell et al., 2002, Nguyen et al., 1996). HeLa cells were irradiated and, immediately after, treated with α-amanitin or DRB, or vehicles. 6 hours later cells were fixed and stained for the HR proteins BRCA1, BRCA2, and RAD51. BRCA1 and RAD51 foci were co-stained together with cyclin A, in order to selectively detect S/G2-positive cells and avoid misleading interpretations of results due to potential cell-cycle variations. For technical reasons, BRCA2 staining could not be coupled with cyclin A staining, and CENP-F, a marker of G2 phase, was instead used. The inhibition of RNA pol II was confirmed by monitoring by qRT-PCR the level of Fos, a short half-life RNA pol II transcript (figure 17).

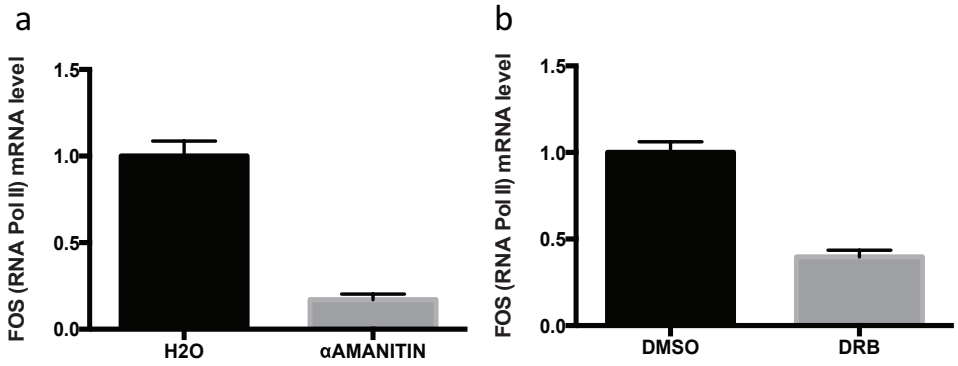

Figure 17: Efficacy of RNA pol II-mediated transcription inhibition
Efficiency of α-amanitin (a) and DRB (b) treatment monitored by qRT-PCR analysis of the levels of FOS, a short-lived RNA pol II transcript.

Strikingly, RNA pol II inhibition with either α-amanitin (figure 18a) or DRB (figure 18c) strongly impaired the formation of BRCA1, BRCA2, and RAD51 foci, as also shown in the relative quantifications (figure 18b and 18d), while not impacting on their protein levels (figure 20). Next, we monitored the impact of RNA pol II inhibition on DNA end resection by probing for the ssDNA binding protein RPA, the DNA damage-induced phosphorylated form of the RPA2 subunit on Ser-4 and Ser-8 (p-RPA Ser4/8), and by directly determining ssDNA by BrdU native staining – cells incubated in the presence of BrdU were stained under native conditions with an antibody against BrdU that detects only extensive stretches of ssDNA. ssDNA by BrdU native staining, RPA, and p-RPA Ser 4/8 stainings (figure 19) revealed no reduction of DNA end resection upon RNA pol II inhibition, rather suggested a moderate increase. Also in these experiments, S/G2 phase cells were selected by co-staining with cyclin A.

This set of results shows that, although DNA end resection is not reduced, actually moderately increased, the recruitment of HR proteins, including BRCA1, BRCA2 and RAD51, is strongly abolished upon RNA pol II inhibition, suggesting a possible role for RNA in the recruitment of these proteins.

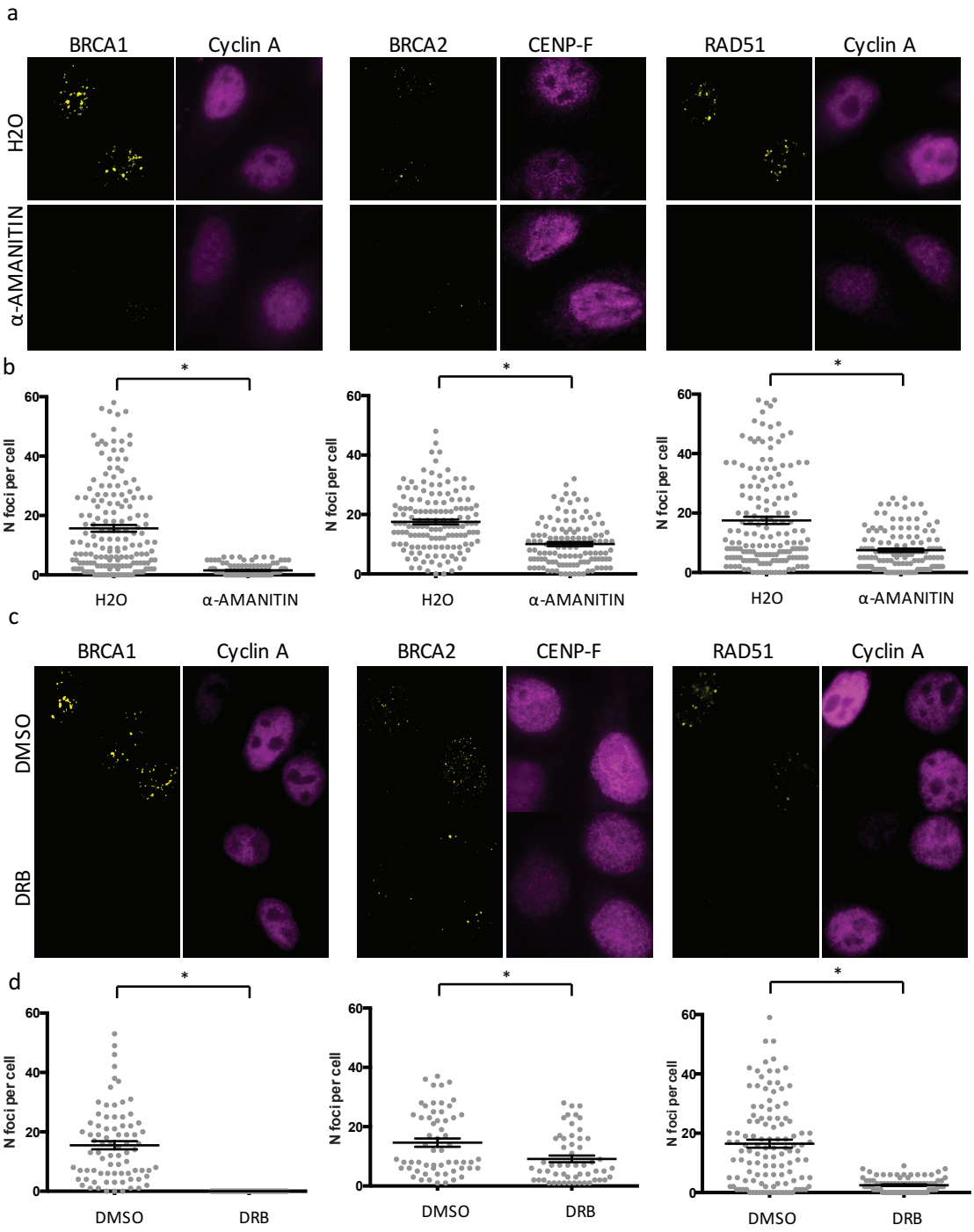

Figure 18: Inhibition of RNA pol II transcription impairs HR proteins foci formation
HeLa cells were treated with α-amanitin (a) or DRB (c), or relative vehicles, and irradiated in parallel. 6 hours later cells were fixed and stained for BRCA1, BRCA2, and RAD51. BRCA1 and BRCA2 staining was coupled with cyclin A, to detect the S/G2 phase cells. BRCA2 staining was coupled with CENP-F, a marker of G2 phase cells. Dot plots of α-amanitin (b) or DRB (d) treated cells represent the number of foci in each nucleus. Error bars indicate s.e.m. ($n \geq 3$).

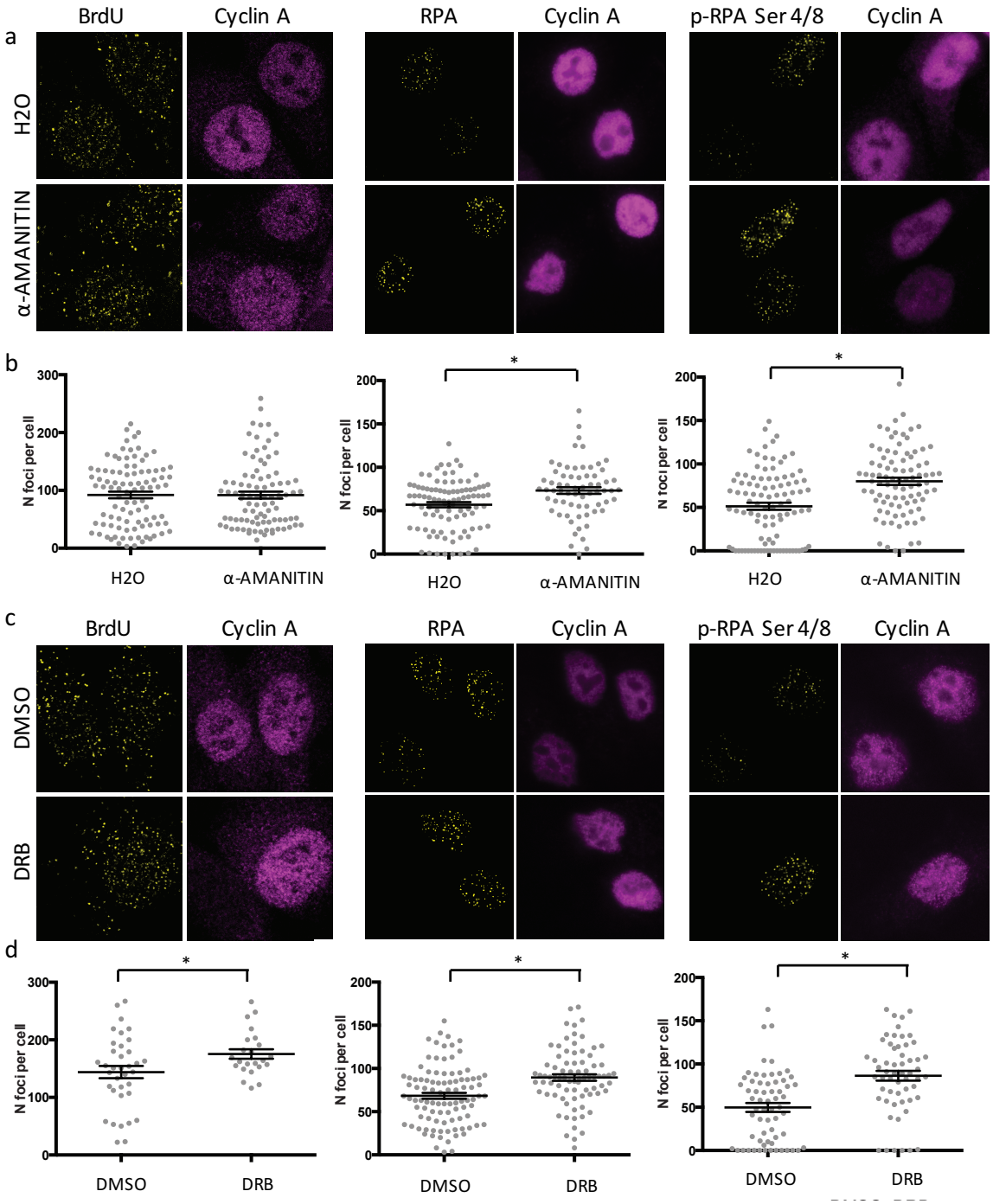

Figure 19: Inhibition of RNA pol II transcription mildly increases DNA end resection
HeLa cells were treated with α-amanitin (a) or DRB (c), or relative vehicles, and irradiated in parallel. 6 hours later cells were fixed and resected DNA ends were visualized by BrdU native staining, RPA, and p-RPA Ser 4/8 staining. Co-staining with cyclin A, allowed to distinguish the S/G2 phase cells. Dot plots of α-amanitin (b) or DRB (b) treated cells represent the number of foci in each nucleus. Error bars indicate s.e.m. ($n \geq 3$).

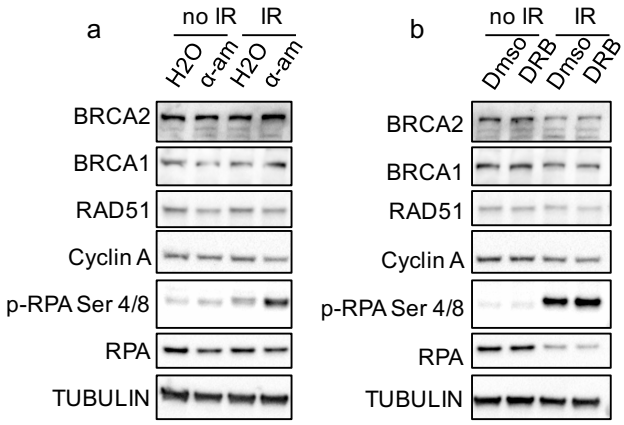

Figure 20: Inhibition of RNA pol II transcription does not affect the level of key HR proteins
Representative immunoblot of control or irradiated HeLa cells treated with α-amanitin (a) or DRB (b) or vehicles (n=2)

3.2.2 Inactivation of dilncRNAs with complementary ASOs inhibits HR

The results previously described show that active transcription is necessary for HR foci formation but do not demonstrate a direct role and sequence-specificity of damage-induced RNAs in this process. According to recent results obtained in our laboratory, four different RNA species are generated from a DSB: two transcribed in opposite orientations away from each end of the DSB (dilncRNAs *from*) and two synthetized toward the DSB (dilncRNAs *to*) (Michelini et al., in press) (figure 21a). In order to test whether RNAs with the sequence of the damaged locus were specifically necessary for HR, we took advantage of a well-known system to study homology-directed repair, the DR-GFP system (Pierce et al., 1999). TRI-DR-U2OS cells contain two non-functional GFP sequences: a sceGFP containing an I-SceI recognition site, which also acts as a stop codon for GFP expression, and a truncated GFP (see figure 21a). Upon induction of I-SceI expression and DSBs formation, only HR between the two non-functional GFP sequences results in the formation of the correct GFP sequence coding for GFP. HR can be monitored by either evaluation of GFP expression by FACS analysis, or, more directly, by PCR amplification of the functional GFP genomic DNA sequence generated upon recombination. In order to inhibit the action of dilncRNAs generated upon cut, I designed Antisense Oligonucleotides (ASOs) complementary to dilncRNAs. In particular, I used Locked Nucleic Acids (LNAs), modified RNA species that

bind the endogenous complementary RNAs and inhibit their functions, as depicted in figure 21a. I transfected different set of ASOs matching the dilncRNAs potentially produced from the damaged I-SceI locus and I induced in parallel the expression of I-SceI, generating a DSB at the I-SceI locus. 72 hours after transfection, I monitored HR by FACS analysis of GFP expression (with the help of Corey Jones-Weinert in the laboratory) and by directly measuring the recombination event by PCR on genomic DNA.

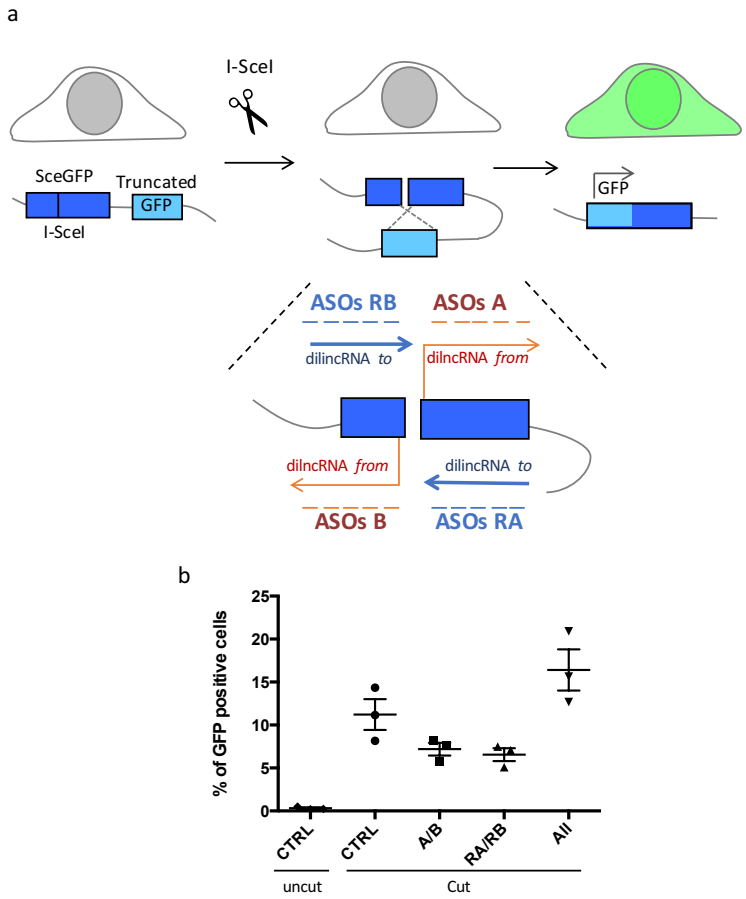

Figure 21: dilncRNAs inactivation by complementary ASOs inhibits HR
a) Use of DR-GFP system to monitor HR (Pierce, 1999). Engineered TRI-DR-U2OS cells contain two non-functional GFP sequences: a sceGFP containing an I-SceI recognition site, that is also a stop codon for GFP expression, and a truncated GFP. Upon induction of I-SceI expression and DSBs formation, HR between the two non-functional GFP sequences restores the correct GFP sequence, coding for a functional GFP, which expression can be monitored by FACS analysis. Upon damage, dilncRNAs are transcribed bi-directionally from (dilncRNAs *from*) and toward (dilncRNAs *to*) the DSB (Michelini et al., in press). For each dilncRNAs, 5 matching Antisense Synthetic Oligonucleotides (ASOs) were used: ASOs pool A and B match the dilncRNA *from* on the right and on the left part of the DSB, respectively; ASOs pool RA and RB match the dilncRNA *to* on the right and on the left part of the DSB, respectively. b) FACS analysis of HR efficiency. TRI-DR-U2OS cells were transfected with 20 nM pool of ASOs in different combinations: A/B, RA/RB, and All. In parallel, I-SceI expression was induced by adding 5 µg/ml doxycycline. 24 hours after, GFP expression was measured by FACS. Dot plots represent 3 independent experiment and error bars indicate s.e.m.

As shown in figure 21b, upon I-SceI induction and DSB generation 10% of the cells transfected with a control ASO matching an unrelated sequence undergo efficient HR and express GFP. Treatment with ASOs matching either the dilncRNAs *from* or *to* reduces GFP expression. As a control, treatment with ASOs that match dilncRNAs *from* or *to* but have been inactivated by annealing to each other (All) does not reduce HR efficiency. Importantly, treatment with ASOs did not cause cell cycle alterations, that could be responsible for a different HR efficiency among the samples (figure 22). In order to further confirm the impact of ASOs on HR, I performed PCR on genomic DNA with primers that only amplify the GFP sequence resulting from HR between the two mutated GFPs (see figure 23a). I observed that treatment with ASOs matching dilncRNAs, but not with control ASOs, strongly reduces HR between the two GFP sequences (figure 23b), thus confirming the impact of ASOs on this repair pathway.

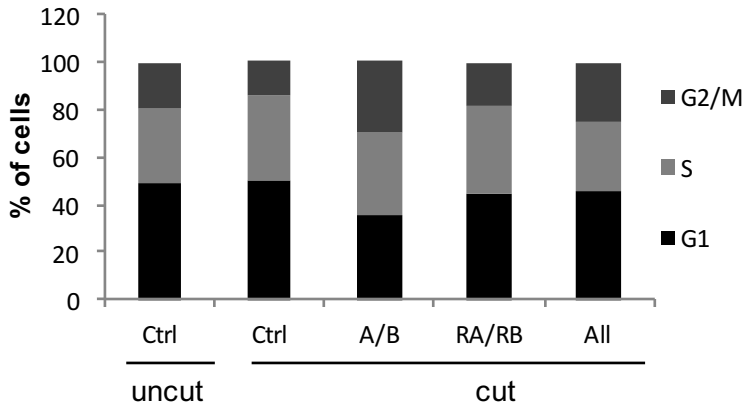

Figure 22: Treatment with ASOs targeting dilncRNAs does not affect cell cycle distribution
FACS analysis of cell cycle distribution of TRI-DR-U2OS cells transfected for 24 hours with 20 nM pool of ASOs in different combinations: A/B, RA/RB, and All. In parallel with ASOs transfection, I-SceI expression is obtained by adding 5 μg/ml doxycycline.

Importantly, PCR on genomic DNA also allows to monitor SSA in the same reporter system. SSA is the result of over-resection of the broken DNA ends and RAD52-mediated annealing of long-tract homology sequences on the exposed resected ends. This process requires DNA end resection but not the recombinase RAD51. As shown in figure 23c, treatment with ASOs matching dilncRNAs *from* or *to* did not inhibit SSA. These results indicate that dilncRNAs

inactivation by complementary ASOs does not impact on DNA end resection, an event required for both HR and SSA, but it only impairs the unique steps of HR.

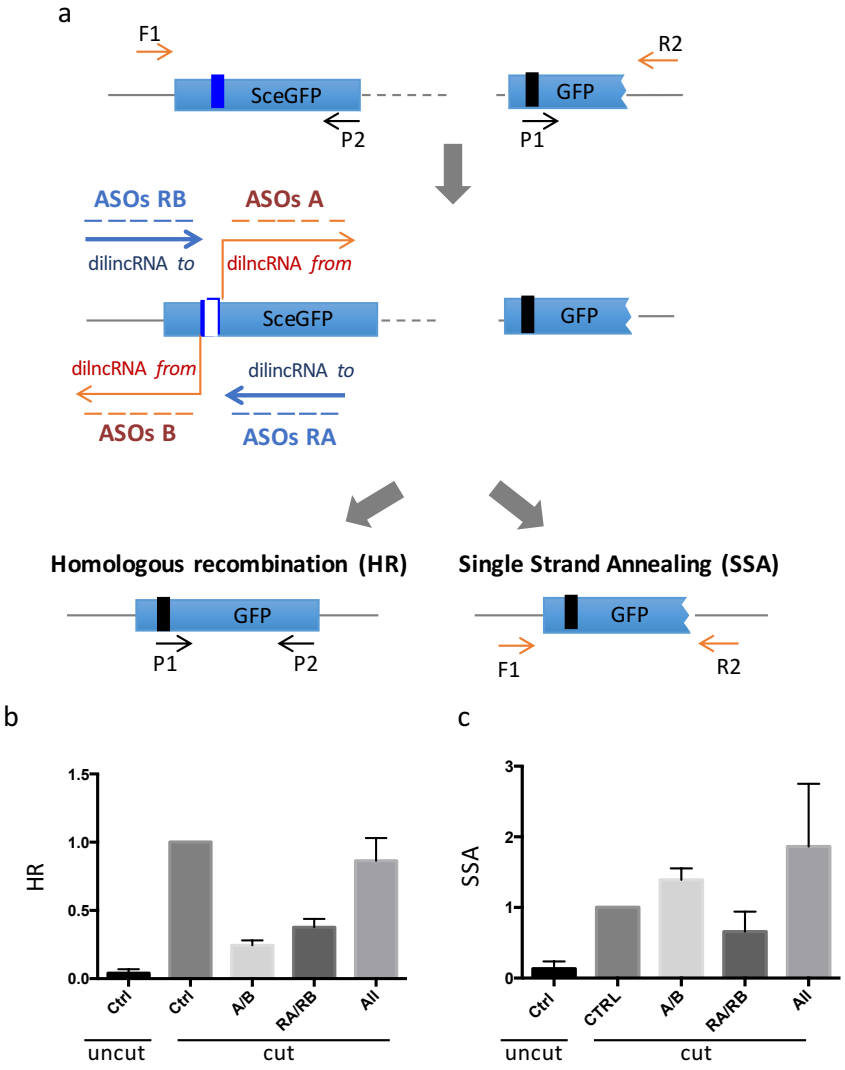

Figure 23: dilncRNAs inactivation by complementary ASOs inhibits HR but not SSA
a) Schematic representation of the ASOs used to block dilncRNAs and the primers used to detect homologous recombination (HR) and single strand annealing (SSA). ASOs A and B target the dilncRNAs *from*, respectively on the right and on the left side of the DSBs. ASOs RA and RB target the dilncRNAs *to*, respectively on the right and on the left side of the DSBs. HR and SSA are two of the possible HDR-based mechanisms to repair the I-SceI induced DSB. Upon HR, the correct GFP sequence containing the 5' portion of the truncated GFP and the 3' of the sceGFP is generated. The HR product can be amplified by PCR using one primer matching the 5' part of the truncated GFP (P1) and one primer matching the 3' part of the sceGFP (P2). Over-resection of the exposed DNA ends results in SSA and generates a 0.8 kb amplicon when PCR with a primer matching a region upstream to the sceGFP (F1) and a primer matching a region downstream of the truncated GFP (R2) are used. b) HR efficiency analyzed by genomic semi-quantitative PCR with primers P1 and P2. c) SSA efficiency analyzed by genomic semi-quantitative PCR with primers F1 and R2. Error bars show the s.e.m. of 2 independent experiments.

3.2.3 RNA species, possibly in the form of DNA:RNA hybrids, contribute to BRCA1 recruitment to DSBs

To confirm the direct role of RNA in HR, I monitored the effect of RNase A or RNase H treatment on HR foci. In particular, I treated irradiated permeabilized U2OS cells with RNase A o RNase H before fixation in order to remove all RNAs in the cells, including dilncRNAs generated upon damage, and DNA:RNA hybrids, respectively. Only after treatment, I fixed and stained for HR factors. I observed that RNase A, as well as RNase H treatment, dismantled BRCA1 foci (figure 24). The same treatment revealed no reduced, if any moderately increased, DNA end resection signals, as monitored by BrdU and RPA stainings (figure 25a and b).

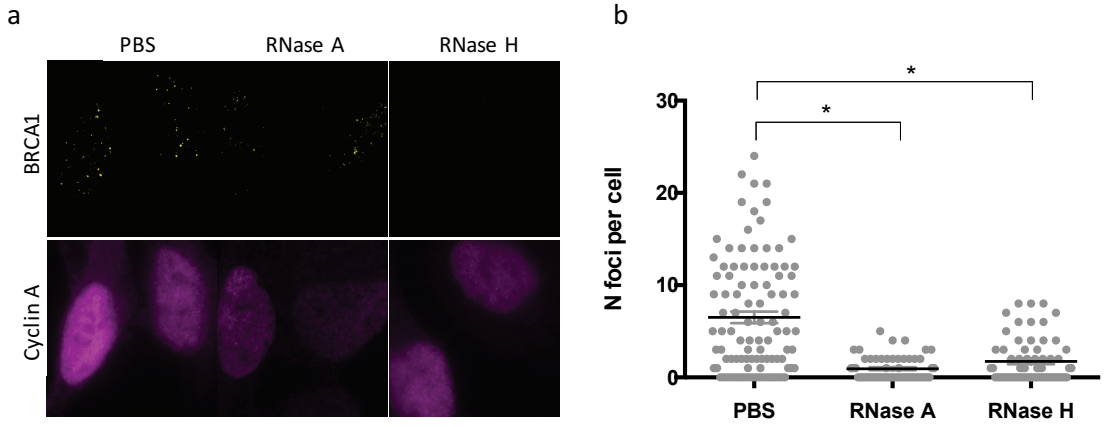

Figure 24: BRCA1 foci are dismantled by treatment with RNase A and RNase H
U2OS irradiated cells were permeabilized and treated with RNase A or RNase H prior to fixation. Representative images (a) and quantification (b) of BRCA1 and cyclin A co-staining of irradiated cells treated with PBS only, RNase A and RNase H. Error bars indicate s.e.m. (n = 3).

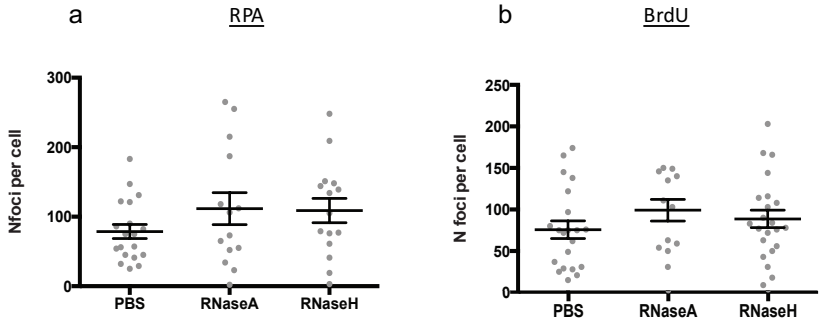

Figure 25: RNase A and RNase H treatment mildly increases BrdU and RPA signal
HeLa and U2OS irradiated cells were permeabilized and treated with RNase A or RNase H prior to fixation. Dot plots of RPA and BrdU foci in irradiated U2OS cells treated with PBS only, RNase A and RNase H. Error bars indicate s.d. of 1 experiment.

In order to further confirm the results obtained with RNase H treatment on permeabilized cells, I overexpressed a GFP tagged RNase H1 in U2OS cells. As shown in figure 26, RNase H1 overexpression impairs BRCA1 foci formation, thus confirming the role of DNA:RNA hybrids in favoring BRCA1 recruitment. However, RAD51 foci formation was not impaired upon RNase H1 overexpression, suggesting that in the absence of DNA:RNA hybrids the loading of RAD51 is not strongly dependent on BRCA1.

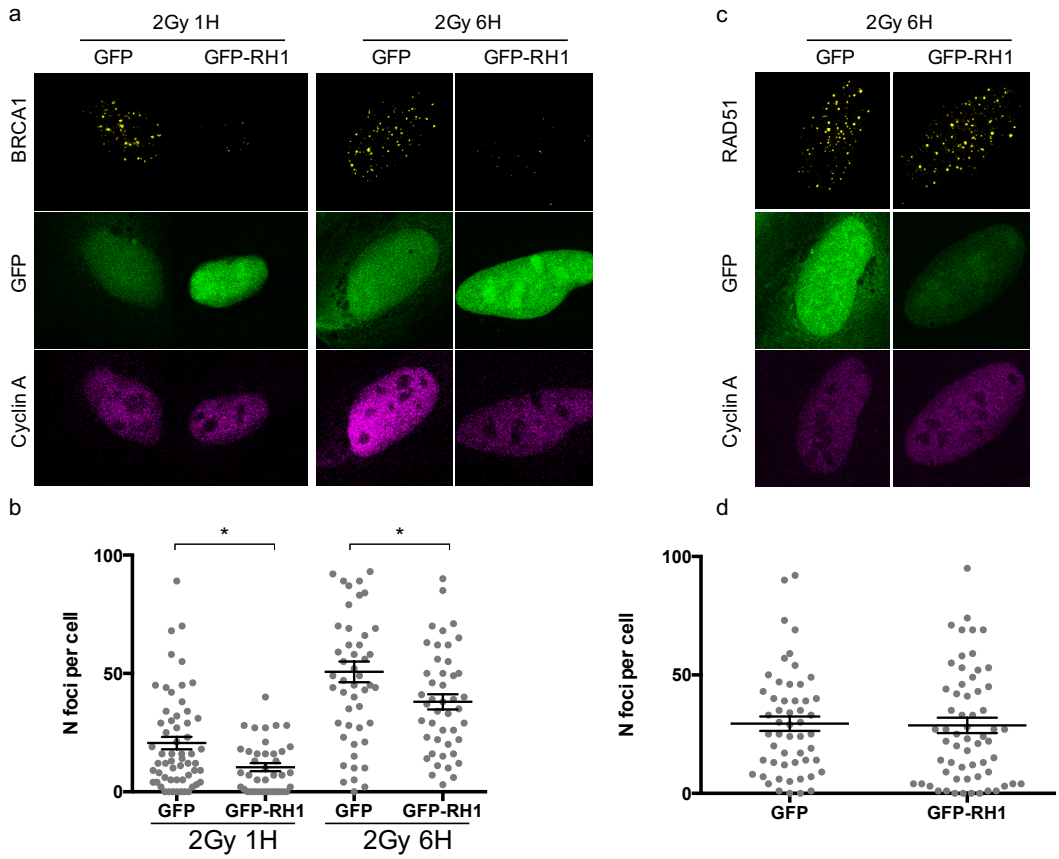

Figure 26: RNase H overexpression impairs BRCA1 but not RAD51 foci formation
U2OS cells overexpressing a control GFP or GFP-RNase H1 were irradiated with 2Gy and fixed 1 hour and 6 hours later. Representative images (a) and relative quantification (b) of BRCA1 foci and representative images (a) and relative quantification (b) of RAD51 foci are shown. Dot plots of represent the number of foci in each nucleus. Error bars indicate s.e.m. (n = 3).

In line with this result, the efficiency of HR-mediated repair, as monitored by GFP expression in the DR-GFP system, is not affected by RNase H1 overexpression (figure 27).

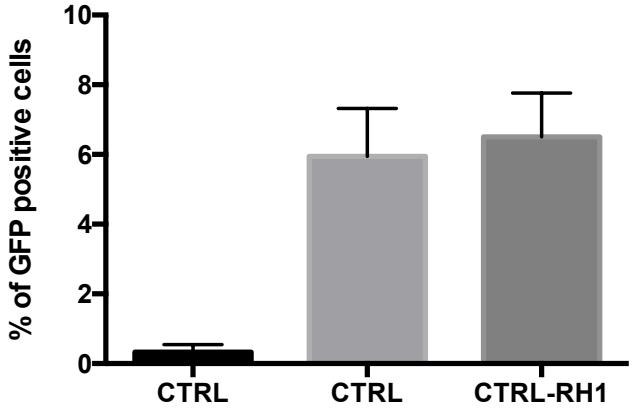

Figure 27: RNase H1 overexpression does not affect HR
TRI-DR-U2OS cells were transfected with RNase H1 and in parallel I-SceI expression was induced by adding doxycycline to the cell medium. 48 hours later GFP expression was monitored by FACS analysis. Error bars indicate s.e.m. (n = 3).

3.2.4 BRCA1 binds in vitro dsDNA and DNA:RNA hybrids

Having observed that BRCA1 recruitment to DSB is affected by inhibition of RNA pol II transcription, as well as RNase A and RNase H treatment, and RNase H1 overexpression, we tested whether BRCA1 could bind to DNA:RNA hybrids. In order to address this we collaborated with Petr Cejka's lab in Bellinzona and his postdoc Sean Michael Howard, who performed electrophoretic mobility shift assay (EMSA) of purified recombinant BRCA1 and BRCA1-BARD1 heterodimer in the presence of DNA duplexes or DNA:RNA hybrids. Radioactively labelled DNA duplexes or DNA:RNA hybrids were incubated with recombinant proteins and separated by electrophoresis on a native polyacrylamide gel. As shown in figure 28a, when nucleic acids were not incubated with recombinant proteins a fast migrating band corresponding to the free nucleic acids was observed. The incubation of nucleic acids with increasing concentrations of either BRCA1 (figure 28a) or BRCA1-BARD1 constitutive heterodimer (figure 28b) determined a "band-shift", indicating protein interaction with the tested nucleic acids. As shown in figure 28a and in the quantification of percentage of free substrate (figure 28c), BRCA1 alone binds DNA:RNA hybrids with an affinity slightly higher compared to DNA duplexes. The constitutive heterodimer BRCA1-BARD1 binds DNA:RNA hybrids to a similar affinity compared to DNA duplexes (figure 28b).

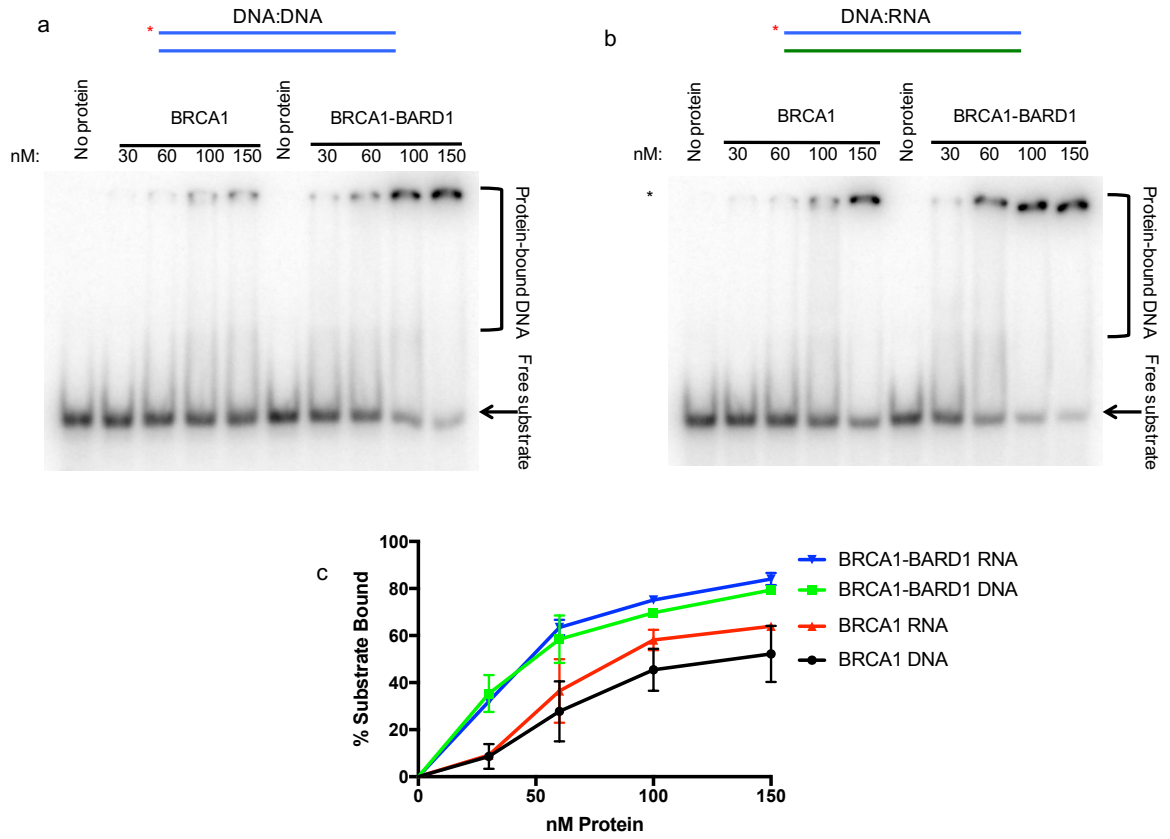

Figure 28: BRCA1 and BRCA1-BARD1 complex bind DNA:RNA hybrids *in vitro*
Different concentrations of the recombinant BRCA1 and BARD1 proteins were incubated with radioactively labelled dsDNA (a) or DNA:RNA hybrids (b) substrates and separated on a non-denaturing polyacrylamide gel. The graph represents the % of substrate bound at different proteins concentration (c).

3.3 RNase H2 is recruited to DSBs and interacts with HR proteins

3.3.1 RNase H1 depletion cannot be obtained by siRNA transfection

To gain further insight into the role of DNA:RNA hybrids on HR modulation, I tried to deplete the two enzymes with RNase H activities in the cell: RNase H1 and RNase H2. I could not deplete RNase H1 since RNase H1 knock-down performed with a pool of commercial siRNA was not efficacious in my hands. Indeed, RNase H1 protein levels did not change reproducibly upon transfection with a pool of different siRNA in several tested conditions. To exclude that the result observed was due technical problems, I tested the specificity of the antibody by western-blot analysis. In particular, I over-expressed a GFP-tagged RNase H1 and I used siRNAs against either GFP or RNase H1. As shown in figure 29, siGFP transfection reduces the GFP-RNase H1 levels, as detected with the RNase H1 antibody, thus showing that the antibody used specifically recognize the RNase H1. However, only a moderate decrease in GFP-RNase H1 level and no decrease in the endogenous RNase H1 level is observed upon siRNase H1 transfection. From this result I concluded that, although the antibody was specific, no efficient RNase H1 depletion could be obtained with the tools available in the lab.

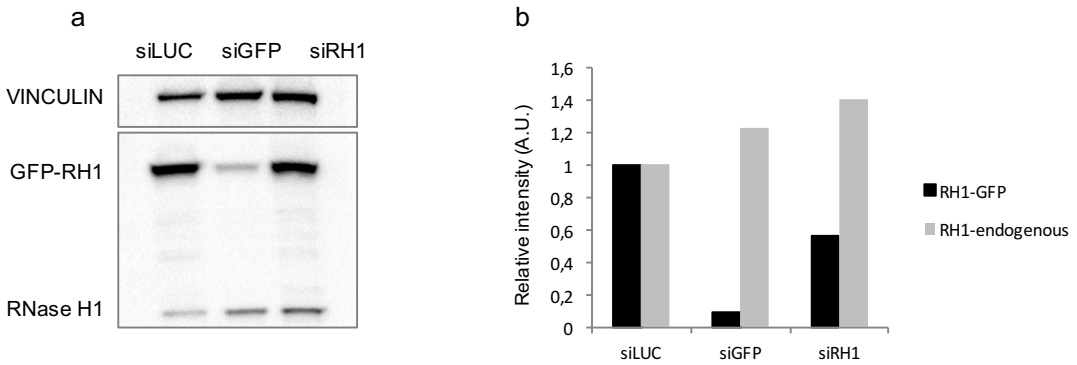

Figure 29: RNase H1 is not depleted upon siRNA transfection
U2OS cells were transfected with 20 nM siRNAs matching luciferase, GFP, and RNase H1 and the day after they were transfected with plasmids expressing GFP or GFP-RNase H1. Immunoblot and relative quantification are shown (n=1)

3.3.2 RNase H2 depletion inhibits HR by impacting on key HR proteins level

I next tested the depletion of RNase H2, the major RNase H activity in mammalian nuclei. RNase H2 depletion was obtained by using siRNAs directed against RNase H2A, the catalytic subunit of the trimeric complex RNase H2, since it is known that depletion of one of the three subunits destabilizes the complex (Cerritelli and Crouch, 2009). The impact of RNase H2 depletion on HR-mediated repair was monitored by using the DR-GFP system (see figure 21a). I transfected TRI-DR-U2OS cells either with siRNA against RNase H2A or against BRCA2, as a positive control, and in parallel I induced I-SceI expression. Three days after, I monitored HR efficiency by both FACS analysis (figure 30a) and genomic DNA PCR (figure 30b). As shown in figure 30a, upon I-SceI expression, the percentage of GFP-positive cells increases in control cells, while a very low increase is observed in cut cells lacking BRCA2. Interestingly, in RNase H2A-depleted cut cells the percentage of GFP positive cells is lower than in the positive control. This result is further confirmed by PCR on genomic DNA. Upon I-SceI expression, a band corresponding to the amplicon generated upon HR (see figure 23a) is observed in the control sample (figure 30b). Instead, the intensity of the band corresponding to the recombination product is lower in both BRCA2 and RNase H2A-depleted samples, thus confirming the results obtained with FACS analyses.

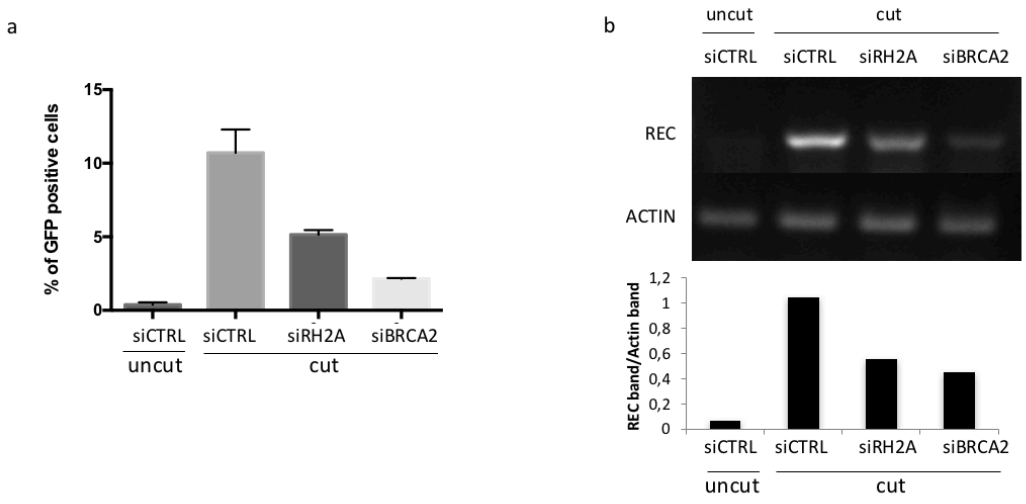

Figure 30: RNase H2 depletion impairs HR as monitored by the DR-GFP system
TRI-DR-U2OS cells were transfected for 72 hours with siRNAs matching a control sequence, RNase H2A, and BRCA2 and in parallel I-SceI expression was induced with doxycycline. HR efficiency monitored by FACS analysis (a) or semi-quantitative PCR on genomic DNA (see figure 23a) (b) in TRI-DR-U2OS cells transfected with siRNA targeting RNase H2A and BRCA1 (n=3)

However, when I tested the efficiency of RNase H2 depletion by either qRT-PCR (figure 31a) and WB analysis (figure 31b), I observed that siRNase H2A not only reduced the RNase H2A levels, but also the levels of key HR proteins, including BRCA1, BRCA2, and RAD51.

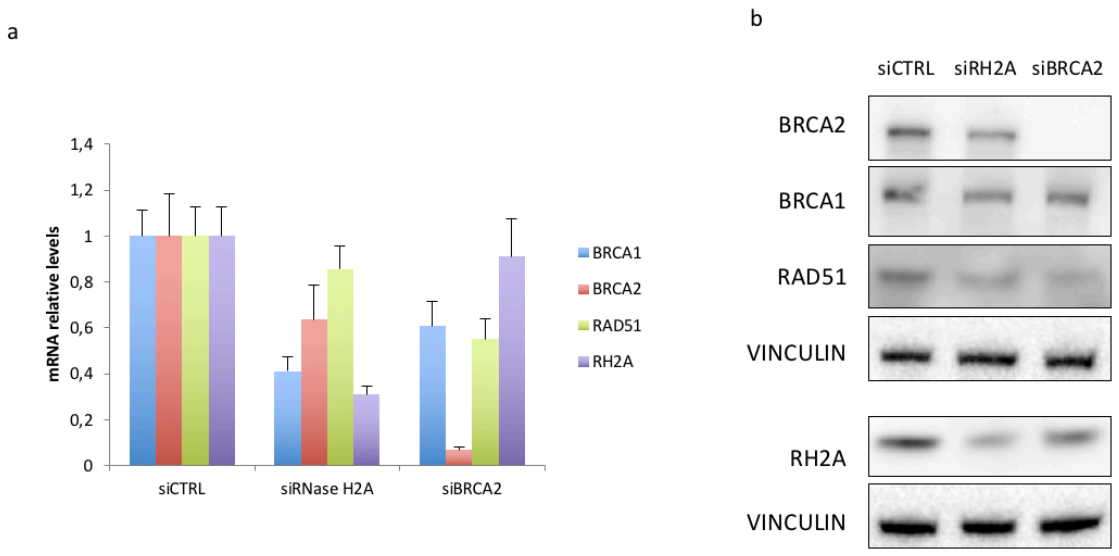

Figure 31: RNase H2 depletion reduces HR proteins levels
mRNA (a) and protein (b) levels of the key HR proteins as monitored, respectively, by qRT-PCR and western blot analysis. (RH2A = RNase H2A)

Since I thought that the reduction in the HR protein level upon RNase H2A siRNA transfection could be due to an off-target effect of the siRNAs used, I deconvolved the siRNAs pool used in the previous RNase H2A depletion experiment and I tested the expression of BRCA2 by qRT-PCR with three different primers pairs matching the 5'-, middle-, and 3'-region of the transcript, to exclude that alternative transcripts were generated upon RNase H2A depletion (figure 32). I observed, that each one of the siRNA used not only reduced RNase H2 levels but also BRCA2 levels, as monitored by qRT-PCR (figure 32a) and immunoblot analysis (figure 32b). From these results it can be concluded that RNase H2 depletion negatively affect HR by reducing the levels of key HR proteins. Although potentially of some interest, as it suggests that RNase H2 and potentially DNA:RNA hybrids are controlling gene expression of HR genes, this result prevented me to use RNase H2 depletion as a tool to modulate DNA:RNA hybrids levels at DSBs.

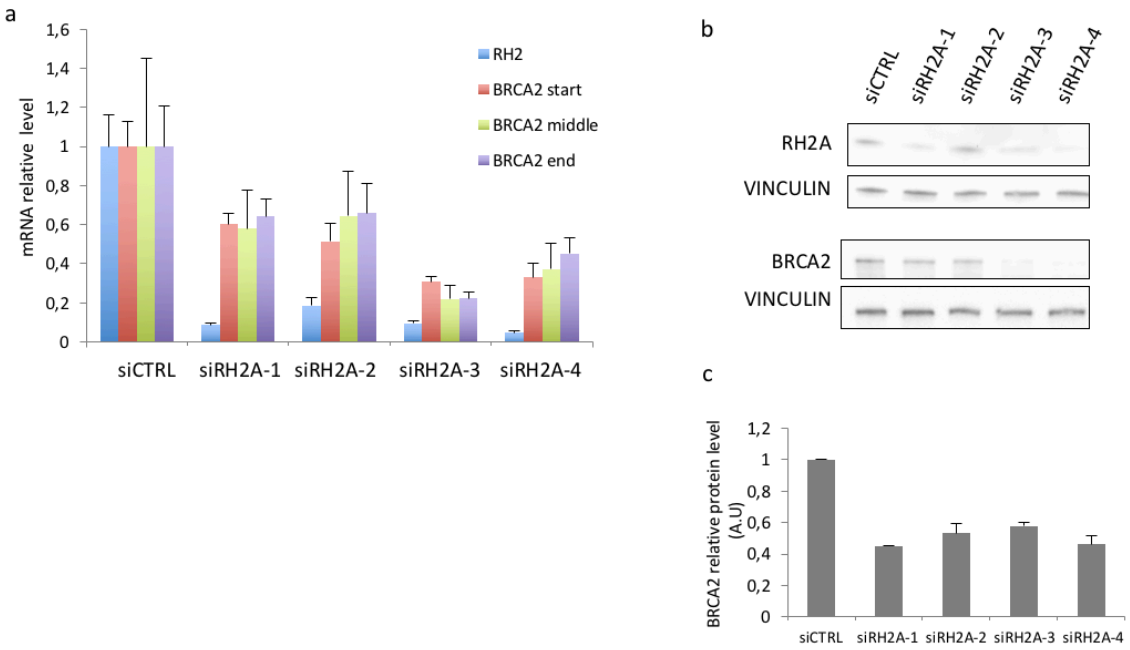

Figure 32: Impact of RNase H2A depletion on BRCA2 expression is not due to siRNA off-target effect
BRCA2 mRNA (a) and protein (b) levels as monitored, respectively, by qRT-PCR using 3 different primers pairs matching the 5' (start), middle, and 3' (end)-region of the transcript and western blot analysis. (RH2A = RNase H2A).

3.3.3 RNase H2 is recruited to DSBs

Having observed that DNA:RNA hybrids form at DSBs, I monitored whether protein responsible for their degradation were recruited to DSBs. In mammalian cells two proteins with RNase H activities have been characterized: RNase H1, which is mainly cytoplasmic, and RNase H2, which is mainly nuclear and represents the major RNase H activity in the cell (Cerritelli and Crouch, 2009). Thus, I tested whether RNase H2 was recruited to DSBs. I thus performed immunofluorescence stainings for all the three RNase H2 subunits on either untreated or irradiated U2OS cells, but I could only detect a pan-nuclear signal in both conditions. I therefore decided to exploit in situ proximity ligation assay (PLA), a technique that allows *in situ* visualization of proximity between two proteins of interest: when two proteins interact or are in close proximity (<40 nm) a signal detectable by fluorescence microscopy is generated. By performing PLA between RNase H2A and γH2AX in untreated and irradiated U2OS cell fixed 1 or 6 hours after irradiation, I observed an increase in PLA signal in irradiated cells compared to not irradiated (figure 33), thus indicating RNase H2A proximity with γH2AX.

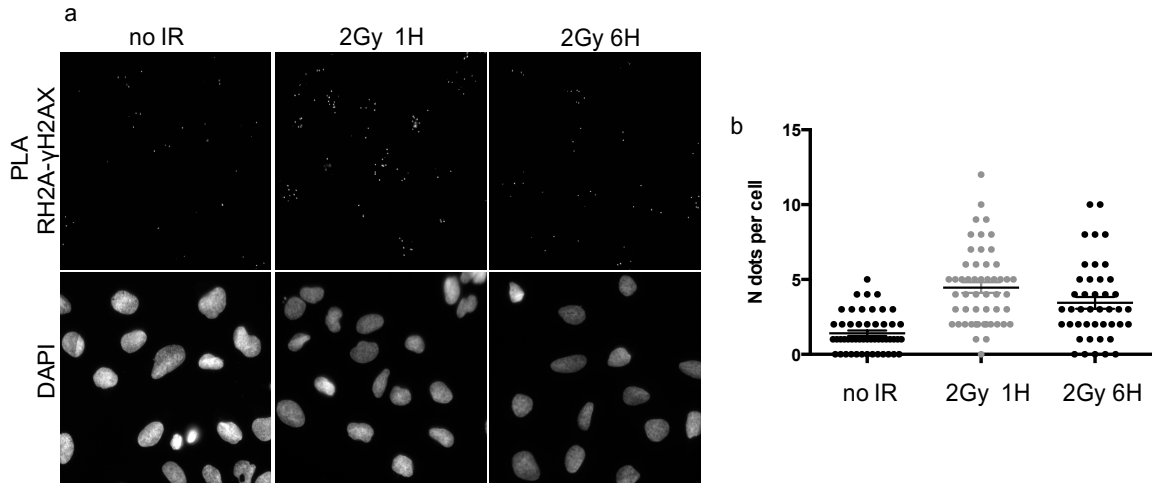

Figure 33: PLA reveals proximity between RNase H2A and γH2AX
PLA between RNase H2A and γH2AX was performed on U2OS cells untreated or irradiated 2Gy and fixed 1 and 6 hours later. Dot plots represent the number of PLA dots per cell and error bars are s.e.m from 3 independent experiments.

To further confirm RNase H2A recruitment to DSBs, I performed Chromatin immunoprecipitation (ChIP) with antibodies against RNase H2A and BRCA1, as a positive control, followed by qPCR amplification of the regions close to the DSB in the DR-GFP system. As already mentioned, in the DR-GFP cells a mutated GFP sequence contains the recognition site for the I-SceI nuclease, whose expression can be induced upon doxycycline administration. As expected, 16 hours upon doxycycline treatment, BRCA1 localizes to the damaged locus (figure 34b). Similarly, RNase H2A accumulates at the DSB, at levels comparable with BRCA1 (figure 34a)

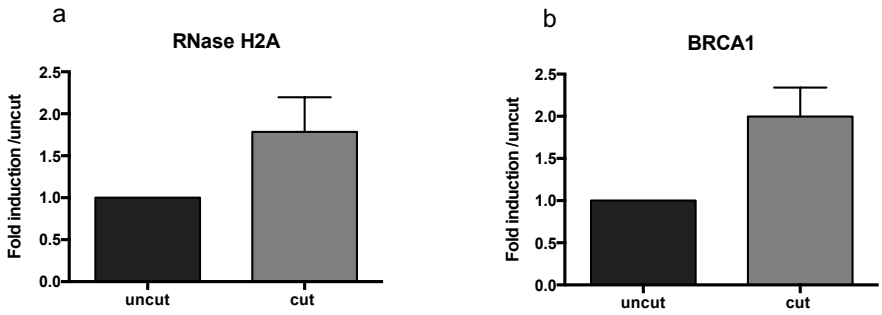

Figure 34: ChIP analysis shows RNase H2A recruitment to DSBs
Accumulation of RNase H2A (a) and BRCA1 (b) as detected by ChIP-qPCR at the I-SceI cleavage site in the DR-GFP system (see figure 23a). The bar plot show the fold induction relative to the uncut (n=3).

3.3.4 RNase H2 recruitment to DSBs is cell-cycle regulated

Since DRIP analysis showed a preferential accumulation of damage-induced DNA:RNA hybrids in S/G2 cell cycle phases, I wanted to test whether also RNase H2A recruitment was cell cycle regulated. For this reason, I performed PLA between γH2AX and either the RNase H2A (by using two different antibodies (Ab-1 and Ab-2)) or the RNase H2B subunits of RNase H2 in untreated or irradiated HeLa-FUCCI cells, in order to distinguish the different cell-cycle phases. I observed that the PLA signal, indicating proximity between γH2AX and each one of the RNase H2 subunits tested, was moderately higher in undamaged S/G2 phase cells compared to G1 cells (figure 35). However, while only a mild increase in PLA signal was observed in damaged G1 cells compared to the undamaged ones, a more pronounced increase in PLA signal was observed for damaged S/G2 cells compared to undamaged ones, with all the antibodies combinations tested.

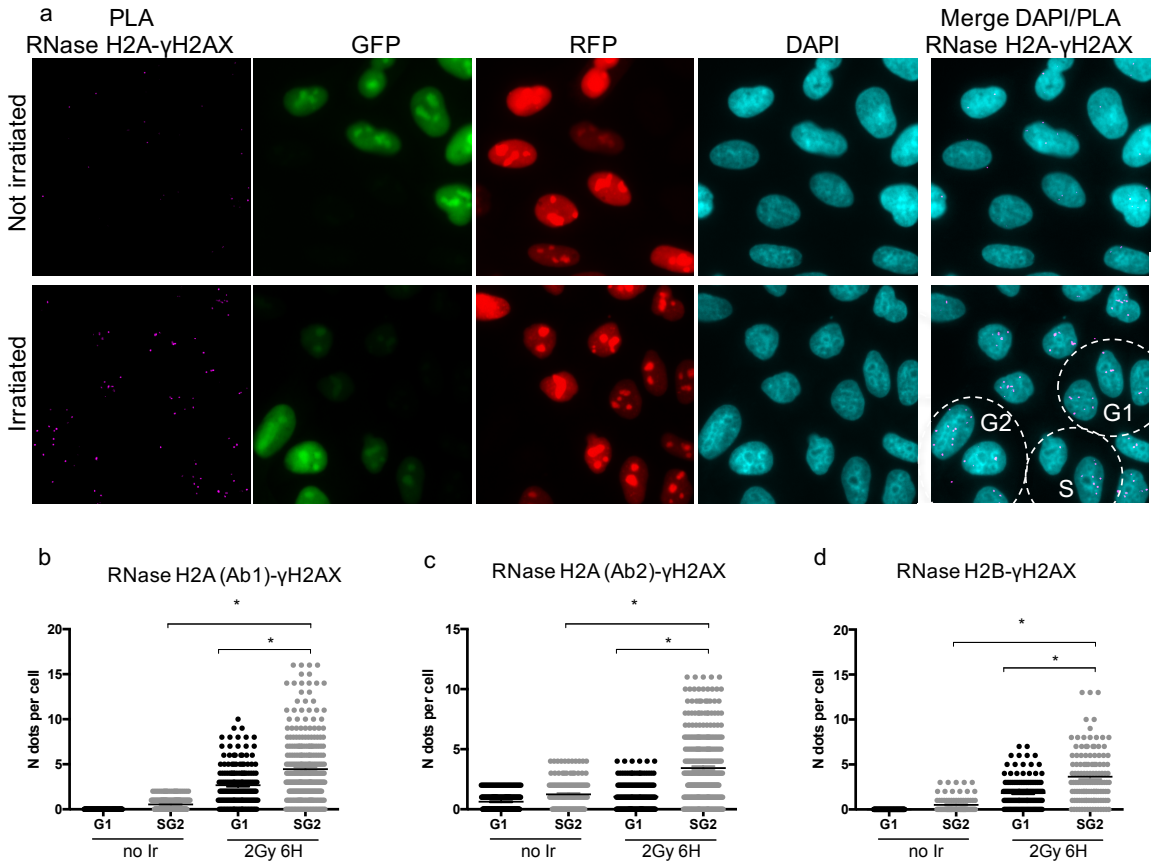

Figure 35: PLA reveals preferential γH2AX-RNase H2 interaction during S/G2 phase
PLA between γH2AX and either RNase H2A, detected with two different antibodies (a and b), and RNase H2B (c), was performed on HeLa-FUCCI cells not irradiated or irradiated 2Gy and fixed 6 hours later. Dot plots represent the number of PLA dots per cell and error bars are s.e.m from 3 independent experiments.

These results indicate that RNase H2 localize to DSBs preferentially during S/G2 phase of the cell cycle and they are not biased by variations of γH2AX foci or RNase H2 protein level during the cell cycle phases analyzed, as demonstrated by the unaltered number of γH2AX foci (figure 36a and b) and the unchanged RNase H2A and RNase H2B pan-nuclear signals (figure 36c) in G1 and S/G2 HeLa-FUCCI cells.

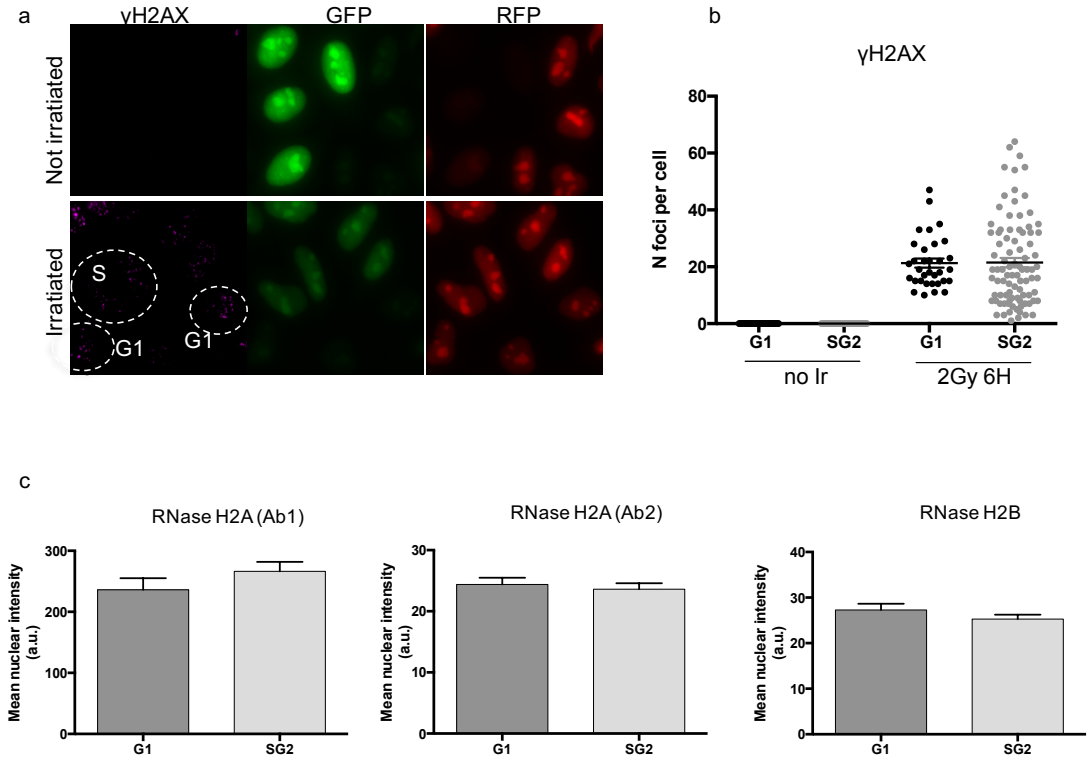

Figure 36: RNase H2 and γH2AX levels are comparable during G1 and S/G2 cell cycle phase
Immunofluorescence analysis was performed on not irradiated and irradiated HeLa-FUCCI cells stained for γH2AX (a), RNase H2A, detected with two different antibodies (b and c), and RNase H2B (d). The dot plot represents the number of foci per nucleus. The bar graphs represent the mean nuclear intensity. Error bars are s.e.m from 2 independent experiments.

Since PLA analyses suggested RNase H2 recruitment to DSBs preferentially during S/G2 cell cycle phase, in collaboration with Eli Rothenberg's group at NYU and his postdoc Donna Whelan, we monitored RNase H2A recruitment to DSBs by super-resolution microscopy throughout the cell cycle. In order to test this, we treated G1 and S/G2 synchronized U2OS cells with the radiomimetic drug NCS and immunostained them for γH2AX and RNase H2A. As shown in figure 37, RNase H2A colocalizes with γH2AX preferentially in S phase damaged cells.

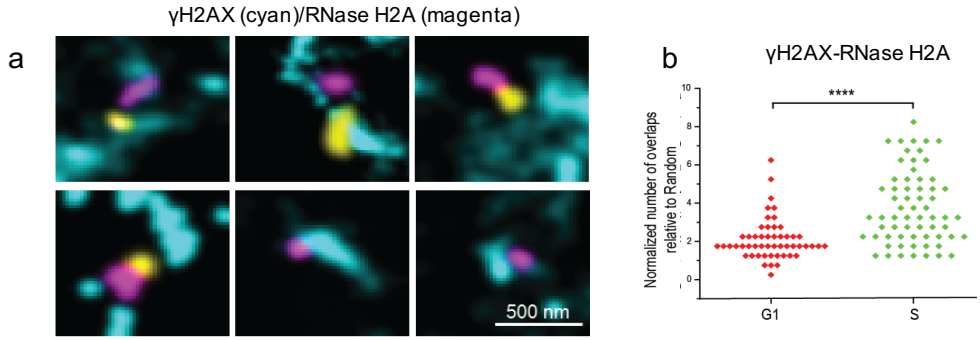

Figure 37: γH2AX and RNase H2A colocalize preferentially in NCS-treated S phase cells
a) Representative images of γH2AX (cyan)-RNase H2A (magenta) colocalization in NCS treated S phase U2OS cells. b) dot plot represents the number of γH2AX and RNase H2A colocalization in G1 and S phase cells relative to random (>50 cells, n=3).

Overall these results, generated through several different techniques and also in collaboration with another lab, consistently indicate that RNase H2 is recruited to DSBs preferentially during S/G2 phase of the cell cycle.

3.3.5 RNase H2A interacts with BRCA1, BRCA2 and RAD51

Based on the observation that RNase H2A localizes to DSBs preferentially in S/G2 phase cells, we decided to monitor the extent of colocalization of RNase H2A with BRCA1 and RAD51. We observed a significant rate of colocalization of RNase H2A with both BRCA1 (figure 38b) and RAD51 (figure 38c) in NCS treated cells.

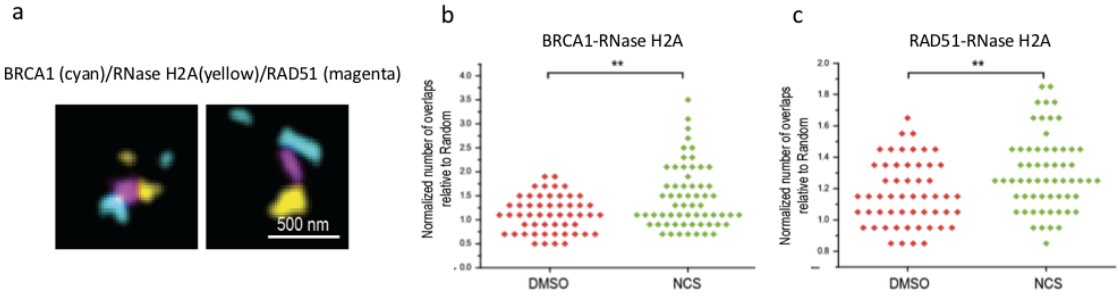

Figure 38: RNaseH2A colocalizes with BRCA1 and RAD51 in NCS-treated S phase cells
a) Representative images of BRCA1 (cyan), RNase H2A (yellow), RAD51 (magenta) colocalization in NCS-treated S phase U2OS cells. Dot plot represents the number of RNase H2A and either BRCA1 (b) and RAD51 (c) colocalization in DMSO or NCS-treated S phase U2OS cells relative to random (>50 cells, n=3).

Next, I planned to test whether RNase H2 colocalization with BRCA1 and RAD51 was a hint of an interaction between the two proteins. For this, I collaborated with Marek Adamowicz, a postdoc in our lab, who performed immunoprecipitation experiments of RNase H2A from cell lysates of HEK293T cells exposed or not to ionizing radiations. We observed that RNase H2A coimmunoprecipitates and thus interacts with BRCA1, RAD51

(figure 39a), BRCA2, and PALB2 (figure 39b), independently of DNA damage induction – these experiments were performed in the presence of benzonase, a nuclease that degrades all nucleic acids in the extract, thus excluding that this interaction was mediated by nucleic acids. Since BRCA1 is found in many different complexes upon damage, we tested whether RNase H2A interaction could also be observed in other BRCA1 complexes, including the BRCA1-A or BRCA1-C, as discussed in the introductory section "The multiple roles of BRCA1 in the DDR" and shown in figure 1. For this reason, we probed the RNase H2A immunoprecipitates for RAP80 and CtIP, two members of the BRCA1-A and BRCA1-C complex, respectively. As shown in figure 39c, no interaction with RAP80 and CtIP was observed. These results indicate that RNase H2A interacts with BRCA1 and RAD51 and that this complex formation is specific to the components of the BRCA1 complex involved in HR.

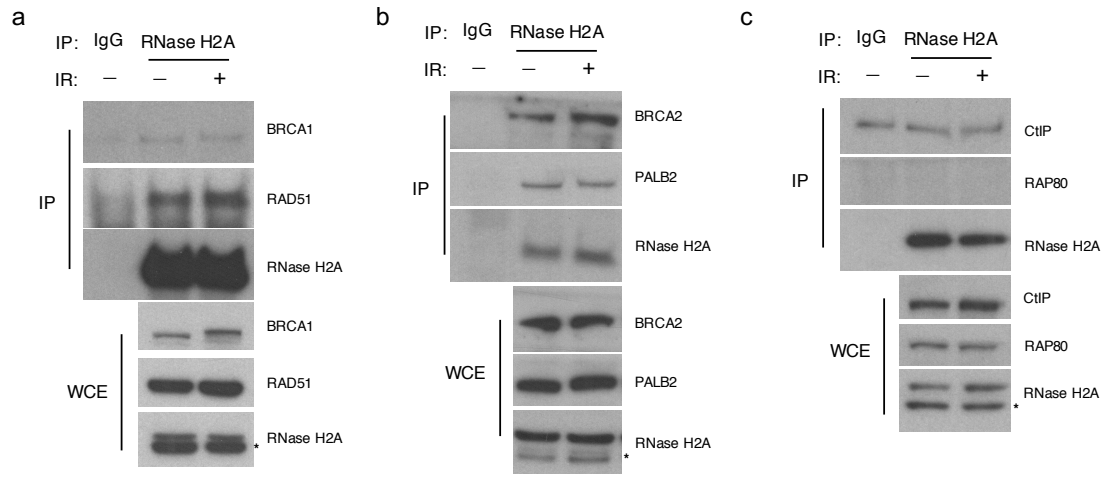

Figure 39: RNase H2A interacts with BRCA1, BRCA2, and RAD51, but is not part of other BRCA1 complexes
Immunoblot analysis of the immunoprecipitations of RNase H2A in not irradiated or irradiated HEK293T cells. BRCA1, RAD51 (a), BRCA2, PALB2 (b), CtIP and Rap80 (c) were probed. (WCE-Whole cell extract).

To determine which of the above proteins was directly binding to RNase H2A, we prepared cell lysates from cells depleted either of BRCA1 or RAD51 by siRNA transfection and we performed RNase H2A immunoprecipitations with them. We observed that, while BRCA1 absence does not affect RNase H2A interaction with RAD51, the interaction of RNase H2A with BRCA1 is lost upon RAD51 depletion. This suggests that RNase H2A interacts with BRCA1 through RAD51 (figure 40).

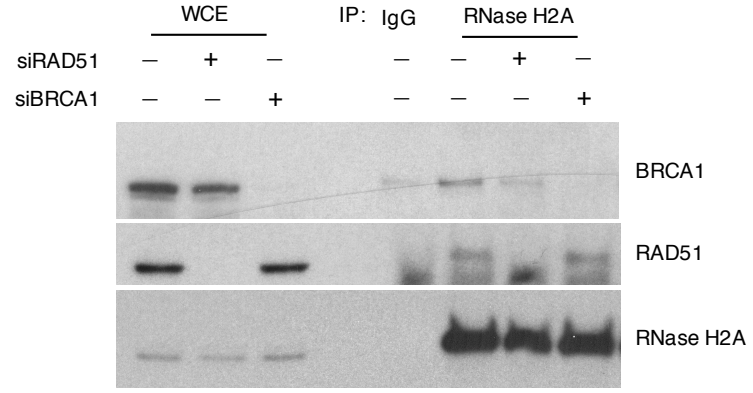

Figure 40: RNase H2A interacts with BRCA1 through RAD51
Immunoblot analysis of RNAse H2A immunoprecipitation in HEK293T cells depleted for BRCA1 or RAD51. (WCE-Whole cell extract).

Next, in order to identify the domain of RAD51 responsible for the interaction with RNase H2A, we used sequential fragments of the RAD51 protein fused with the glutathione S-transferase (GST) to perform GST-pulldowns in cells expressing YFP-tagged RNase H2A. We observed a specific interaction between recombinant RNase H2A and GST-RAD51 fragment encoding for the middle portion of RAD51 (184-257aa). Additionally, we noticed a much weaker interaction with the 101-184aa and 257-337aa fragments (Figure 41).

Altogether, these results show that RNase H2A interacts directly with RAD51 through the RAD51 region responsible for the interaction with BRCA2 and PALB2. Moreover, RNase H2A, through RAD51, also interacts with BRCA1 and BRCA2.

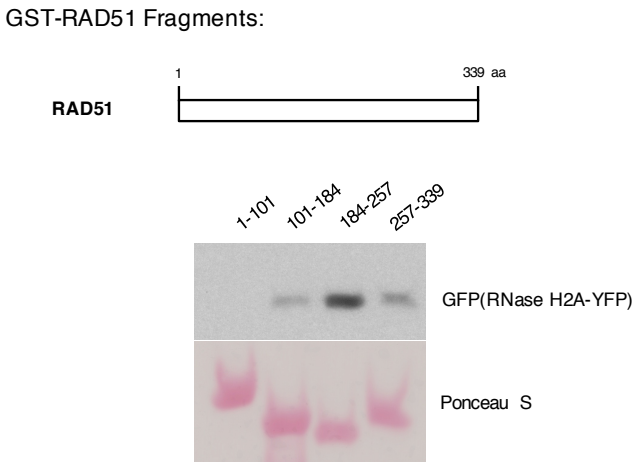

Figure 41: GST pulldown reveals the RAD51 fragments interacting with RNase H2A
Immunoblot analysis of GST pulldowns with sequential non-overlapping GST-RAD51 fragments. HEK293T cells were transfected with RNase H2A-YFP, lysed and used in the pull down experiment.

4 Discussion

4.1 The impact of DSB-induced RNAs and DNA:RNA hybrids on HR

4.1.1 DSB-induced transcription: RNA joins the DNA damage world

For years, DDR has been considered a proteins-only signaling cascade. However, recently, evidence supporting a role for RNA in this process has emerged. In 2012 our group and others reported the generation upon DSB of sncRNAs with the sequence of the damaged locus (Francia et al., 2012, Wei et al., 2012, Michalik et al., 2012). These RNA species, named DDRNAs and diRNAs, were reported to be involved in DDR signaling (Francia et al., 2012, Francia et al., 2016) and HR (Gao et al., 2014, Wei et al., 2012), respectively. Such damage-induced sncRNAs generation was reported to require RNAi proteins-mediated nuclease activities, thus suggesting the existence of a longer precursor transcript.

The affinity of RNA pol II for DNA ends was known for several years (Dynan and Burgess, 1981), but no physiological relevance was attributed to this observation. However, very recently our lab demonstrated in different *in vivo* and *in vitro* systems that the apical DDR protein complex MRN contributes to the recruitment of the transcriptionally active RNA pol II to exposed DNA ends upon damage (Michelini et al., in press). Upon DSB generation, RNA pol II-mediated bi-directional transcription from the DNA ends generates two RNA species, named dilncRNAs *from* (see figure 42). In addition, RNA pol II transcription toward the break generates other RNA species known as dilncRNAs *to,* at a lower extent compared to dilncRNAs *from*. dilncRNAs are processed by DROSHA and DICER to generate DDRNAs whose localization is mediated by their binding to the unprocessed complementary dilncRNA, via RNA:RNA interaction. Although the exact mechanism of DDRNAs function in DDR has not been fully understood, our lab demonstrated that DDRNAs promote DDR at least in part by associating with 53BP1 and mediating its recruitment to the damaged locus (Michelini et al., in press). However, whether the interaction is direct or it requires additional proteins or their modifications remains to be addressed.

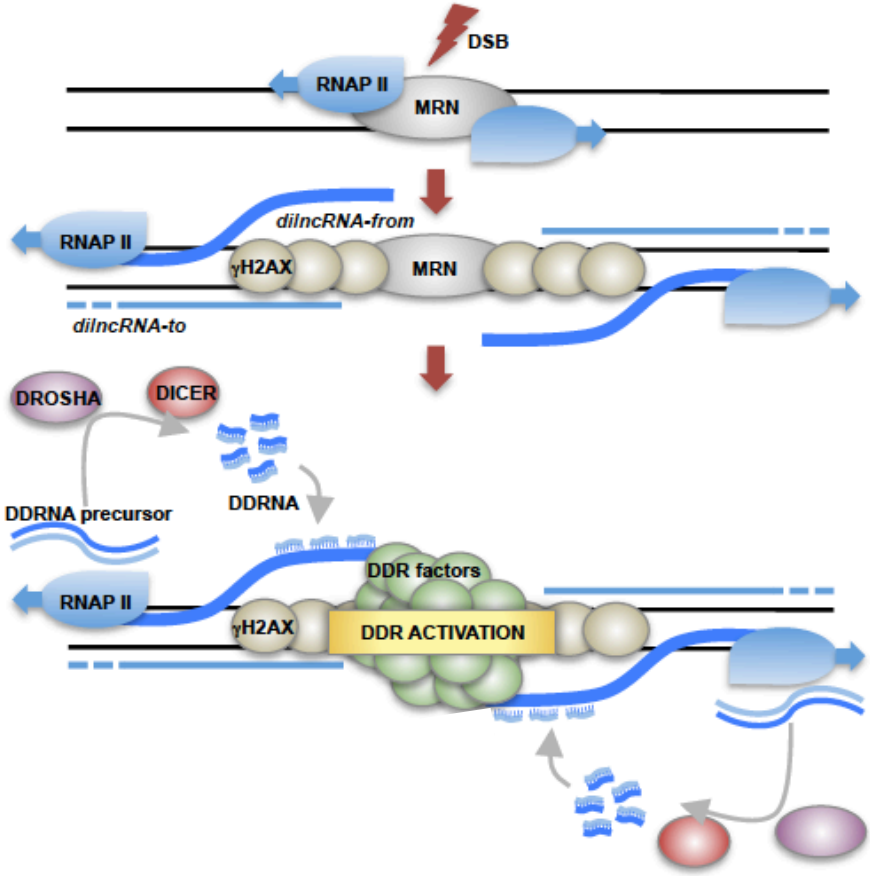

adapted from (Michelini et al., in press)

Figure 42: DilncRNAs synthesis at DSBs
Upon DSB, RNA pol II is recruited to the DNA ends. RNA pol II bi-directional transcription generates two different RNA species, named dilncRNAs *from* and dilncRNAs *to*. dilncRNAs are processed by DROSHA and DICER to produce DDRNAs, which localize at DSBs via RNA:RNA interaction with the precursors dilncRNAs and contribute to DDR activation.

4.1.2 DSB-induced de novo transcription and DSB-induced silencing: a compromise exists.

Although an increasing amount of evidence supports *de novo* transcription from sites of damage, the observation of damage-induced transcriptional silencing could seem in contrast with this (Shanbhag et al., 2010, Pankotai et al., 2012). Indeed, it has been observed that transcription of a reporter gene is inhibited via ATM-mediated chromatin condensation when a cluster of DSBs is generated in close proximity of the gene (Shanbhag et al., 2010). Additionally, RNA pol II exclusion from laser microirradiation sites has been observed (Beli

et al., 2012, Chou et al., 2010). DSB-induced *de novo* transcription and transcriptional silencing are clearly two distinct events but they are not mutually exclusive. It is important to note, for example, that, while DSB-induced transcriptional repression is ATM-dependent, dilncRNAs transcription is not affected by ATM inhibition (Michelini et al., in press). The observed RNA pol II depletion from sites of laser microirradiation is hard to interpret unambiguously since the low resolution of the canonical imaging techniques may not allow to discriminate between RNA pol II exclusion, associated with transcriptional inhibition, and DSB-induced RNA pol II recruitment, as we observed both by super-resolution imaging and ChIP (Michelini et al., in press). It is possible that DSB-induced *de novo* transcription and transcriptional silencing are temporally regulated: the first is an early event in DDR and, by promoting DDR and, in particular, ATM activation, may even contribute to RNA pol II exclusion from sites of damage, thus causing transcriptional silencing.

4.1.3 DNA:RNA hybrids are formed at DSBs

A possible consequence of RNA pol II transcription from DSBs is the generation of DNA:RNA hybrids. Although usually considered a by-product of cellular metabolism and one of the causes of genome instability, the role of DNA:RNA hybrids in several physiological processes has been recently appreciated (Aguilera and Gomez-Gonzalez, 2017). For example, it has been shown that DNA:RNA hybrids control gene expression (Ginno et al., 2013, Ginno et al., 2012) and termination of transcription (Skourti-Stathaki et al., 2011, Skourti-Stathaki et al., 2014). Exposed DNA ends such as those generated upon DSB resection are potential templates for RNA pairing and, thus, DNA:RNA hybrids formation. DNA:RNA hybrids accumulation at DSBs has been recently described in *Schizosaccharomyces pombe* (Ohle et al., 2016). In human cells, DNA:RNA hybrids formation at DSBs has not been demonstrated yet, although some data seem to suggest it. It has been observed, for example, that catalytically inactive *Escherichia coli* RNase H, used as a tool to detect DNA:RNA hybrids, accumulates at laser micro-irradiation regions (Britton

et al., 2014). Moreover, it has been proposed that the human RNA-unwinding protein DEAD box 1 (DDX1) is recruited to DSBs possibly via DNA:RNA hybrids (Li et al., 2016). Although these data indirectly suggested DNA:RNA hybrids formation upon DNA damage, a better characterization of the process that may lead to their formation was still missing. It was not clear, for example, whether the DNA:RNA hybrids observed upon damage where the result of *de novo* transcription, according to the recent model of damage-induced RNA pol II transcription from the broken DNA ends (Michelini et al., in press) (see figure 42), or were the result of pairing of pre-existing transcripts to a more open and easily accessible DNA template generated upon damage. Here, I document DNA:RNA hybrids formation at DSBs by independent imaging techniques and DNA:RNA hybrids immunoprecipitation (DRIP). More specifically, I show DNA:RNA hybrids accumulation at a damaged repetitive exogenous site integrated within the genome by immunofluorescence with the S9.6 antibody; I observe an increase in DNA:RNA hybrids levels in the nucleus of irradiated cells, as detected by a GFP-tagged catalytically inactive RNase H1 expressed in cells lacking the endogenous one; I also describe DNA:RNA hybrids accumulation at DSBs in two different cellular systems (I-PpoI or AsiSI endonucleases expressed in different cell lines) at genic and inter-genic regions, by performing DRIP with the S9.6 antibody. Importantly, the observation that DNA:RNA hybrids accumulate upon damage at DSBs located in non-genic regions excludes the possibility that damage-induced DNA:RNA hybrids are the result of the annealing of pre-existing transcripts with the template DNA. It seems, instead, that these hybrids are the result of the hybridization of dilncRNAs with the damaged template DNA. Similarly to dilncRNAs, DNA:RNA hybrids do not accumulate at DSBs when RNA pol II transcription is acutely inhibited, thus confirming that they are the result of RNA pol II-mediated *de novo* transcription. The possibility that DNA:RNA hybrids are the result of DDRNAs hybridization to the template DNA can be excluded since we observed that DDRNAs localization to DSBs is not affected by RNase H1 overexpression (Michelini et al., 2017).

4.1.4 DSB-induced DNA:RNA hybrids form preferentially in S/G2 phase cells on resected DNA ends

Since the accessibility of the template DNA is a crucial step in DNA:RNA hybrids formation, it is likely that damage-induced DNA:RNA hybrids form preferentially during the S/G2 phase of the cell cycle, when resected DNA ends are available. In yeast, although not supported by experimental data, it has been proposed that DNA:RNA hybrids are generated at DSBs by pairing of RNA species to the resected DNA ends (Ohle et al., 2016). Our results obtained by DRIP in G1 and S/G2 cells and by immunofluorescence analyses with canonical and super-resolution microscopy reveal that damage-induced DNA:RNA hybrids accumulate preferentially in the S/G2 cell cycle phase, when they colocalize with HR proteins including BRCA1 and RAD51. DRIP experiments in cells depleted of CtIP, a key protein in DNA end resection, further confirm the hypothesis that DNA:RNA hybrids accumulate only on resected DNA ends and reveal indeed a strong decrease in damage-induced DNA:RNA hybrids accumulation upon CtIP depletion. However, it is known that CtIP interacts with MRN to promote DNA end resection (Sartori et al., 2007) and we reported that MRN activity is required for dilncRNAs generation (Michelini et al., in press). Therefore, it cannot be excluded that the reduction of DNA:RNA hybrids levels at DSBs upon CtIP depletion is caused by impaired MRN activity, which in turn results in lower dilncRNAs synthesis. In order to further confirm the impact of DNA end resection on DNA:RNA hybrids formation at DSBs, I plan to monitor DNA:RNA hybrids levels at DSBs upon EXO1 depletion, an exonuclease which only acts in the later steps of DNA end resection and does not impact on the early steps of the process.

In line with the hypothesis that DNA:RNA hybrids form on the resected DNA ends, the DNA:RNA hybrids-dependent recruitment of the RNA-unwinding protein DDX1 to DSBs has also been reported to be dependent on DNA end resection (Li et al., 2016). The possibility that DNA:RNA hybrids stronger detection in S/G2 is due to an increase of their processing and degradation in G1 phase is unlikely since G1 exposed DNA ends may not be

as good a template for RNA pairing as resected and easily accessible DNA ends. In addition, the recruitment of RNase H2 to S/G2 phase damaged cells, as discussed below, independently supports the notion of DNA:RNA hybrids accumulation in this specific cell cycle phase. The observation that DNA:RNA hybrids accumulation is regulated by DNA end resection also suggests that the dilncRNAs forming DNA:RNA hybrids likely are "dilncRNAs *from*" RNAs, that are complementary to the resected DNA ends.

4.1.5 A new connection between DNA:RNA hybrids and DSB repair

Once established that DNA:RNA hybrids form at DSBs, it remains to be elucidated what is their function. It is known that RAD51 mediates DNA:RNA hybrids formation in yeast RNA processing mutants (Wahba et al., 2013). On the contrary, it has been shown that DNA:RNA hybrids accumulate in BRCA1 and BRCA2 depleted cells (Bhatia et al., 2014, Tan et al., 2017). This is in line with the model I propose in which BRCA2 recruits the RAD51-RNase H2 complex to DSBs to degrade DNA:RNA hybrids. The increased DNA:RNA hybrids level observed by Bhatia et al. in BRCA1 and BRCA2 depleted cells could be caused by the inability of RNase H2 to recognize and degrade DNA:RNA hybrids formed at endogenous DSBs. Overall, the impact of HR proteins on DNA:RNA hybrids levels suggests a strong link between these proteins and DNA:RNA hybrids metabolism. It has been shown, for example, that DNA:RNA hybrids accumulation upon DDX1 depletion impairs HR in the DR-GFP system (Li et al., 2016). Conversely, in yeast, a tight regulation of DNA:RNA hybrids level at DSBs seems to be necessary for HR since excessive or insufficient DNA:RNA hybrids levels have been reported to negatively affect this repair phatway (Ohle et al., 2016). Recent data also suggest a role for SENATAXIN in DNA repair (Becherel et al., 2013, Yuce and West, 2013). SENATAXIN prevents transcription-associated DNA:RNA hybrids accumulation (Mischo et al., 2011) and in yeasts it associates with replication forks and protects their stability when they encounter highly transcribed genes (Alzu et al., 2012). It has been shown in mice that SENATAXIN facilitates meiotic

recombination (Becherel et al., 2013) and in human cells, it forms transcription- and DNA:RNA hybrids-dependent DNA damage foci in S/G2 phase, when it colocalizes with DDR proteins, including 53BP1 and BRCA1 (Yuce and West, 2013). Although a clear picture has not been yet drawn, all these findings support a role for DNA:RNA hybrids in HR.

4.1.6 The role of DSB-induced RNA in HR

The observation that RNA is necessary for the recruitment of HR proteins to DSB suggests a role for DNA:RNA hybrids in this process. Here, I show that inhibition of RNA pol II transcription impairs BRCA1, BRCA2, and RAD51 foci formation upon DSB. Interestingly, impaired RAD51 recruitment to DSBs is not caused by defective DNA end resection, since the efficiency of this process is mildly increased upon transcriptional inhibition. The observed proficient resection in the absence of BRCA1 recruitment may appear controversial, since BRCA1 modulates DNA end resection by interacting with CtIP. However, it has been shown that BRCA1-CtIP interaction is dispensable for resection (Reczek et al., 2013) and BRCA1 mainly controls this process by counteracting the inhibitory effect of 53BP1 (Escribano-Diaz et al., 2013). Upon transcriptional inhibition 53BP1 recruitment to DSBs is inhibited as much as BRCA1 recruitment (Michelini et al., in press). As a consequence, in the absence of both 53BP1 and BRCA1, DNA end resection is likely to be proficient. Indeed, the undiminished number of RPA and P-RPA Ser4/8 foci detected by immunofluorescence upon transcriptional inhibition is consistent with that and their actual increase may be caused by either a higher efficiency of the process, or, more likely, by an increased availability of the ssDNA strand for the single-strand DNA binding protein RPA, since no complementary RNA species are transcribed. Similarly, detection of BrdU on ssDNA, as measured by native staining, may be masked by the presence of a DNA:RNA hybrid and thus transcriptional inhibition may improve its detection. Increase of the BrdU signal upon RNase H treatment in damaged cells could confirm this hypothesis.

Potential applications of ASOs-mediated HR inhibition

The involvement of dilncRNAs in HR is further confirmed by the observation that ASOs matching and inhibiting the function of dilncRNAs potentially forming in the DR-GFP system inhibit homologous recombination (HR)-mediated repair. HR and single strand annealing (SSA) are two pathways that exploit sequence homology to repair damaged DNA, as described in the paragraph "HDR" of the introduction. Once broken DNA ends are resected, HR-mediated repair occurs via RAD51-mediatd invasion of the homologous sequence, while SSA anneals two homologous sequences exposed on the resected DNA ends through RAD52, with the consequent loss of genetic material. Interestingly, treatment of TRI-DR-U2OS cells with ASOs matching either dilncRNAs *from* or *to* only impairs HR, while not significantly affecting SSA, thus confirming that dilncRNAs are necessary for HR proteins recruitment to the DSBs and not for the DNA end resection step of the HDR-based pathways. It is possible to envision that ASOs treatment, as well as transcriptional inhibition, affects BRCA1 and RAD51 recruitment to DSBs thus impairing HR-mediated repair. The impact of ASOs treatment on recruitment of HR factors should be checked to confirm this hypothesis. According to the previously discussed role of BRCA1 in controlling DNA end resection, it would be expected that impaired BRCA1 localization to DSBs would also impact on DNA end resection. On the contrary, I observe that SSA is efficient upon ASOs treatment. Since others in the lab observed that ASOs treatment inhibit 53BP1 recruitment to DSBs (Michelini et al., in press), the same reasoning applied for the results obtained upon transcriptional inhibition can be useful to interpret these results. In brief, since BRCA1 mainly controls DNA end resection by counteracting the barriers posed by 53BP1 to this process, in the absence of both 53BP1 and BRCA1, DNA end resection efficiency, and consequently SSA, is not affected.

The observation that HR is inhibited upon treatment with ASOs matching either dilncRNAs *from* or *to* supports the idea that dilncRNAs control this process through a complex and multi-layered mechanism. It is known already that diRNAs, RNA species similar to

DDRNAs, control HR by acting on BRCA1 and RAD51 recruitment to DSBs (Gao et al., 2014, Wang and Goldstein, 2016). Similarly to DDRNAs, diRNAs are generated by processing of a longer precursor transcript. By targeting dilncRNAs *from* and *to*, ASOs inhibit DDRNAs biogenesis. Additionally, they may also directly inhibit DDRNAs function, thus inhibiting HR by impairing the recruitment of HR proteins to the DSB.

ASOs are becoming a widely used tool to block the functions of RNA molecules, including ncRNAs (McClorey and Wood, 2015) and they were recently used in our lab to inhibit DDR at site-specific loci (Michelini et al., in press), including telomeres in cultured cells and in mice (Rossiello et al., 2017). HR modulation by ASOs may be a powerful tool with several applications. Although inhibiting repair of a single DSB may not kill the cells, it is possible that cell death could be achieved by inhibiting repair of several DSBs with a known sequence. This is the case of oncogene induced fragile sites, whose sequence can be mapped, thus allowing inhibition of DDR and HR-repair by treatment with complementary ASOs. It could also be conceived that restriction enzymes selectively targeted to tumor cells and treatment with sequence-specific ASOs could allow DDR and HR-inhibition in these cells, thus resulting in tumor cells death.

4.1.7 RNA and DNA:RNA hybrids mediate BRCA1 recruitment to DSB

The specific role of RNA in HR is further confirmed by the observed disruption of BRCA1 foci upon RNase A treatment of irradiated cells, which degrades both RNAs and DNA:RNA hybrids in the experimental conditions used. Further confirming the contribute of DNA:RNA hybrids in BRCA1 recruitment to DSBs, BRCA1 foci are also dismantled upon RNase H treatment. Persistency of RPA foci upon treatment with RNase A and RNase H not only demonstrates the specificity of the treatment, but confirms the results obtained with RNA pol II inhibitors and ASOs treatment. Impaired BRCA1 recruitment is also observed upon RNase H1 overexpression. Moreover, *in vitro* BRCA1 and the BRCA1-BARD1 constitutive heterodimer bind DNA:RNA hybrids even with higher affinity compared to dsDNA, thus

strengthening the idea that BRCA1 recruitment to DNA lesions may be facilitated by DNA:RNA hybrids formation. A similar scenario has been already envisioned by a recent publication suggesting DNA:RNA hybrids-mediated BRCA1 recruitment to the termination site of the β-actin gene where it recruits, in turn, SENATAXIN, thus suppressing DNA:RNA hybrids associated genome instability (Hatchi et al., 2015). The link between BRCA1 and transcription has been known since long time. The interaction between BRCA1 and RNA pol II and its ability to modulate transcription was known since the 90ies (Scully et al., 1997, Chapman and Verma, 1996, Anderson et al., 1998, Neish et al., 1998) and recent data further strengthen this link by showing, for example, that BRCA1 recognizes miRNA precursor and promotes their processing by interacting with DROSHA (Kawai and Amano, 2012).

Given the impact of transcription inhibition, RNase A and RNase H treatment on focal accumulation of HR factors, and the decreased HR efficiency upon ASOs treatment, it can be concluded that dilncRNAs control HR, in part by modulating BRCA1 recruitment to DSBs via DNA:RNA hybrids formation. The complete abrogation of BRCA1 focal accumulation at DSBs upon transcriptional inhibition compared to the moderate reduction observed upon RNase H treatment and RNase H overexpression, further suggests that RNA pol II-mediated transcription controls BRCA1 recruitment through several redundant pathways. As already mentioned for ASOs treatment, it is possible that DDRNAs contribute to this process (Gao et al., 2014, Wang and Goldstein, 2016). Moreover, the possibility that BRCA1 recruitment to DSBs is controlled by direct interaction with RNA pol II cannot be excluded. It is possible that the residual BRCA1 recruitment upon RNase H overexpression is sufficient to mediate RAD51 recruitment and HR. Another possibility is that RNase H overexpression only delays BRCA1 loading and this can be the reason why no defect in RAD51 loading to DSBs and HR-mediated repair is observed upon RNase H overexpression.

4.2 RNase H2: a new player in DSB repair

While a certain level of DNA:RNA hybrids at DSBs may promote repair by facilitating BRCA1 recruitment, it is also possible that accumulation of these hybrids may negatively affect DSB repair. It has already been reported in a recent paper that accumulation of DNA:RNA hybrids at the DR-GFP locus in human cells impairs HR (Li et al., 2016). In line with these results, it has been demonstrated in human and drosophila cells that EXOSC10/RRP6, the catalytic component of the RNA exosome with a 3' to 5' exoribonuclease activity (Houseley et al., 2006), localizes to DSBs, interacts with RAD51, and its activity is required for RAD51 loading to DSBs, although no impact on DNA end resection has been tested (Marin-Vicente et al., 2015). Yeast Rrp6 is necessary for RPA, but not RAD51, loading on resected ssDNA ends (Manfrini et al., 2015). Although the two observations do not fit perfectly, they support the idea that in the absence of RRP6, excessive RNA and, possibly, DNA:RNA hybrids accumulation at DSBs inhibit the loading of RPA and RAD51 on the resected DNA ends. However, in yeast Rrp6 mutants defective RPA loading is not restored by RNase H1 overexpression (Manfrini et al., 2015). Differently, at telomeres, DNA:RNA hybrids seem to favor HR: RNase H1 has been shown to regulate TERRA DNA:RNA hybrids at telomeres that uses ALT, an HR-based telomere elongation mechanism (Arora et al., 2014); in yeast, increased DNA:RNA hybrids caused by impaired RNase H2 localization, favors telomere elongation (Graf et al., 2017). In yeast, only a certain level of DNA:RNA hybrids at DSBs facilitates DSB repair: too many hybrids inhibit RPA binding on the resected DNA ends; on the other hand, lack of hybrids allows excessive resection and inhibit HR because other pathways, such as SSA, are preferred (Ohle et al., 2016). For this reason, DNA:RNA hybrids levels at the damaged loci must be tightly regulated. At the cellular level, control of DNA:RNA hybrids level is continuously guaranteed by either avoiding DNA:RNA hybrids formation, through binding of nascent RNA with RNA binding proteins, or by resolution or degradation of already formed hybrids

by helicases like SENATAXIN, and RNase H enzymes, respectively. In eukaryotic cells, DNA:RNA hybrids are degraded by RNase H1 and RNase H2, a trimeric protein composed of RNase H2A, B, and C subunits (Cerritelli and Crouch, 2009). In particular, RNase H2 has already been shown to resolve DNA:RNA generated by RNA polymerases during transcription (El Hage et al., 2010, Lin et al., 2010).

4.2.1 RNase H2 depletion impacts on HR by reducing HR proteins levels

Yeast mutants for the cellular RNase H enzymes show decreased HR levels (Ohle et al., 2016). In our case, depletion of either RNase H1 or RNase H2 to study the impact of DNA:RNA hybrids accumulation on HR could not be used: while RNase H1 knock-down could not be obtained with the tools available in the lab, RNase H2 depletion reduced the levels of key HR proteins. Although this result did not allow us to recapitulate in our hands the impact of DNA:RNA hybrids accumulation on HR, it revealed a new layer of control of this pathway by RNase H2, possibly through DNA:RNA hybrids accumulation. Indeed, in the last few years DNA:RNA hybrids have emerged as regulators of gene expression (Skourti-Stathaki and Proudfoot, 2014). It is possible, therefore that expression of HR genes is modulated by DNA:RNA hybrids and aberrant DNA:RNA hybrids accumulation, caused by RNase H2 depletion, could impact on expression of those genes. This could be a mechanism that cells have evolved to push repair toward NHEJ in the absence of a key enzyme responsible for removal of DNA:RNA hybrids that would impede, when too many, HR repair. Moreover, it could also be possible that the reduced expression of HR proteins in the absence of RNase H2 is the result of a feedback mechanism that controls the expression of components of the same complex to keep the right stoichiometry. For example, feedback regulation of gene expression at the post-transcriptional level is common. There are examples of ribosomal and RNA-binding proteins which repress their translation by binding their mRNAs (Philippe et al., 1993, Dabeva and Warner, 1993, Boelens et al., 1993).

Another example is the negative regulation of DGCR8 expression by the Drosha-DGCR8 complex through cleavage of DGCR8 mRNA (Han et al., 2009).

4.2.2 RNase H2 joins BRCA2 and RAD51

The formation of DNA:RNA hybrids at DSBs and the requirement of a tight regulation of their levels suggest that proteins involved in DNA:RNA hybrids resolution could localize to DSBs. It has already been shown that the human RNA-unwinding protein DDX1 (Li et al., 2016) and the DNA/RNA helicase SENATAXIN (Yuce and West, 2013) localize to DSBs in S/G2 phase cells in a transcription- and DNA:RNA hybrids-dependent way. Here we show by ChIP analysis, PLA, and super-resolution microscopy that RNase H2A, which accounts for the major RNase H activity in mammalian cells, is recruited to DSBs. In line with the cell-cycle regulation of DNA:RNA hybrids accumulation, RNase H2A localization to DSBs is limited to the S/G2 cell cycle phase, despite its level does not change throughout the cell cycle phases as shown here and in mouse cells (Reijns et al., 2012). In S/G2 damaged cells, RNase H2 colocalizes with the HR proteins BRCA1 and RAD51 through direct interaction with RAD51. Immunoprecipitation of the endogenous RNase H2A indeed reveals interaction with BRCA1, BRCA2, and RAD51, but not with RAP80 and CtIP, which form with BRCA1 the BRCA1-A and the BRCA1-C complexes, respectively. The direct interaction of RNase H2A with RAD51 has been shown by RNase H2A immunoprecipitation on cells depleted for BRCA1 and RAD51: in the absence of BRCA1 RNase H2A-RAD51 interaction is kept, while in the absence of RAD51 BRCA1-RNaseH2A interaction is lost. From this result it can also be inferred that the binding of RNase H2A with RAD51 is not mediated by BRCA2. Indeed, in the context of RAD51 depletion BRCA2 would still bind both RNase H2 and BRCA1, therefore the BRCA1-RNAse H2 indirect interaction would have not been lost, as we see instead. GST-pulldowns using GST fragments of the entire RAD51 proteins further confirm the specificity of RNase H2A-RAD51 interaction. Moreover, the GST-pulldown not only provides evidence of the specific

RNase H2A-RAD51 interaction, but also allows to exactly localize the RNase H2 interaction domain in the RAD51 fragment already involved in BRCA2 and PALB2 binding. RAD51-mediated RNase H2 recruitment to DSBs would allow the degradation of the DSB-induced DNA:RNA hybrids in the later steps of HR, when DNA:RNA hybrids are not anymore needed, thus facilitating RAD51 loading on the ssDNA ends. This model could also explain the recently emerging link between BRCA1, BRCA2 and DNA:RNA hybrids. However, since the DNA:RNA hybrids accumulation in BRCA1 and BRCA2 depleted cells is not cell-cycle dependent and is not observed upon RAD51 depletion, it is possible that BRCA2 favors DNA:RNA hybrids resolution through two distinct mechanisms: in undamaged cells, it recognizes the branched structures in R-loops, that are similar to the replicative intermediates to which it binds (Lomonosov et al., 2003, Schlacher et al., 2011) and exposes the DNA:RNA hybrids to further processing by other factors (Bhatia et al., 2014); in damaged cells, BRCA2 recruits RAD51 and RNase H2, thus directly contributing to DNA:RNA hybrids degradation. The effect of BRCA2 and RAD51 depletion on DNA:RNA hybrids level at DSBs will finally prove whether RAD51-mediated RNase H2 recruitment to DSBs is needed for DNA:RNA hybrids degradation. The discrepancy between the observation that RAD51 favors DNA:RNA hybrids formation in RNA processing mutants in yeast (Wahba et al., 2013) and our results could be explained by a different role of RAD51 at damaged and undamaged loci, although we observe that RAD51 binding with RNase H2 is independent of DNA damage induction.

4.2.3 A possible link between RNase H2 activity and AGS

RNase H2 mutations are associated to the neuroinflammatory AGS syndrome, which pathogenesis is possibly associated to an excessive inflammatory response due to the accumulation of DNA:RNA hybrids (Crow et al., 2006). RNase H2 mutant mice are not viable and an increased genome instability and DNA-damage response is observed during the early embryogenesis (Reijns et al., 2012). This phenotype has been associated to

ribonucleotides incorporation in the genome, although the possibility that DNA:RNA hybrids accumulate in these embryos has not been excluded. Interestingly RNase H2 is expressed globally during embryogenesis and mainly in the highly proliferative cells in adults (Reijns et al., 2012). Highly proliferating cells are the ones that have a higher chance to incorporated ribonucleotides during DNA replication, but they are also the ones that can undergo repair by HR and both are good reasons for a cell to express high levels of RNase H2. It is possible, therefore, that the genome instability observed in the RNase H2 null mice is not only caused by ribonucleotides incorporation, but also by impaired HR-mediated repair. As a consequence of this speculation, stimulating repair by NHEJ in cells lacking the RNase H activity could be a strategy to partially reduce genome instability in these cells. Inhibition of MRN endonuclease activity has been shown to inhibit DNA end resection and HR (Shibata et al., 2014). It could be concluded, therefore, that using this inhibitor in AGC cells could at least reduce the genomic instability associated to HR defects.

4.3 A model of the sequence of events occurring at DSBs

In conclusion, from the results discussed above the following working model can be proposed (figure 43). Upon DSB generation, RNA pol II binds to the DNA ends and transcribes dilncRNAs *from* and *to* (Michelini et al., in press) (figure 43a and b). Pairing of dilncRNA *from* and *to* forms dsRNAs that are cleaved by DICER to generate DDRNAs. Hairpin secondary structures possibly present in the dilncRNAs may require an additional DROSHA-mediated cleavage step for DDRNAs production (figure 43c). DDRNAs contribute to DDR focus formation and signaling and consequently to HR, as already reported by several authors (Wang and Goldstein, 2016, Gao et al., 2014, Wei et al., 2012). If then DNA end resection takes place, dilncRNAs *from* can match the 3' protruding DNA end, thus forming a DNA:RNA hybrid (figure 43d). In principle, DNA:RNA hybrids formation could favor antisense transcription (dilncRNAs *to*), as already proposed at gene terminators (Skourti-Stathaki et al., 2014). However, this needs to be reconciled with the observation that DNA:RNA hybrids form by hybridization of the dilncRNA from with the 3' protruding DNA end (Figure 43 d). At this step, the 5' protruding end which should be used as a template for synthesis of dilncRNAs *to* should have been already degraded.

DNA:RNA hybrids formed on the resected DNA ends contribute to BRCA1 recruitment which, in turn, recruits other HR proteins, including BRCA2 and RAD51. Through direct binding with RAD51, RNase H2 localizes to DSB during S/G2 phase, where it probably degrades DNA:RNA hybrids, thus allowing RAD51 loading and HR completion.

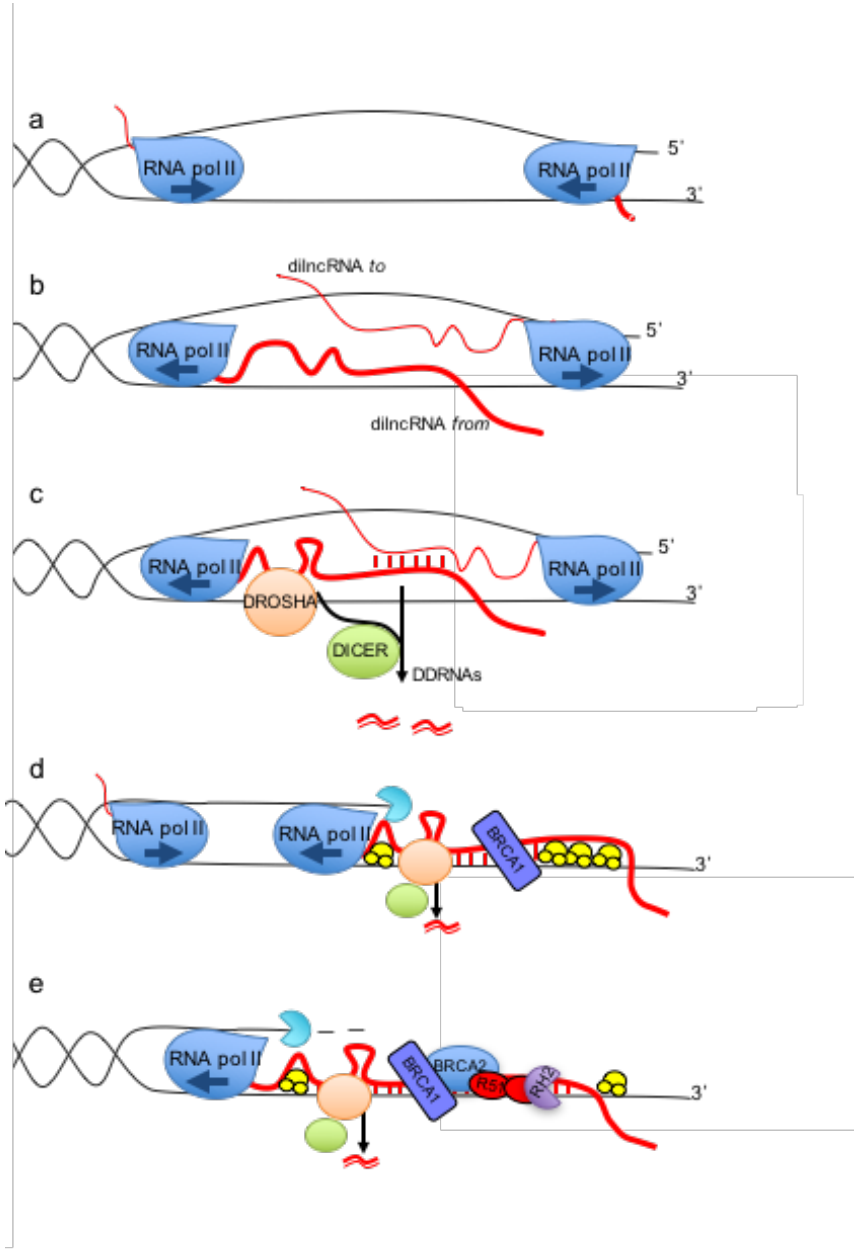

Figure 43: Hypothetical sequence of events occurring at DSBs
RNA pol II transcription at DSBs generates dilncRNAs *from* and *to*. a) Hybridization of dilncRNAs *from* and *to* mediates the formation of dsRNAs that are processed by DICER to generate DDRNAs. RNA hairpin secondary structures may require an additional processing step mediated by DROSHA to produce DDRNAs. b) When DNA end resection takes place, less template for dilncRNA *to* synthesis is available and dilncRNA *from* hybridize to the exposed resected DNA ends. DNA:RNA hybrids recruit BRCA1, which, in turn, promotes their degradation via RAD51-mediated RNase H2 recruitment. Possibly, RNase H2A degrades the DNA:RNA hybrids, thus allowing RAD51 loading and HR.

5 References

AGUILERA, A. 2002. The connection between transcription and genomic instability. *EMBO J,* 21**,** 195-201.
AGUILERA, A. & GAILLARD, H. 2014. Transcription and recombination: when RNA meets DNA. *Cold Spring Harb Perspect Biol,* 6.
AGUILERA, A. & GARCIA-MUSE, T. 2012. R loops: from transcription byproducts to threats to genome stability. *Mol Cell,* 46**,** 115-24.
AGUILERA, A. & GOMEZ-GONZALEZ, B. 2017. DNA-RNA hybrids: the risks of DNA breakage during transcription. *Nat Struct Mol Biol,* 24**,** 439-443.
ALZU, A., BERMEJO, R., BEGNIS, M., LUCCA, C., PICCINI, D., CAROTENUTO, W., SAPONARO, M., BRAMBATI, A., COCITO, A., FOIANI, M. & LIBERI, G. 2012. Senataxin associates with replication forks to protect fork integrity across RNA-polymerase-II-transcribed genes. *Cell,* 151**,** 835-46.
AN, J., HUANG, Y. C., XU, Q. Z., ZHOU, L. J., SHANG, Z. F., HUANG, B., WANG, Y., LIU, X. D., WU, D. C. & ZHOU, P. K. 2010. DNA-PKcs plays a dominant role in the regulation of H2AX phosphorylation in response to DNA damage and cell cycle progression. *BMC Mol Biol,* 11**,** 18.
ANDERSON, S. F., SCHLEGEL, B. P., NAKAJIMA, T., WOLPIN, E. S. & PARVIN, J. D. 1998. BRCA1 protein is linked to the RNA polymerase II holoenzyme complex via RNA helicase A. *Nat Genet,* 19**,** 254-6.
ANDO, Y., TOMARU, Y., MORINAGA, A., BURROUGHS, A. M., KAWAJI, H., KUBOSAKI, A., KIMURA, R., TAGATA, M., INO, Y., HIRANO, H., CHIBA, J., SUZUKI, H., CARNINCI, P. & HAYASHIZAKI, Y. 2011. Nuclear pore complex protein mediated nuclear localization of dicer protein in human cells. *PLoS One,* 6**,** e23385.
ARORA, R., LEE, Y., WISCHNEWSKI, H., BRUN, C. M., SCHWARZ, T. & AZZALIN, C. M. 2014. RNaseH1 regulates TERRA-telomeric DNA hybrids and telomere maintenance in ALT tumour cells. *Nat Commun,* 5**,** 5220.
AYMARD, F., BUGLER, B., SCHMIDT, C. K., GUILLOU, E., CARON, P., BRIOIS, S., IACOVONI, J. S., DABURON, V., MILLER, K. M., JACKSON, S. P. & LEGUBE, G. 2014. Transcriptionally active chromatin recruits homologous recombination at DNA double-strand breaks. *Nat Struct Mol Biol,* 21**,** 366-74.
BALK, B., MAICHER, A., DEES, M., KLERMUND, J., LUKE-GLASER, S., BENDER, K. & LUKE, B. 2013. Telomeric RNA-DNA hybrids affect telomere-length dynamics and senescence. *Nat Struct Mol Biol,* 20**,** 1199-205.
BECHEREL, O. J., YEO, A. J., STELLATI, A., HENG, E. Y., LUFF, J., SURAWEERA, A. M., WOODS, R., FLEMING, J., CARRIE, D., MCKINNEY, K., XU, X., DENG, C. & LAVIN, M. F. 2013. Senataxin plays an essential role with DNA damage response proteins in meiotic recombination and gene silencing. *PLoS Genet,* 9**,** e1003435.
BEKKER-JENSEN, S. & MAILAND, N. 2010. Assembly and function of DNA double-strand break repair foci in mammalian cells. *DNA Repair (Amst),* 9**,** 1219-28.
BELI, P., LUKASHCHUK, N., WAGNER, S. A., WEINERT, B. T., OLSEN, J. V., BASKCOMB, L., MANN, M., JACKSON, S. P. & CHOUDHARY, C. 2012. Proteomic investigations reveal a role for RNA processing factor THRAP3 in the DNA damage response. *Mol Cell,* 46**,** 212-25.
BENNETZEN, M. V., LARSEN, D. H., BUNKENBORG, J., BARTEK, J., LUKAS, J. & ANDERSEN, J. S. 2010. Site-specific phosphorylation dynamics of the nuclear proteome during the DNA damage response. *Mol Cell Proteomics,* 9**,** 1314-23.
BENSIMON, A., SCHMIDT, A., ZIV, Y., ELKON, R., WANG, S. Y., CHEN, D. J., AEBERSOLD, R. & SHILOH, Y. 2010. ATM-dependent and -independent dynamics of the nuclear phosphoproteome after DNA damage. *Sci Signal,* 3**,** rs3.

BHATIA, V., BARROSO, S. I., GARCIA-RUBIO, M. L., TUMINI, E., HERRERA-MOYANO, E. & AGUILERA, A. 2014. BRCA2 prevents R-loop accumulation and associates with TREX-2 mRNA export factor PCID2. *Nature,* 511**,** 362-5.

BILLY, E., BRONDANI, V., ZHANG, H., MULLER, U. & FILIPOWICZ, W. 2001. Specific interference with gene expression induced by long, double-stranded RNA in mouse embryonal teratocarcinoma cell lines. *Proc Natl Acad Sci U S A,* 98**,** 14428-33.

BLACKFORD, A. N. & JACKSON, S. P. 2017. ATM, ATR, and DNA-PK: The Trinity at the Heart of the DNA Damage Response. *Mol Cell,* 66**,** 801-817.

BOELENS, W. C., JANSEN, E. J., VAN VENROOIJ, W. J., STRIPECKE, R., MATTAJ, I. W. & GUNDERSON, S. I. 1993. The human U1 snRNP-specific U1A protein inhibits polyadenylation of its own pre-mRNA. *Cell,* 72**,** 881-92.

BRANZEI, D. & FOIANI, M. 2008. Regulation of DNA repair throughout the cell cycle. *Nat Rev Mol Cell Biol,* 9**,** 297-308.

BRANZEI, D. & FOIANI, M. 2010. Maintaining genome stability at the replication fork. *Nat Rev Mol Cell Biol,* 11**,** 208-19.

BRITTON, S., DERNONCOURT, E., DELTEIL, C., FROMENT, C., SCHILTZ, O., SALLES, B., FRIT, P. & CALSOU, P. 2014. DNA damage triggers SAF-A and RNA biogenesis factors exclusion from chromatin coupled to R-loops removal. *Nucleic Acids Res,* 42**,** 9047-62.

BUNTING, S. F., CALLEN, E., WONG, N., CHEN, H. T., POLATO, F., GUNN, A., BOTHMER, A., FELDHAHN, N., FERNANDEZ-CAPETILLO, O., CAO, L., XU, X., DENG, C. X., FINKEL, T., NUSSENZWEIG, M., STARK, J. M. & NUSSENZWEIG, A. 2010. 53BP1 inhibits homologous recombination in Brca1-deficient cells by blocking resection of DNA breaks. *Cell,* 141**,** 243-54.

BURGER, K., SCHLACKOW, M., POTTS, M., HESTER, S., MOHAMMED, S. & GULLEROVA, M. 2017. Nuclear phosphorylated Dicer processes double-stranded RNA in response to DNA damage. *J Cell Biol,* 216**,** 2373-2389.

BUSHNELL, D. A., CRAMER, P. & KORNBERG, R. D. 2002. Structural basis of transcription: alpha-amanitin-RNA polymerase II cocrystal at 2.8 A resolution. *Proc Natl Acad Sci U S A,* 99**,** 1218-22.

CALLEN, E., DI VIRGILIO, M., KRUHLAK, M. J., NIETO-SOLER, M., WONG, N., CHEN, H. T., FARYABI, R. B., POLATO, F., SANTOS, M., STARNES, L. M., WESEMANN, D. R., LEE, J. E., TUBBS, A., SLECKMAN, B. P., DANIEL, J. A., GE, K., ALT, F. W., FERNANDEZ-CAPETILLO, O., NUSSENZWEIG, M. C. & NUSSENZWEIG, A. 2013. 53BP1 mediates productive and mutagenic DNA repair through distinct phosphoprotein interactions. *Cell,* 153**,** 1266-80.

CARPENTER, A. E., JONES, T. R., LAMPRECHT, M. R., CLARKE, C., KANG, I. H., FRIMAN, O., GUERTIN, D. A., CHANG, J. H., LINDQUIST, R. A., MOFFAT, J., GOLLAND, P. & SABATINI, D. M. 2006. CellProfiler: image analysis software for identifying and quantifying cell phenotypes. *Genome Biol,* 7**,** R100.

CELESTE, A., FERNANDEZ-CAPETILLO, O., KRUHLAK, M. J., PILCH, D. R., STAUDT, D. W., LEE, A., BONNER, R. F., BONNER, W. M. & NUSSENZWEIG, A. 2003. Histone H2AX phosphorylation is dispensable for the initial recognition of DNA breaks. *Nat Cell Biol,* 5**,** 675-9.

CERRITELLI, S. M. & CROUCH, R. J. 2009. Ribonuclease H: the enzymes in eukaryotes. *FEBS J,* 276**,** 1494-505.

CERRITELLI, S. M., FROLOVA, E. G., FENG, C., GRINBERG, A., LOVE, P. E. & CROUCH, R. J. 2003. Failure to produce mitochondrial DNA results in embryonic lethality in Rnaseh1 null mice. *Mol Cell,* 11**,** 807-15.

CHAKRABORTY, A., TAPRYAL, N., VENKOVA, T., HORIKOSHI, N., PANDITA, R. K., SARKER, A. H., SARKAR, P. S., PANDITA, T. K. & HAZRA, T. K. 2016.

Classical non-homologous end-joining pathway utilizes nascent RNA for error-free double-strand break repair of transcribed genes. *Nat Commun,* 7**,** 13049.
CHANG, H. H. Y., PANNUNZIO, N. R., ADACHI, N. & LIEBER, M. R. 2017. Non-homologous DNA end joining and alternative pathways to double-strand break repair. *Nat Rev Mol Cell Biol,* 18**,** 495-506.
CHAPMAN, J. R., BARRAL, P., VANNIER, J. B., BOREL, V., STEGER, M., TOMAS-LOBA, A., SARTORI, A. A., ADAMS, I. R., BATISTA, F. D. & BOULTON, S. J. 2013. RIF1 is essential for 53BP1-dependent nonhomologous end joining and suppression of DNA double-strand break resection. *Mol Cell,* 49**,** 858-71.
CHAPMAN, J. R., SOSSICK, A. J., BOULTON, S. J. & JACKSON, S. P. 2012a. BRCA1-associated exclusion of 53BP1 from DNA damage sites underlies temporal control of DNA repair. *J Cell Sci,* 125**,** 3529-34.
CHAPMAN, J. R., TAYLOR, M. R. & BOULTON, S. J. 2012b. Playing the end game: DNA double-strand break repair pathway choice. *Mol Cell,* 47**,** 497-510.
CHAPMAN, M. S. & VERMA, I. M. 1996. Transcriptional activation by BRCA1. *Nature,* 382**,** 678-9.
CHAURASIA, P., SEN, R., PANDITA, T. K. & BHAUMIK, S. R. 2012. Preferential repair of DNA double-strand break at the active gene in vivo. *J Biol Chem,* 287**,** 36414-22.
CHIB, S., BYRD, A. K. & RANEY, K. D. 2016. Yeast Helicase Pif1 Unwinds RNA:DNA Hybrids with Higher Processivity than DNA:DNA Duplexes. *J Biol Chem,* 291**,** 5889-901.
CHON, H., VASSILEV, A., DEPAMPHILIS, M. L., ZHAO, Y., ZHANG, J., BURGERS, P. M., CROUCH, R. J. & CERRITELLI, S. M. 2009. Contributions of the two accessory subunits, RNASEH2B and RNASEH2C, to the activity and properties of the human RNase H2 complex. *Nucleic Acids Res,* 37**,** 96-110.
CHOU, D. M., ADAMSON, B., DEPHOURE, N. E., TAN, X., NOTTKE, A. C., HUROV, K. E., GYGI, S. P., COLAIACOVO, M. P. & ELLEDGE, S. J. 2010. A chromatin localization screen reveals poly (ADP ribose)-regulated recruitment of the repressive polycomb and NuRD complexes to sites of DNA damage. *Proc Natl Acad Sci U S A,* 107**,** 18475-80.
CHOWDHURY, D., CHOI, Y. E. & BRAULT, M. E. 2013. Charity begins at home: non-coding RNA functions in DNA repair. *Nat Rev Mol Cell Biol,* 14**,** 181-9.
CICCIA, A. & ELLEDGE, S. J. 2010. The DNA damage response: making it safe to play with knives. *Mol Cell,* 40**,** 179-204.
CROW, Y. J., LEITCH, A., HAYWARD, B. E., GARNER, A., PARMAR, R., GRIFFITH, E., ALI, M., SEMPLE, C., AICARDI, J., BABUL-HIRJI, R., BAUMANN, C., BAXTER, P., BERTINI, E., CHANDLER, K. E., CHITAYAT, D., CAU, D., DERY, C., FAZZI, E., GOIZET, C., KING, M. D., KLEPPER, J., LACOMBE, D., LANZI, G., LYALL, H., MARTINEZ-FRIAS, M. L., MATHIEU, M., MCKEOWN, C., MONIER, A., OADE, Y., QUARRELL, O. W., RITTEY, C. D., ROGERS, R. C., SANCHIS, A., STEPHENSON, J. B., TACKE, U., TILL, M., TOLMIE, J. L., TOMLIN, P., VOIT, T., WESCHKE, B., WOODS, C. G., LEBON, P., BONTHRON, D. T., PONTING, C. P. & JACKSON, A. P. 2006. Mutations in genes encoding ribonuclease H2 subunits cause Aicardi-Goutieres syndrome and mimic congenital viral brain infection. *Nat Genet,* 38**,** 910-6.
CRUZ-GARCIA, A., LOPEZ-SAAVEDRA, A. & HUERTAS, P. 2014. BRCA1 accelerates CtIP-mediated DNA-end resection. *Cell Rep,* 9**,** 451-9.
D'ADDA DI FAGAGNA, F. 2008. Living on a break: cellular senescence as a DNA-damage response. *Nat Rev Cancer,* 8**,** 512-22.
D'ADDA DI FAGAGNA, F. 2014. A direct role for small non-coding RNAs in DNA damage response. *Trends Cell Biol,* 24**,** 171-8.
D'ALESSANDRO, G. & D'ADDA DI FAGAGNA, F. 2016. Transcription and DNA Damage: Holding Hands or Crossing Swords? *J Mol Biol*.

DABEVA, M. D. & WARNER, J. R. 1993. Ribosomal protein L32 of Saccharomyces cerevisiae regulates both splicing and translation of its own transcript. *J Biol Chem,* 268**,** 19669-74.

DAVIES, O. R. & PELLEGRINI, L. 2007. Interaction with the BRCA2 C terminus protects RAD51-DNA filaments from disassembly by BRC repeats. *Nat Struct Mol Biol,* 14**,** 475-83.

DIMITROVA, N., CHEN, Y. C., SPECTOR, D. L. & DE LANGE, T. 2008. 53BP1 promotes non-homologous end joining of telomeres by increasing chromatin mobility. *Nature,* 456**,** 524-8.

DOYLE, M., BADERTSCHER, L., JASKIEWICZ, L., GUTTINGER, S., JURADO, S., HUGENSCHMIDT, T., KUTAY, U. & FILIPOWICZ, W. 2013. The double-stranded RNA binding domain of human Dicer functions as a nuclear localization signal. *RNA,* 19**,** 1238-52.

DROLET, M. 2006. Growth inhibition mediated by excess negative supercoiling: the interplay between transcription elongation, R-loop formation and DNA topology. *Mol Microbiol,* 59**,** 723-30.

DROLET, M., PHOENIX, P., MENZEL, R., MASSE, E., LIU, L. F. & CROUCH, R. J. 1995. Overexpression of RNase H partially complements the growth defect of an Escherichia coli delta topA mutant: R-loop formation is a major problem in the absence of DNA topoisomerase I. *Proc Natl Acad Sci U S A,* 92**,** 3526-30.

DUTERTRE, M., LAMBERT, S., CARREIRA, A., AMOR-GUERET, M. & VAGNER, S. 2014. DNA damage: RNA-binding proteins protect from near and far. *Trends Biochem Sci,* 39**,** 141-9.

DYNAN, W. S. & BURGESS, R. R. 1981. In vitro transcription by wheat germ RNA polymerase II. Initiation of RNA synthesis on relaxed, closed circular template. *J Biol Chem,* 256**,** 5866-73.

EL HAGE, A., FRENCH, S. L., BEYER, A. L. & TOLLERVEY, D. 2010. Loss of Topoisomerase I leads to R-loop-mediated transcriptional blocks during ribosomal RNA synthesis. *Genes Dev,* 24**,** 1546-58.

ESASHI, F., GALKIN, V. E., YU, X., EGELMAN, E. H. & WEST, S. C. 2007. Stabilization of RAD51 nucleoprotein filaments by the C-terminal region of BRCA2. *Nat Struct Mol Biol,* 14**,** 468-74.

ESCRIBANO-DIAZ, C., ORTHWEIN, A., FRADET-TURCOTTE, A., XING, M., YOUNG, J. T., TKAC, J., COOK, M. A., ROSEBROCK, A. P., MUNRO, M., CANNY, M. D., XU, D. & DUROCHER, D. 2013. A cell cycle-dependent regulatory circuit composed of 53BP1-RIF1 and BRCA1-CtIP controls DNA repair pathway choice. *Mol Cell,* 49**,** 872-83.

FERRETTI, L. P., LAFRANCHI, L. & SARTORI, A. A. 2013. Controlling DNA-end resection: a new task for CDKs. *Front Genet,* 4**,** 99.

FRANCIA, S., CABRINI, M., MATTI, V., OLDANI, A. & D'ADDA DI FAGAGNA, F. 2016. DICER, DROSHA and DNA damage response RNAs are necessary for the secondary recruitment of DNA damage response factors. *J Cell Sci,* 129**,** 1468-76.

FRANCIA, S., MICHELINI, F., SAXENA, A., TANG, D., DE HOON, M., ANELLI, V., MIONE, M., CARNINCI, P. & D'ADDA DI FAGAGNA, F. 2012. Site-specific DICER and DROSHA RNA products control the DNA-damage response. *Nature,* 488**,** 231-5.

GAGNON, K. T., LI, L., CHU, Y., JANOWSKI, B. A. & COREY, D. R. 2014. RNAi factors are present and active in human cell nuclei. *Cell Rep,* 6**,** 211-21.

GAN, W., GUAN, Z., LIU, J., GUI, T., SHEN, K., MANLEY, J. L. & LI, X. 2011. R-loop-mediated genomic instability is caused by impairment of replication fork progression. *Genes Dev,* 25**,** 2041-56.

GAO, M., WEI, W., LI, M. M., WU, Y. S., BA, Z., JIN, K. X., LI, M. M., LIAO, Y. Q., ADHIKARI, S., CHONG, Z., ZHANG, T., GUO, C. X., TANG, T. S., ZHU, B. T.,

XU, X. Z., MAILAND, N., YANG, Y. G., QI, Y. & RENDTLEW DANIELSEN, J. M. 2014. Ago2 facilitates Rad51 recruitment and DNA double-strand break repair by homologous recombination. *Cell Res,* 24**,** 532-41.

GARCIA-RUBIO, M. L., PEREZ-CALERO, C., BARROSO, S. I., TUMINI, E., HERRERA-MOYANO, E., ROSADO, I. V. & AGUILERA, A. 2015. The Fanconi Anemia Pathway Protects Genome Integrity from R-loops. *PLoS Genet,* 11**,** e1005674.

GHILDIYAL, M. & ZAMORE, P. D. 2009. Small silencing RNAs: an expanding universe. *Nat Rev Genet,* 10**,** 94-108.

GINNO, P. A., LIM, Y. W., LOTT, P. L., KORF, I. & CHEDIN, F. 2013. GC skew at the 5' and 3' ends of human genes links R-loop formation to epigenetic regulation and transcription termination. *Genome Res,* 23**,** 1590-600.

GINNO, P. A., LOTT, P. L., CHRISTENSEN, H. C., KORF, I. & CHEDIN, F. 2012. R-loop formation is a distinctive characteristic of unmethylated human CpG island promoters. *Mol Cell,* 45**,** 814-25.

GOTTIPATI, P., CASSEL, T. N., SAVOLAINEN, L. & HELLEDAY, T. 2008. Transcription-associated recombination is dependent on replication in Mammalian cells. *Mol Cell Biol,* 28**,** 154-64.

GRABCZYK, E., MANCUSO, M. & SAMMARCO, M. C. 2007. A persistent RNA.DNA hybrid formed by transcription of the Friedreich ataxia triplet repeat in live bacteria, and by T7 RNAP in vitro. *Nucleic Acids Res,* 35**,** 5351-9.

GRAF, M., BONETTI, D., LOCKHART, A., SERHAL, K., KELLNER, V., MAICHER, A., JOLIVET, P., TEIXEIRA, M. T. & LUKE, B. 2017. Telomere Length Determines TERRA and R-Loop Regulation through the Cell Cycle. *Cell,* 170**,** 72-85 e14.

GUDJONSSON, T., ALTMEYER, M., SAVIC, V., TOLEDO, L., DINANT, C., GROFTE, M., BARTKOVA, J., POULSEN, M., OKA, Y., BEKKER-JENSEN, S., MAILAND, N., NEUMANN, B., HERICHE, J. K., SHEARER, R., SAUNDERS, D., BARTEK, J., LUKAS, J. & LUKAS, C. 2012. TRIP12 and UBR5 suppress spreading of chromatin ubiquitylation at damaged chromosomes. *Cell,* 150**,** 697-709.

GULLEROVA, M. & PROUDFOOT, N. J. 2012. Convergent transcription induces transcriptional gene silencing in fission yeast and mammalian cells. *Nat Struct Mol Biol,* 19**,** 1193-201.

HAN, J., PEDERSEN, J. S., KWON, S. C., BELAIR, C. D., KIM, Y. K., YEOM, K. H., YANG, W. Y., HAUSSLER, D., BLELLOCH, R. & KIM, V. N. 2009. Posttranscriptional crossregulation between Drosha and DGCR8. *Cell,* 136**,** 75-84.

HANAHAN, D. & WEINBERG, R. A. 2011. Hallmarks of cancer: the next generation. *Cell,* 144**,** 646-74.

HATCHI, E., SKOURTI-STATHAKI, K., VENTZ, S., PINELLO, L., YEN, A., KAMIENIARZ-GDULA, K., DIMITROV, S., PATHANIA, S., MCKINNEY, K. M., EATON, M. L., KELLIS, M., HILL, S. J., PARMIGIANI, G., PROUDFOOT, N. J. & LIVINGSTON, D. M. 2015. BRCA1 recruitment to transcriptional pause sites is required for R-loop-driven DNA damage repair. *Mol Cell,* 57**,** 636-47.

HELMRICH, A., BALLARINO, M., NUDLER, E. & TORA, L. 2013. Transcription-replication encounters, consequences and genomic instability. *Nat Struct Mol Biol,* 20**,** 412-8.

HELMRICH, A., BALLARINO, M. & TORA, L. 2011. Collisions between replication and transcription complexes cause common fragile site instability at the longest human genes. *Mol Cell,* 44**,** 966-77.

HOUSELEY, J., LACAVA, J. & TOLLERVEY, D. 2006. RNA-quality control by the exosome. *Nat Rev Mol Cell Biol,* 7**,** 529-39.

HU, Y., SCULLY, R., SOBHIAN, B., XIE, A., SHESTAKOVA, E. & LIVINGSTON, D. M. 2011. RAP80-directed tuning of BRCA1 homologous recombination function at ionizing radiation-induced nuclear foci. *Genes Dev,* 25**,** 685-700.

HUEN, M. S., SY, S. M. & CHEN, J. 2010. BRCA1 and its toolbox for the maintenance of genome integrity. *Nat Rev Mol Cell Biol,* 11**,** 138-48.

HUERTAS, P. & JACKSON, S. P. 2009. Human CtIP mediates cell cycle control of DNA end resection and double strand break repair. *J Biol Chem,* 284**,** 9558-65.

HUSTEDT, N. & DUROCHER, D. 2016. The control of DNA repair by the cell cycle. *Nat Cell Biol,* 19**,** 1-9.

IACOVONI, J. S., CARON, P., LASSADI, I., NICOLAS, E., MASSIP, L., TROUCHE, D. & LEGUBE, G. 2010. High-resolution profiling of gammaH2AX around DNA double strand breaks in the mammalian genome. *EMBO J,* 29**,** 1446-57.

IANNELLI, F., GALBIATI, A., CAPOZZO, I., NGUYEN, Q., MAGNUSON, B., MICHELINI, F., D'ALESSANDRO, G., CABRINI, M., RONCADOR, M., FRANCIA, S., CROSETTO, N., LJUNGMAN, M., CARNINCI, P. & D'ADDA DI FAGAGNA, F. 2017. A damaged genome's transcriptional landscape through multilayered expression profiling around in situ-mapped DNA double-strand breaks. *Nat Commun,* 8**,** 15656.

IZHAR, L., ADAMSON, B., CICCIA, A., LEWIS, J., PONTANO-VAITES, L., LENG, Y., LIANG, A. C., WESTBROOK, T. F., HARPER, J. W. & ELLEDGE, S. J. 2015. A Systematic Analysis of Factors Localized to Damaged Chromatin Reveals PARP-Dependent Recruitment of Transcription Factors. *Cell Rep,* 11**,** 1486-500.

JACKSON, S. P. & BARTEK, J. 2009. The DNA-damage response in human biology and disease. *Nature,* 461**,** 1071-8.

JACKSON, S. P. & DUROCHER, D. 2013. Regulation of DNA damage responses by ubiquitin and SUMO. *Mol Cell,* 49**,** 795-807.

JASIN, M. & ROTHSTEIN, R. 2013. Repair of strand breaks by homologous recombination. *Cold Spring Harb Perspect Biol,* 5**,** a012740.

KAIDI, A., WEINERT, B. T., CHOUDHARY, C. & JACKSON, S. P. 2010. Human SIRT6 promotes DNA end resection through CtIP deacetylation. *Science,* 329**,** 1348-53.

KASAHARA, M., CLIKEMAN, J. A., BATES, D. B. & KOGOMA, T. 2000. RecA protein-dependent R-loop formation in vitro. *Genes Dev,* 14**,** 360-5.

KAWAI, S. & AMANO, A. 2012. BRCA1 regulates microRNA biogenesis via the DROSHA microprocessor complex. *J Cell Biol,* 197**,** 201-8.

KESKIN, H., SHEN, Y., HUANG, F., PATEL, M., YANG, T., ASHLEY, K., MAZIN, A. V. & STORICI, F. 2014. Transcript-RNA-templated DNA recombination and repair. *Nature,* 515**,** 436-9.

KRUHLAK, M., CROUCH, E. E., ORLOV, M., MONTANO, C., GORSKI, S. A., NUSSENZWEIG, A., MISTELI, T., PHAIR, R. D. & CASELLAS, R. 2007. The ATM repair pathway inhibits RNA polymerase I transcription in response to chromosome breaks. *Nature,* 447**,** 730-4.

KUROSAWA, A., KOYAMA, H., TAKAYAMA, S., MIKI, K., AYUSAWA, D., FUJII, M., IIIZUMI, S. & ADACHI, N. 2008. The requirement of Artemis in double-strand break repair depends on the type of DNA damage. *DNA Cell Biol,* 27**,** 55-61.

LEE, S. E., PELLICIOLI, A., DEMETER, J., VAZE, M. P., GASCH, A. P., MALKOVA, A., BROWN, P. O., BOTSTEIN, D., STEARNS, T., FOIANI, M. & HABER, J. E. 2000. Arrest, adaptation, and recovery following a chromosome double-strand break in Saccharomyces cerevisiae. *Cold Spring Harb Symp Quant Biol,* 65**,** 303-14.

LEMAITRE, C., GRABARZ, A., TSOUROULA, K., ANDRONOV, L., FURST, A., PANKOTAI, T., HEYER, V., ROGIER, M., ATTWOOD, K. M., KESSLER, P., DELLAIRE, G., KLAHOLZ, B., REINA-SAN-MARTIN, B. & SOUTOGLOU, E. 2014. Nuclear position dictates DNA repair pathway choice. *Genes Dev,* 28**,** 2450-63.

LI, L., GERMAIN, D. R., POON, H. Y., HILDEBRANDT, M. R., MONCKTON, E. A., MCDONALD, D., HENDZEL, M. J. & GODBOUT, R. 2016. DEAD Box 1 Facilitates Removal of RNA and Homologous Recombination at DNA Double-Strand Breaks. *Mol Cell Biol,* 36**,** 2794-2810.

LI, L., MONCKTON, E. A. & GODBOUT, R. 2008. A role for DEAD box 1 at DNA double-strand breaks. *Mol Cell Biol,* 28**,** 6413-25.

LI, M. & YU, X. 2013. Function of BRCA1 in the DNA damage response is mediated by ADP-ribosylation. *Cancer Cell,* 23**,** 693-704.

LIN, Y., DENT, S. Y., WILSON, J. H., WELLS, R. D. & NAPIERALA, M. 2010. R loops stimulate genetic instability of CTG.CAG repeats. *Proc Natl Acad Sci U S A,* 107**,** 692-7.

LINDAHL, T. & BARNES, D. E. 2000. Repair of endogenous DNA damage. *Cold Spring Harb Symp Quant Biol,* 65**,** 127-33.

LOK, B. H., CARLEY, A. C., TCHANG, B. & POWELL, S. N. 2013. RAD52 inactivation is synthetically lethal with deficiencies in BRCA1 and PALB2 in addition to BRCA2 through RAD51-mediated homologous recombination. *Oncogene,* 32**,** 3552-8.

LOMONOSOV, M., ANAND, S., SANGRITHI, M., DAVIES, R. & VENKITARAMAN, A. R. 2003. Stabilization of stalled DNA replication forks by the BRCA2 breast cancer susceptibility protein. *Genes Dev,* 17**,** 3017-22.

MAILAND, N., BEKKER-JENSEN, S., FAUSTRUP, H., MELANDER, F., BARTEK, J., LUKAS, C. & LUKAS, J. 2007. RNF8 ubiquitylates histones at DNA double-strand breaks and promotes assembly of repair proteins. *Cell,* 131**,** 887-900.

MANFRINI, N., CLERICI, M., WERY, M., COLOMBO, C. V., DESCRIMES, M., MORILLON, A., D'ADDA DI FAGAGNA, F. & LONGHESE, M. P. 2015. Resection is responsible for loss of transcription around a double-strand break in Saccharomyces cerevisiae. *Elife,* 4.

MARECHAL, A., LI, J. M., JI, X. Y., WU, C. S., YAZINSKI, S. A., NGUYEN, H. D., LIU, S., JIMENEZ, A. E., JIN, J. & ZOU, L. 2014. PRP19 transforms into a sensor of RPA-ssDNA after DNA damage and drives ATR activation via a ubiquitin-mediated circuitry. *Mol Cell,* 53**,** 235-46.

MARIN-VICENTE, C., DOMINGO-PRIM, J., EBERLE, A. B. & VISA, N. 2015. RRP6/EXOSC10 is required for the repair of DNA double-strand breaks by homologous recombination. *J Cell Sci,* 128**,** 1097-107.

MATSUI, M., LI, L., JANOWSKI, B. A. & COREY, D. R. 2015. Reduced Expression of Argonaute 1, Argonaute 2, and TRBP Changes Levels and Intracellular Distribution of RNAi Factors. *Sci Rep,* 5**,** 12855.

MATSUOKA, S., BALLIF, B. A., SMOGORZEWSKA, A., MCDONALD, E. R., 3RD, HUROV, K. E., LUO, J., BAKALARSKI, C. E., ZHAO, Z., SOLIMINI, N., LERENTHAL, Y., SHILOH, Y., GYGI, S. P. & ELLEDGE, S. J. 2007. ATM and ATR substrate analysis reveals extensive protein networks responsive to DNA damage. *Science,* 316**,** 1160-6.

MAZINA, O. M., KESKIN, H., HANAMSHET, K., STORICI, F. & MAZIN, A. V. 2017. Rad52 Inverse Strand Exchange Drives RNA-Templated DNA Double-Strand Break Repair. *Mol Cell,* 67**,** 19-29 e3.

MCCLOREY, G. & WOOD, M. J. 2015. An overview of the clinical application of antisense oligonucleotides for RNA-targeting therapies. *Curr Opin Pharmacol,* 24**,** 52-8.

MICHALIK, K. M., BOTTCHER, R. & FORSTEMANN, K. 2012. A small RNA response at DNA ends in Drosophila. *Nucleic Acids Res,* 40**,** 9596-603.

MISCHO, H. E., GOMEZ-GONZALEZ, B., GRZECHNIK, P., RONDON, A. G., WEI, W., STEINMETZ, L., AGUILERA, A. & PROUDFOOT, N. J. 2011. Yeast Sen1 helicase protects the genome from transcription-associated instability. *Mol Cell,* 41**,** 21-32.

MUCH, C., AUCHYNNIKAVA, T., PAVLINIC, D., BUNESS, A., RAPPSILBER, J., BENES, V., ALLSHIRE, R. & O'CARROLL, D. 2016. Endogenous Mouse Dicer Is an Exclusively Cytoplasmic Protein. *PLoS Genet,* 12**,** e1006095.

NEALE, M. J. & KEENEY, S. 2006. Clarifying the mechanics of DNA strand exchange in meiotic recombination. *Nature,* 442**,** 153-8.

NEISH, A. S., ANDERSON, S. F., SCHLEGEL, B. P., WEI, W. & PARVIN, J. D. 1998. Factors associated with the mammalian RNA polymerase II holoenzyme. *Nucleic Acids Res,* 26**,** 847-53.

NEVE, J., BURGER, K., LI, W., HOQUE, M., PATEL, R., TIAN, B., GULLEROVA, M. & FURGER, A. 2016. Subcellular RNA profiling links splicing and nuclear DICER1 to alternative cleavage and polyadenylation. *Genome Res,* 26**,** 24-35.

NGUYEN, V. T., GIANNONI, F., DUBOIS, M. F., SEO, S. J., VIGNERON, M., KEDINGER, C. & BENSAUDE, O. 1996. In vivo degradation of RNA polymerase II largest subunit triggered by alpha-amanitin. *Nucleic Acids Res,* 24**,** 2924-9.

OCHS, F., SOMYAJIT, K., ALTMEYER, M., RASK, M. B., LUKAS, J. & LUKAS, C. 2016. 53BP1 fosters fidelity of homology-directed DNA repair. *Nat Struct Mol Biol,* 23**,** 714-21.

OHLE, C., TESORERO, R., SCHERMANN, G., DOBREV, N., SINNING, I. & FISCHER, T. 2016. Transient RNA-DNA Hybrids Are Required for Efficient Double-Strand Break Repair. *Cell,* 167**,** 1001-1013 e7.

OHRT, T., MUETZE, J., SVOBODA, P. & SCHWILLE, P. 2012. Intracellular localization and routing of miRNA and RNAi pathway components. *Curr Top Med Chem,* 12**,** 79-88.

ORTHWEIN, A., NOORDERMEER, S. M., WILSON, M. D., LANDRY, S., ENCHEV, R. I., SHERKER, A., MUNRO, M., PINDER, J., SALSMAN, J., DELLAIRE, G., XIA, B., PETER, M. & DUROCHER, D. 2015. A mechanism for the suppression of homologous recombination in G1 cells. *Nature,* 528**,** 422-6.

PANKOTAI, T., BONHOMME, C., CHEN, D. & SOUTOGLOU, E. 2012. DNAPKcs-dependent arrest of RNA polymerase II transcription in the presence of DNA breaks. *Nat Struct Mol Biol,* 19**,** 276-82.

PAULSEN, R. D., SONI, D. V., WOLLMAN, R., HAHN, A. T., YEE, M. C., GUAN, A., HESLEY, J. A., MILLER, S. C., CROMWELL, E. F., SOLOW-CORDERO, D. E., MEYER, T. & CIMPRICH, K. A. 2009. A genome-wide siRNA screen reveals diverse cellular processes and pathways that mediate genome stability. *Mol Cell,* 35**,** 228-39.

PFEIFFER, V., CRITTIN, J., GROLIMUND, L. & LINGNER, J. 2013. The THO complex component Thp2 counteracts telomeric R-loops and telomere shortening. *EMBO J,* 32**,** 2861-71.

PHILIPPE, C., EYERMANN, F., BENARD, L., PORTIER, C., EHRESMANN, B. & EHRESMANN, C. 1993. Ribosomal protein S15 from Escherichia coli modulates its own translation by trapping the ribosome on the mRNA initiation loading site. *Proc Natl Acad Sci U S A,* 90**,** 4394-8.

PIERCE, A. J., JOHNSON, R. D., THOMPSON, L. H. & JASIN, M. 1999. XRCC3 promotes homology-directed repair of DNA damage in mammalian cells. *Genes Dev,* 13**,** 2633-8.

PIZZI, S., SERTIC, S., ORCESI, S., CEREDA, C., BIANCHI, M., JACKSON, A. P., LAZZARO, F., PLEVANI, P. & MUZI-FALCONI, M. 2015. Reduction of hRNase H2 activity in Aicardi-Goutieres syndrome cells leads to replication stress and genome instability. *Hum Mol Genet,* 24**,** 649-58.

POLATO, F., CALLEN, E., WONG, N., FARYABI, R., BUNTING, S., CHEN, H. T., KOZAK, M., KRUHLAK, M. J., RECZEK, C. R., LEE, W. H., LUDWIG, T., BAER, R., FEIGENBAUM, L., JACKSON, S. & NUSSENZWEIG, A. 2014. CtIP-

mediated resection is essential for viability and can operate independently of BRCA1. *J Exp Med,* 211**,** 1027-36.

POLO, S. E., BLACKFORD, A. N., CHAPMAN, J. R., BASKCOMB, L., GRAVEL, S., RUSCH, A., THOMAS, A., BLUNDRED, R., SMITH, P., KZHYSHKOWSKA, J., DOBNER, T., TAYLOR, A. M., TURNELL, A. S., STEWART, G. S., GRAND, R. J. & JACKSON, S. P. 2012. Regulation of DNA-end resection by hnRNPU-like proteins promotes DNA double-strand break signaling and repair. *Mol Cell,* 45**,** 505-16.

POLYAK, K. & GARBER, J. 2011. Targeting the missing links for cancer therapy. *Nat Med,* 17**,** 283-4.

PRAKASH, R., ZHANG, Y., FENG, W. & JASIN, M. 2015. Homologous recombination and human health: the roles of BRCA1, BRCA2, and associated proteins. *Cold Spring Harb Perspect Biol,* 7**,** a016600.

PRICE, B. D. & D'ANDREA, A. D. 2013. Chromatin remodeling at DNA double-strand breaks. *Cell,* 152**,** 1344-54.

PROVOST, P., DISHART, D., DOUCET, J., FRENDEWEY, D., SAMUELSSON, B. & RADMARK, O. 2002. Ribonuclease activity and RNA binding of recombinant human Dicer. *EMBO J,* 21**,** 5864-74.

REABAN, M. E., LEBOWITZ, J. & GRIFFIN, J. A. 1994. Transcription induces the formation of a stable RNA.DNA hybrid in the immunoglobulin alpha switch region. *J Biol Chem,* 269**,** 21850-7.

RECZEK, C. R., SZABOLCS, M., STARK, J. M., LUDWIG, T. & BAER, R. 2013. The interaction between CtIP and BRCA1 is not essential for resection-mediated DNA repair or tumor suppression. *J Cell Biol,* 201**,** 693-707.

REDDY, K., TAM, M., BOWATER, R. P., BARBER, M., TOMLINSON, M., NICHOL EDAMURA, K., WANG, Y. H. & PEARSON, C. E. 2011. Determinants of R-loop formation at convergent bidirectionally transcribed trinucleotide repeats. *Nucleic Acids Res,* 39**,** 1749-62.

REIJNS, M. A., RABE, B., RIGBY, R. E., MILL, P., ASTELL, K. R., LETTICE, L. A., BOYLE, S., LEITCH, A., KEIGHREN, M., KILANOWSKI, F., DEVENNEY, P. S., SEXTON, D., GRIMES, G., HOLT, I. J., HILL, R. E., TAYLOR, M. S., LAWSON, K. A., DORIN, J. R. & JACKSON, A. P. 2012. Enzymatic removal of ribonucleotides from DNA is essential for mammalian genome integrity and development. *Cell,* 149**,** 1008-22.

RIBALLO, E., KUHNE, M., RIEF, N., DOHERTY, A., SMITH, G. C., RECIO, M. J., REIS, C., DAHM, K., FRICKE, A., KREMPLER, A., PARKER, A. R., JACKSON, S. P., GENNERY, A., JEGGO, P. A. & LOBRICH, M. 2004. A pathway of double-strand break rejoining dependent upon ATM, Artemis, and proteins locating to gamma-H2AX foci. *Mol Cell,* 16**,** 715-24.

RIJKERS, T., VAN DEN OUWELAND, J., MOROLLI, B., ROLINK, A. G., BAARENDS, W. M., VAN SLOUN, P. P., LOHMAN, P. H. & PASTINK, A. 1998. Targeted inactivation of mouse RAD52 reduces homologous recombination but not resistance to ionizing radiation. *Mol Cell Biol,* 18**,** 6423-9.

ROGAKOU, E. P., BOON, C., REDON, C. & BONNER, W. M. 1999. Megabase chromatin domains involved in DNA double-strand breaks in vivo. *J Cell Biol,* 146**,** 905-16.

ROSSIELLO, F., AGUADO, J., SEPE, S., IANNELLI, F., NGUYEN, Q., PITCHIAYA, S., CARNINCI, P. & D'ADDA DI FAGAGNA, F. 2017. DNA damage response inhibition at dysfunctional telomeres by modulation of telomeric DNA damage response RNAs. *Nat Commun,* 8**,** 13980.

ROY, D. & LIEBER, M. R. 2009. G clustering is important for the initiation of transcription-induced R-loops in vitro, whereas high G density without clustering is sufficient thereafter. *Mol Cell Biol,* 29**,** 3124-33.

ROY, D., ZHANG, Z., LU, Z., HSIEH, C. L. & LIEBER, M. R. 2010. Competition between the RNA transcript and the nontemplate DNA strand during R-loop formation in vitro: a nick can serve as a strong R-loop initiation site. *Mol Cell Biol,* 30**,** 146-59.

SAKAUE-SAWANO, A., KUROKAWA, H., MORIMURA, T., HANYU, A., HAMA, H., OSAWA, H., KASHIWAGI, S., FUKAMI, K., MIYATA, T., MIYOSHI, H., IMAMURA, T., OGAWA, M., MASAI, H. & MIYAWAKI, A. 2008. Visualizing spatiotemporal dynamics of multicellular cell-cycle progression. *Cell,* 132**,** 487-98.

SANTOS-PEREIRA, J. M. & AGUILERA, A. 2015. R loops: new modulators of genome dynamics and function. *Nat Rev Genet,* 16**,** 583-97.

SARTORI, A. A., LUKAS, C., COATES, J., MISTRIK, M., FU, S., BARTEK, J., BAER, R., LUKAS, J. & JACKSON, S. P. 2007. Human CtIP promotes DNA end resection. *Nature,* 450**,** 509-14.

SAVAGE, K. I. & HARKIN, D. P. 2015. BRCA1, a 'complex' protein involved in the maintenance of genomic stability. *FEBS J,* 282**,** 630-46.

SCHLACHER, K., CHRIST, N., SIAUD, N., EGASHIRA, A., WU, H. & JASIN, M. 2011. Double-strand break repair-independent role for BRCA2 in blocking stalled replication fork degradation by MRE11. *Cell,* 145**,** 529-42.

SCHWAB, R. A., NIEMINUSZCZY, J., SHAH, F., LANGTON, J., LOPEZ MARTINEZ, D., LIANG, C. C., COHN, M. A., GIBBONS, R. J., DEANS, A. J. & NIEDZWIEDZ, W. 2015. The Fanconi Anemia Pathway Maintains Genome Stability by Coordinating Replication and Transcription. *Mol Cell,* 60**,** 351-61.

SCULLY, R., ANDERSON, S. F., CHAO, D. M., WEI, W., YE, L., YOUNG, R. A., LIVINGSTON, D. M. & PARVIN, J. D. 1997. BRCA1 is a component of the RNA polymerase II holoenzyme. *Proc Natl Acad Sci U S A,* 94**,** 5605-10.

SHANBHAG, N. M., RAFALSKA-METCALF, I. U., BALANE-BOLIVAR, C., JANICKI, S. M. & GREENBERG, R. A. 2010. ATM-dependent chromatin changes silence transcription in cis to DNA double-strand breaks. *Cell,* 141**,** 970-81.

SHAO, Z., DAVIS, A. J., FATTAH, K. R., SO, S., SUN, J., LEE, K. J., HARRISON, L., YANG, J. & CHEN, D. J. 2012. Persistently bound Ku at DNA ends attenuates DNA end resection and homologous recombination. *DNA Repair (Amst),* 11**,** 310-6.

SHEN, Y., NANDI, P., TAYLOR, M. B., STUCKEY, S., BHADSAVLE, H. P., WEISS, B. & STORICI, F. 2011. RNA-driven genetic changes in bacteria and in human cells. *Mutat Res,* 717**,** 91-8.

SHIBATA, A., MOIANI, D., ARVAI, A. S., PERRY, J., HARDING, S. M., GENOIS, M. M., MAITY, R., VAN ROSSUM-FIKKERT, S., KERTOKALIO, A., ROMOLI, F., ISMAIL, A., ISMALAJ, E., PETRICCI, E., NEALE, M. J., BRISTOW, R. G., MASSON, J. Y., WYMAN, C., JEGGO, P. A. & TAINER, J. A. 2014. DNA double-strand break repair pathway choice is directed by distinct MRE11 nuclease activities. *Mol Cell,* 53**,** 7-18.

SINKKONEN, L., HUGENSCHMIDT, T., FILIPOWICZ, W. & SVOBODA, P. 2010. Dicer is associated with ribosomal DNA chromatin in mammalian cells. *PLoS One,* 5**,** e12175.

SKOURTI-STATHAKI, K., KAMIENIARZ-GDULA, K. & PROUDFOOT, N. J. 2014. R-loops induce repressive chromatin marks over mammalian gene terminators. *Nature,* 516**,** 436-9.

SKOURTI-STATHAKI, K. & PROUDFOOT, N. J. 2014. A double-edged sword: R loops as threats to genome integrity and powerful regulators of gene expression. *Genes Dev,* 28**,** 1384-96.

SKOURTI-STATHAKI, K., PROUDFOOT, N. J. & GROMAK, N. 2011. Human senataxin resolves RNA/DNA hybrids formed at transcriptional pause sites to promote Xrn2-dependent termination. *Mol Cell,* 42**,** 794-805.

SOLLIER, J., STORK, C. T., GARCIA-RUBIO, M. L., PAULSEN, R. D., AGUILERA, A. & CIMPRICH, K. A. 2014. Transcription-coupled nucleotide excision repair factors promote R-loop-induced genome instability. *Mol Cell,* 56**,** 777-85.

SOULAS-SPRAUEL, P., RIVERA-MUNOZ, P., MALIVERT, L., LE GUYADER, G., ABRAMOWSKI, V., REVY, P. & DE VILLARTAY, J. P. 2007. V(D)J and immunoglobulin class switch recombinations: a paradigm to study the regulation of DNA end-joining. *Oncogene,* 26**,** 7780-91.

SPARKS, J. L., CHON, H., CERRITELLI, S. M., KUNKEL, T. A., JOHANSSON, E., CROUCH, R. J. & BURGERS, P. M. 2012. RNase H2-initiated ribonucleotide excision repair. *Mol Cell,* 47**,** 980-6.

STEGER, M., MURINA, O., HUHN, D., FERRETTI, L. P., WALSER, R., HANGGI, K., LAFRANCHI, L., NEUGEBAUER, C., PALIWAL, S., JANSCAK, P., GERRITS, B., DEL SAL, G., ZERBE, O. & SARTORI, A. A. 2013. Prolyl isomerase PIN1 regulates DNA double-strand break repair by counteracting DNA end resection. *Mol Cell,* 50**,** 333-43.

STORICI, F., BEBENEK, K., KUNKEL, T. A., GORDENIN, D. A. & RESNICK, M. A. 2007. RNA-templated DNA repair. *Nature,* 447**,** 338-41.

TAN, S. L. W., CHADHA, S., LIU, Y., GABASOVA, E., PERERA, D., AHMED, K., CONSTANTINOU, S., RENAUDIN, X., LEE, M., AEBERSOLD, R. & VENKITARAMAN, A. R. 2017. A Class of Environmental and Endogenous Toxins Induces BRCA2 Haploinsufficiency and Genome Instability. *Cell,* 169**,** 1105-1118 e15.

TAN-WONG, S. M. & PROUDFOOT, N. J. 2013. Rad51, friend or foe? *Elife,* 2**,** e00914.

TANG, J., CHO, N. W., CUI, G., MANION, E. M., SHANBHAG, N. M., BOTUYAN, M. V., MER, G. & GREENBERG, R. A. 2013. Acetylation limits 53BP1 association with damaged chromatin to promote homologous recombination. *Nat Struct Mol Biol,* 20**,** 317-25.

TAUB, R., KIRSCH, I., MORTON, C., LENOIR, G., SWAN, D., TRONICK, S., AARONSON, S. & LEDER, P. 1982. Translocation of the c-myc gene into the immunoglobulin heavy chain locus in human Burkitt lymphoma and murine plasmacytoma cells. *Proc Natl Acad Sci U S A,* 79**,** 7837-41.

TOMIMATSU, N., MUKHERJEE, B., DELAND, K., KURIMASA, A., BOLDERSON, E., KHANNA, K. K. & BURMA, S. 2012. Exo1 plays a major role in DNA end resection in humans and influences double-strand break repair and damage signaling decisions. *DNA Repair (Amst),* 11**,** 441-8.

TRAN, P. L. T., POHL, T. J., CHEN, C. F., CHAN, A., POTT, S. & ZAKIAN, V. A. 2017. PIF1 family DNA helicases suppress R-loop mediated genome instability at tRNA genes. *Nat Commun,* 8**,** 15025.

TUDURI, S., CRABBE, L., CONTI, C., TOURRIERE, H., HOLTGREVE-GREZ, H., JAUCH, A., PANTESCO, V., DE VOS, J., THOMAS, A., THEILLET, C., POMMIER, Y., TAZI, J., COQUELLE, A. & PASERO, P. 2009. Topoisomerase I suppresses genomic instability by preventing interference between replication and transcription. *Nat Cell Biol,* 11**,** 1315-24.

VENKITARAMAN, A. R. 2002. Cancer susceptibility and the functions of BRCA1 and BRCA2. *Cell,* 108**,** 171-82.

VERMA, P. & GREENBERG, R. A. 2016. Noncanonical views of homology-directed DNA repair. *Genes Dev,* 30**,** 1138-54.

WAHBA, L., AMON, J. D., KOSHLAND, D. & VUICA-ROSS, M. 2011. RNase H and multiple RNA biogenesis factors cooperate to prevent RNA:DNA hybrids from generating genome instability. *Mol Cell,* 44**,** 978-88.

WAHBA, L., GORE, S. K. & KOSHLAND, D. 2013. The homologous recombination machinery modulates the formation of RNA-DNA hybrids and associated chromosome instability. *Elife,* 2**,** e00505.

WANG, Q. & GOLDSTEIN, M. 2016. Small RNAs Recruit Chromatin-Modifying Enzymes MMSET and Tip60 to Reconfigure Damaged DNA upon Double-Strand Break and Facilitate Repair. *Cancer Res,* 76**,** 1904-15.

WATT, D. L., JOHANSSON, E., BURGERS, P. M. & KUNKEL, T. A. 2011. Replication of ribonucleotide-containing DNA templates by yeast replicative polymerases. *DNA Repair (Amst),* 10**,** 897-902.

WEI, W., BA, Z., GAO, M., WU, Y., MA, Y., AMIARD, S., WHITE, C. I., RENDTLEW DANIELSEN, J. M., YANG, Y. G. & QI, Y. 2012. A role for small RNAs in DNA double-strand break repair. *Cell,* 149**,** 101-12.

WEINSTOCK, D. M., NAKANISHI, K., HELGADOTTIR, H. R. & JASIN, M. 2006. Assaying double-strand break repair pathway choice in mammalian cells using a targeted endonuclease or the RAG recombinase. *Methods Enzymol,* 409**,** 524-40.

WELLINGER, R. E., PRADO, F. & AGUILERA, A. 2006. Replication fork progression is impaired by transcription in hyperrecombinant yeast cells lacking a functional THO complex. *Mol Cell Biol,* 26**,** 3327-34.

WHITE, E., SCHLACKOW, M., KAMIENIARZ-GDULA, K., PROUDFOOT, N. J. & GULLEROVA, M. 2014. Human nuclear Dicer restricts the deleterious accumulation of endogenous double-stranded RNA. *Nat Struct Mol Biol,* 21**,** 552-9.

WILLIAMS, G. J., LEES-MILLER, S. P. & TAINER, J. A. 2010. Mre11-Rad50-Nbs1 conformations and the control of sensing, signaling, and effector responses at DNA double-strand breaks. *DNA Repair (Amst),* 9**,** 1299-306.

WU, L. C., WANG, Z. W., TSAN, J. T., SPILLMAN, M. A., PHUNG, A., XU, X. L., YANG, M. C., HWANG, L. Y., BOWCOCK, A. M. & BAER, R. 1996. Identification of a RING protein that can interact in vivo with the BRCA1 gene product. *Nat Genet,* 14**,** 430-40.

YAN, W. X., MIRZAZADEH, R., GARNERONE, S., SCOTT, D., SCHNEIDER, M. W., KALLAS, T., CUSTODIO, J., WERNERSSON, E., LI, Y., GAO, L., FEDEROVA, Y., ZETSCHE, B., ZHANG, F., BIENKO, M. & CROSETTO, N. 2017. BLISS is a versatile and quantitative method for genome-wide profiling of DNA double-strand breaks. *Nat Commun,* 8**,** 15058.

YU, K., CHEDIN, F., HSIEH, C. L., WILSON, T. E. & LIEBER, M. R. 2003. R-loops at immunoglobulin class switch regions in the chromosomes of stimulated B cells. *Nat Immunol,* 4**,** 442-51.

YU, T. Y., KAO, Y. W. & LIN, J. J. 2014. Telomeric transcripts stimulate telomere recombination to suppress senescence in cells lacking telomerase. *Proc Natl Acad Sci U S A,* 111**,** 3377-82.

YU, X. & CHEN, J. 2004. DNA damage-induced cell cycle checkpoint control requires CtIP, a phosphorylation-dependent binding partner of BRCA1 C-terminal domains. *Mol Cell Biol,* 24**,** 9478-86.

YUCE, O. & WEST, S. C. 2013. Senataxin, defective in the neurodegenerative disorder ataxia with oculomotor apraxia 2, lies at the interface of transcription and the DNA damage response. *Mol Cell Biol,* 33**,** 406-17.

ZAITSEV, E. N. & KOWALCZYKOWSKI, S. C. 2000. A novel pairing process promoted by Escherichia coli RecA protein: inverse DNA and RNA strand exchange. *Genes Dev,* 14**,** 740-9.

ZHU, Q., PAO, G. M., HUYNH, A. M., SUH, H., TONNU, N., NEDERLOF, P. M., GAGE, F. H. & VERMA, I. M. 2011. BRCA1 tumour suppression occurs via heterochromatin-mediated silencing. *Nature,* 477**,** 179-84.

ZIMMERMANN, M., LOTTERSBERGER, F., BUONOMO, S. B., SFEIR, A. & DE LANGE, T. 2013. 53BP1 regulates DSB repair using Rif1 to control 5' end resection. *Science,* 339**,** 700-4.

ZOU, L. & ELLEDGE, S. J. 2003. Sensing DNA damage through ATRIP recognition of RPA-ssDNA complexes. *Science,* 300**,** 1542-8.